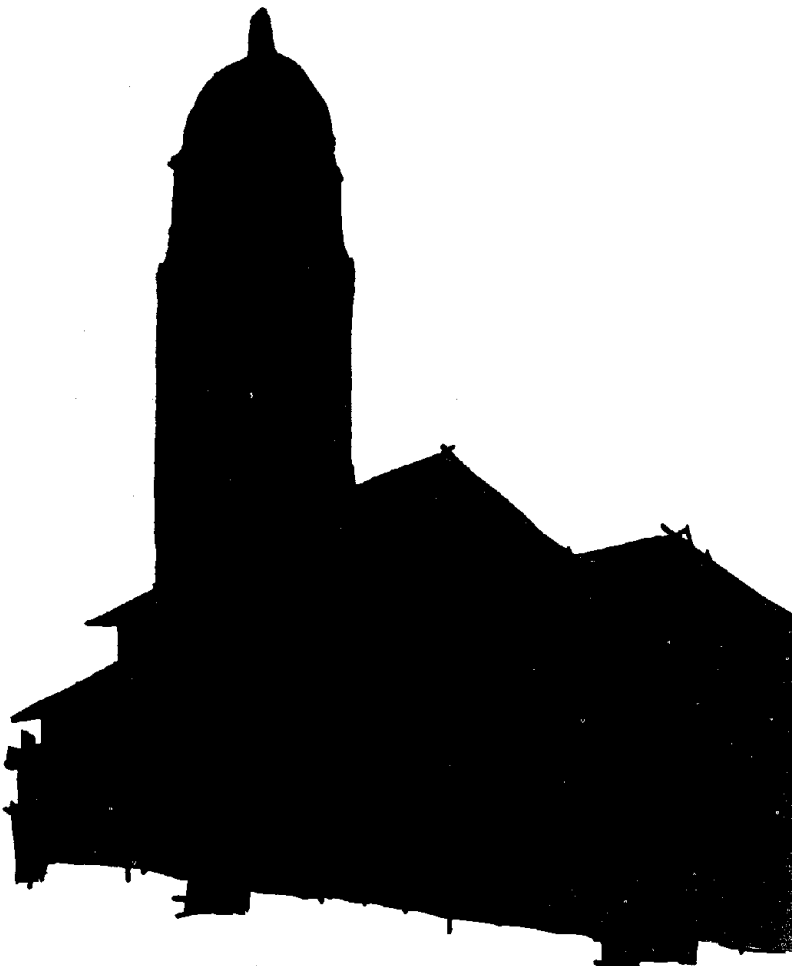# The John A. Blume Earthquake Engineering Center

Department of Civil Engineering
Stanford University

VIBRATION ANALYSIS OF SKELETAL SYSTEMS USING A MIXED FORMULATION WITH AN ARNOLDI-BASED NONLINEAR EIGENSOLUTION TECHNIQUE

by

Rajesh K. Singh

and

H. Allison Smith

Report No. 109

December 1993

The John A. Blume Earthquake Engineering Center was established to promote research and education in earthquake engineering. Through its activities our understanding of earthquakes and their effects on mankind's facilities and structures is improving. The Center conducts research, provides instruction, publishes reports and articles, conducts seminars and conferences, and provides financial support for students. The Center is named for Dr. John A. Blume, a well-known consulting engineer and Stanford alumnus.

Address

The John A. Blume Earthquake Engineering Center
Department of Civil Engineering
Stanford University
Stanford, California 94305

Report Nos:

Title: Vibration Analysis of Skeletal Systems Using a Mixed Formulation with an Arnoldi-Based Nonlinear Eigensolution Technique.

Date: Dec 93

Authors: R. K. Singh and H. A. Smith.

Performing Organization: Stanford Univ., CA. John A. Blume Earthquake Engineering Center.

Sponsoring Organization: *National Science Foundation, Washington, DC.

Contract Nos: NSF-BCS-9058316

Supplemental Notes: Also pub. as Stanford Univ., CA. John A. Blume Earthquake Engineering Center rept. no. REPT-109.

NTIS Field/Group Codes: 89D (Structural Analyses), 46E (Structural Mechanics)

Price: PC A08/MF A02

Availability: Available from the National Technical Information Service, Springfield, VA. 22161

Number of Pages: 175p

Keywords: *Structural vibration, *Structural analysis, *Eigenvalues, *Nonlinear systems, Dynamic response, Earthquake engineering, Algorithms, Finite element method, Degrees of freedom, Matrices(Mathematics), Vibration mode, Vibration damping, Resonant frequency.

Abstract: Vibration analyses of structural systems are concerned with accurately predicting the natural frequencies and mode shapes of the vibrating system. This analysis process involves two general parts: the dynamic finite element model of the physical system and the numerical algorithm for determining the frequencies and mode shapes from the model. The finite element model establishes the number of equations of motion (degrees-of-freedom) needed to accurately define the behavior of the vibrating system, and the numerical algorithm extracts the frequencies and mode shapes of the system from the resulting eigenproblem. To optimize the effectiveness of a dynamic analysis procedure, both the finite element model and the eigensolution technique must be chosen such that the desired accuracy can be obtained with the most efficient use of computer resources.

VIBRATION ANALYSIS OF SKELETAL SYSTEMS USING A MIXED FORMULATION WITH AN ARNOLDI-BASED NONLINEAR EIGENSOLUTION TECHNIQUE

by

Rajesh K. Singh

and

H. Allison Smith

The John A. Blume Earthquake Engineering Center

Department of Civil Engineering

Stanford University

Stanford, CA 94305-4020

Report No. 109

December, 1993

Abstract

Vibration analyses of structural systems are concerned with accurately predicting the natural frequencies and mode shapes of the vibrating system. This analysis process involves two general parts: the dynamic finite element model of the physical system and the numerical algorithm for determining the frequencies and mode shapes from the model. The finite element model establishes the number of equations of motion (degrees-of-freedom) needed to accurately define the behavior of the vibrating system, and the numerical algorithm extracts the frequencies and mode shapes of the system from the resulting eigenproblem. To optimize the effectiveness of a dynamic analysis procedure, both the finite element model and the eigensolution technique must be chosen such that the desired accuracy can be obtained with the most efficient use of computer resources.

The research presented here is in four parts, addressing separate aspects of free vibration analysis. Part one of this study presents a frequency dependent finite element modeling procedure that is more accurate than the conventional finite element models, and a nonlinear eigensolver for determining the natural frequencies and mode shapes from finite element models. The new solution methodology is based upon the ability to evaluate a specific set of parameterized nonlinear eigenvalue curves through an implicitly restarted Lanczos technique. Numerical examples illustrate that this method coupled with a secant based zero finder accurately evaluates the exact natural frequencies and modes of the nonlinear eigenproblem and is more computationally

ii

efficient than the determinant search technique.

Part two presents a performance comparison of the frequency dependent mixed finite element formulation with the $h-$ and $p-$formulations of the conventional finite element method for free vibration analysis. Performance is evaluated through a detailed study of accuracy and computational efficiency in obtaining the natural frequencies and modes of skeletal systems. Additional studies compare the computational effectiveness of the mixed finite element formulation with the dynamic element method which involves use of a quadratic eigenvalue problem. Results show that for lower accuracy requirements, the $h-$formulation is more efficient than the $p-$formulation but this trend is reversed for higher accuracy requirements. When very high accuracy is needed, especially for higher-order modes, the mixed formulation is more computationally efficient than both the $h-$ and $p-$formulations.
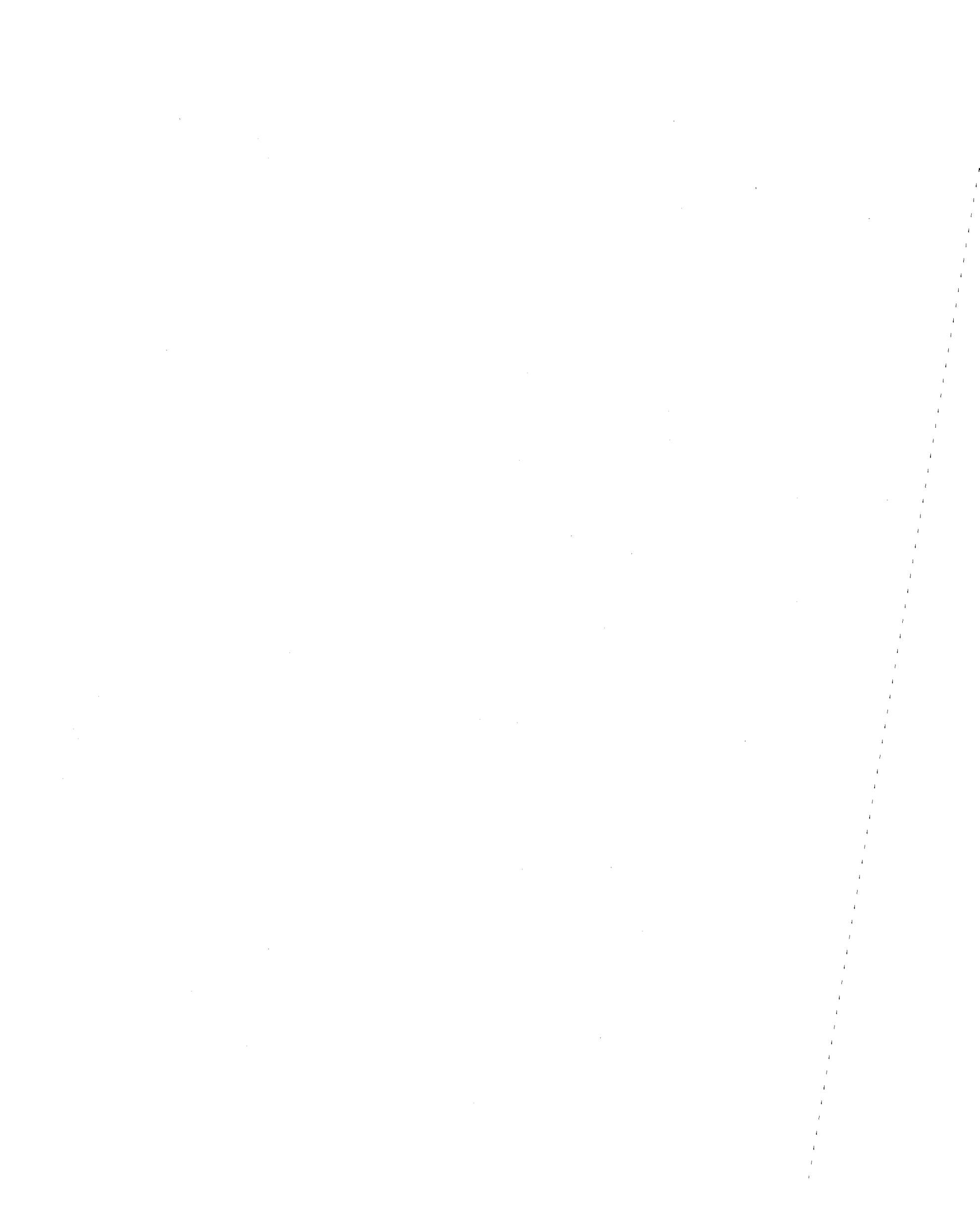
Part three formulates the interior eigenvalue problem that is used to extract frequencies higher than a specified shift. The eigensolver is modified to solve the nonpositive definite eigenproblem and to extract eigenvalues from the interior of the spectrum. A numerical example is presented to demonstrate the effectiveness of this method. It is also shown that beyond a threshold it is economical to solve the shifted eigenproblem despite the increased cost of factoring a nonpositive definite matrix.

The last part of this study extends the mixed finite element method to model nonclassically damped structures. A new form of frequency dependent damping matrix is presented that better models the nonhomogenous nature of the energy loss mechanisms in structures. The eigenproblem resulting from this model is unsymmetric; the $k-$step Arnoldi method with implicit restart is used to extract the complex frequencies and mode shapes without resorting to costly complex arithmetic.

Acknowledgements

Contents

Tables

Figures

Notation

a   vector of nodal degrees-of-freedom

a_0, a_1 coefficients of the cubic polynomial for the conventional formulation; nodal displacements

$\bar{a}_0, \bar{a}_1$ coefficients of the linear polynomial for the conventional formulation; nodal displacements

b parameter for exact solution to the axial vibration

$\bar{b}$ parameter for exact solution to the lateral vibration

b_0, b_1 coefficients of the 5th order polynomial for the P_1 formulation

$\bar{b}_0, \bar{b}_1$ coefficients of the 3rd order polynomial for the P_1 formulation

c $\cos \bar{b}l$

d vector of element continuous displacements

e_j jth coordinate vector of length j

$\mathbf{f}_j$ residual vector after j steps of the one-sided Lanczos iteration

h_{ij} elements of an upper Hessenberg matrix

$\mathbf{k}_p$ polynomial based stiffness matrix for axial vibrations

$\bar{\mathbf{k}}_p$ polynomial based stiffness matrix for lateral vibrations

l length of an element

m uniform mass distribution of an element

$\mathbf{m}_p$ polynomial based mass matrix for axial vibrations

$\bar{\mathbf{m}}_p$ polynomial based mass matrix for lateral vibrations

$\mathbf{m}_e$	frequency dependent mass matrix for axial vibrations
$\bar{\mathbf{m}}_e$	frequency dependent mass matrix for lateral vibrations
$\mathbf{p}_j$	left residual vector after j steps of the two-sided Lanczos iteration
$\mathbf{r}_j$	right residual vector after j steps of the two-sided Lanczos iteration
s	$\sin \bar{b}l$
u	axial displacement
u_e	exact axial displacement
$\tilde{u}$	finite element representation of the axial displacement
$\tilde{u}_p$	finite element representation of the axial displacement using the conventional formulation
v	lateral displacement
v_e	exact lateral displacement
$\tilde{v}$	finite element representation of the lateral displacement
$\tilde{v}_p$	finite element representation of the lateral displacement using the conventional formulation
$\mathbf{v}_j$	jth right Lanczos vector for the two-sided Lanczos iteration
$\mathbf{w}_j$	jth left Lanczos vector for the two sided Lanczos iteration
x	spanwise coordinate
$\mathbf{x}$	eigenvector and mode shape
$\hat{\mathbf{x}}$	complex eigenvector and mode shape
$\mathbf{y}$	eigenvector of the reduced tridiagonal system
A	area of cross-section of an element
$\mathbf{A}$	large, sparse, symmetric or unsymmetric matrix

$\mathbf{B}$	large, sparse, symmetric and positive definite matrix
C	$\cosh \bar{b}l$
C_1, C_2	constants of integration corresponding to the axial modes for the mixed formulation
$\tilde{C}_1, \tilde{C}_2$	constants of integration corresponding to the axial modes for the conventional formulation
$\bar{C}_1, \bar{C}_2$	constants of integration corresponding to the lateral modes for the mixed formulation
$\mathbf{C}$	damping matrix
$\mathbf{C}(\hat{\omega})$	frequency dependent damping matrix
$\mathbf{D}(\omega)$	dynamic stiffness matrix
$\mathbf{D}_a$	dynamic stiffness matrix for axial vibrations
$\mathbf{D}_f$	dynamic stiffness matrix for lateral vibrations
$\mathbf{D}(\mu)$	frequency dependent, complex symmetric matrix
$\mathbf{D}(\lambda)$	$[\mathbf{A} - \lambda \mathbf{B}(\lambda)]$, used in the determinant search method
$\hat{\mathbf{D}}$	diagonal part of the symmetric factorization of $\mathbf{D}(\lambda)$
E	Young's modulus of elasticity
$\mathbf{F}$	vector of element inertia forces
$\mathbf{F}(\lambda)$	frequency dependent matrix function
$\mathbf{H}$	upper Hessenberg matrix
$\mathbf{H}_j$	upper Hessenberg matrix after j steps of the Arnoldi iteration
I	moment of inertia of an element cross-section about z-axis
$\mathbf{I}$	identity matrix

$\mathbf{K}$	stiffness matrix
$\mathbf{K}_e$	mixed formulation stiffness matrix
$\mathbf{K}_0$	stiffness matrix based on the static displacement field
$\mathbf{K}_4, \mathbf{K}_8$	dynamic correction terms to the stiffness matrix
$\mathbf{K}(\lambda)$	frequency dependent stiffness matrix
$\hat{\mathbf{K}}$	$[\mathbf{K} - \sigma\mathbf{M}]$, the shifted stiffness matrix
$\mathbf{L}, \mathbf{L}^T$	lower and upper triangular parts of the the symmetric factorization of $\mathbf{D}(\lambda)$
$\mathbf{M}$	mass matrix
$\mathbf{M}_e$	mixed formulation frequency dependent mass matrix
$\mathbf{M}_0$	mass matrix based on the static displacement field
$\mathbf{M}_2, \mathbf{M}_4$	dynamic correction terms to the mass matrix
$\mathbf{M}(\lambda)$	λ—dependent mass matrix
$\mathbf{M}_0$	frequency independent part of the decomposed $\mathbf{M}(\lambda)$
$\mathbf{M}_1(\lambda)$	frequency dependent part of the decomposed $\mathbf{M}(\lambda)$
$\mathbf{N}$	shape function matrix
$\mathbf{N}(\omega)$	frequency dependent shape function matrix
$\mathbf{N}_0$	shape function matrix based on static displacement field
$\mathbf{N}_1(\omega), \mathbf{N}_2(\omega)$	dynamic corrections terms for the shape function matrix
$\mathbf{P}$	nodal force vector
S	$\sinh \bar{b}l$
$\mathbf{T}_j$	symmetric (unsymmetric) tridiagonal matrix after j steps of the one-sided (two-sided) Lanczos iteration

U	amplitude of the harmonic axial displacement
V	amplitude of the harmonic lateral displacement
$\mathbf{V}_j$	the set of right Lanczos vectors $\{\mathbf{v}_1, \mathbf{v}_2, \ldots, \mathbf{v}_j\}$
$\mathbf{W}_j$	the set of left Lanczos vectors $\{\mathbf{w}_1, \mathbf{w}_2, \ldots, \mathbf{w}_j\}$
α_j	jth diagonal of the tridiagonal matrix $\mathbf{T}_j$
α_n	nth root of equation $\quad 1 + \cos\alpha \cdot \cosh\alpha = 0$
β_j	jth subdiagonal of the tridiagonal matrix $\mathbf{T}_j$
γ_j	jth superdiagonal of the tridiagonal matrix $\mathbf{T}_j$
$\{\delta\}$	nodal displacement vector
η	spanwise nondimensional coordinate
θ	rotation about the z-axis
λ	eigenvalue for the undamped structure
$\hat{\lambda}$	eigenvalue for the nonproportionally damped structure
μ	reciprocal of the eigenvalue λ
$\hat{\mu}$	reciprocal of the complex eigenvalue $\hat{\lambda}$
ξ	modal damping
$\hat{\xi}$	pseudo modal damping
σ	shift frequency
ω	undamped natural frequency ($\omega^2 = \lambda$)
$\hat{\omega}$	pseudo undamped natural frequency ($\hat{\omega} = |\hat{\lambda}|$)

CHAPTER 1

Introduction

This chapter presents an introduction to modeling linear beam, frame and truss structures for undamped and damped free vibration analysis using the various finite element formulations. Section 1.2 is an introduction to finite elements models used for undamped free vibration analysis. Section 1.3 describes the damped free vibration problem, the associated quadratic eigenvalue problem and its transformation to state-space formulation. Eigensolution techniques typically used to solve the undamped and damped free vibration problems are presented in Section 1.4. This section also presents a brief summary of existing methods for solving frequency dependent (nonlinear) eigenvalue problems in structural dynamics, their disadvantages and the need for better, more efficient, and more robust eigensolvers that are scalable to large problems. Section 1.5 presents motivation for the current research and outlines its objectives. This chapter concludes with the outline for the remainder of this dissertation.

1.1 Problem Description

The first step in studying the vibrating behavior of structures subjected to seismic excitations, wind loading or other transient, dynamic loads is to derive a mathematical

model of the dynamical system. The differential equations of motion thus obtained describe the behavior of the physical system subject to modeling assumptions. These equations can be solved in closed form only for some structures with very simple geometry and boundary conditions. For a majority of analysis and design problems, these differential equations of motion are discretized in the space and/or time domain, using well established and thoroughly researched methodologies such as finite difference, finite element and boundary element methods. This research pertains to spatial discretization using the finite element method. Any such discretization has to accurately model the structural systems, and, in order to be useful to the engineer, must require a minimum of computational resources with results obtainable to a specified accuracy.

In analysis and design of structures subjected to dynamic loads, it is a common practice (often a necessity) to perform a free vibration analysis before performing a forced vibration analysis. Free vibration analyses of structural systems are concerned with accurately predicting the free vibration modes and frequencies of the vibrating system. This analysis process involves two general parts: the dynamic finite element model of the physical system and the numerical algorithm for determining the modal shapes and frequencies from the model. The finite element model establishes the number of equations of motion (degrees-of-freedom) needed to accurately define the behavior of the vibrating system, and the numerical algorithm extracts the vibration modes and frequencies of the system from the resulting eigenproblem. The effectiveness of a dynamic analysis procedure depends on careful selection of both the finite element model and the eigensolution technique.

1.2   Undamped Free Vibration Analysis

Accurate representation of the displacement field is the main consideration in developing an effective finite element representation of the dynamical system. The displacement field is used to derive the shape functions and, ultimately, element and system stiffness and mass matrices. Przemieniecki [39] showed that the shape function matrices derived from element displacement fields can be expressed by a series expression as a function of the natural frequency ω as follows

$$\mathbf{N}(\omega) = \mathbf{N}_0 + \omega\mathbf{N}_1 + \omega^2\mathbf{N}_2 + \cdots \tag{1.1}$$

where $\mathbf{N}(\omega)$ is the exact, frequency dependent shape function matrix based on the solution to the differential equation of motion for the continuous system, $\mathbf{N}_0$ is the shape function matrix based on the static displacement, and $\mathbf{N}_1, \mathbf{N}_2, \cdots$ are the shape function matrices representing the dynamic correction terms, and are obtained using a Taylor series expansion of the exact, frequency dependent shape function.

For skeletal systems, the stiffness and mass matrices derived using the shape functions of Eq. (1.1) can also be expressed by series expressions as a function of ω

$$\mathbf{K}(\omega) = \mathbf{K}_0 + \omega^4\mathbf{K}_4 + \omega^8\mathbf{K}_8 + \cdots$$
$$\mathbf{M}(\omega) = \mathbf{M}_0 + \omega^2\mathbf{M}_2 + \omega^4\mathbf{M}_4 + \cdots \tag{1.2}$$

where $\mathbf{K}(\omega)$ and $\mathbf{M}(\omega)$ are the exact, frequency dependent stiffness and mass matrices, $\mathbf{K}_0$ and $\mathbf{M}_0$ are the stiffness and mass matrices based on the element's static displacement field, and $\mathbf{K}_4, \mathbf{K}_{\varepsilon}, \cdots$, and $\mathbf{M}_2, \mathbf{M}_4, \cdots$, are the corresponding dynamic corrections terms. Note that the only nontrivial terms in $\mathbf{K}(\omega)$ and $\mathbf{M}(\omega)$ are of the

type ω^{4n} and ω^{2n}, respectively.

1.2.1 Conventional Finite Element Method

The conventional finite element model, which uses only the static displacement field to derive the element shape functions and system matrices, is equivalent to using only the first terms from each of the two series in Eqs. (1.1) and (1.2). The resulting eigenvalue problem is

$$\mathbf{Kx} = \lambda \mathbf{Mx} \tag{1.3}$$

where $\lambda = \omega^2$ (circular natural frequency squared) is the eigenvalue and $\mathbf{x}$ is the mode shape. After rigid body modes have been eliminated, both the stiffness and mass matrices in Eq. (1.3) are frequency independent, symmetric and positive definite.

Since the conventional model uses only the static displacement field to discretize the dynamic problem, the associated structural model is stiffer than the actual system. Consequently, the natural frequencies obtained from Eq. (1.3) are higher than the actual vibrating frequencies of the structure. Thus, the conventional finite element solution provides an upper bound to the exact natural frequencies, where the solution difference is referred to as discretization error. It should be noted that this error increases for higher modes. This formulation is further discussed in the following chapter in Section 2.3.

There are at least two basic parameters that can be varied to reduce the discretization error and improve the solution accuracy and convergence of the conventional finite element method: $h-$refinement, where the number of degrees-of-freedom used to model the system is increased by refining the finite element mesh parameter h; and

p—refinement, where the order of the polynomial defining the element displacement field is increased. As the mesh parameter h approaches zero, that is, as the number of degrees-of-freedom approaches infinity, all discretization error is avoided and exact solutions are obtained. However, as the number of degrees-of-freedom increases, so does the computational intensity. The discretization error can also be systematically reduced by increasing the order of the polynomial in the displacement field used to derive shape functions and element stiffness and mass matrices. Zienkewicz [73] has analyzed the situation when these parameters vary independently ($h \rightarrow 0$, $p \rightarrow \infty$) and has presented estimates for asymptotic reduction in the discretization error. The case where both these parameters are varied simultaneously is less understood in terms of error analysis. Details of three levels of the $h-$ and $p-$formulations and numerical examples to compare their relative accuracy and computational intensity are presented in Chapter 4.

Babuska [5, 6] has presented theoretical results that suggested that exponential rate of convergence can be achieved with an 'optimal' combination of variation of the h and p parameters for a special class of one-dimensional problems. Rachowicz, Oden and Demkowicz [40, 41] have presented an approximate technique to vary the h and p parameters simultaneously in some optimal sense. A systematic approach for optimally varying these parameters simultaneously with respect to a prespecified level of accuracy is not available. A practical implementation of the optimal h-p strategy poses very difficult requirements on meshing. Zienkiewicz [74, 75] has provided some heuristics while noting that no commercial or research finite element codes exist that are satisfactory.

1.2.2 The Exact Method

Another way to reduce the discretization error is to use the frequency correction terms in Eqs. (1.1) and (1.2); thus, effectively retaining all the terms in the series expansion. This results in a nonlinear eigenvalue problem

$$\mathbf{K}(\lambda)\mathbf{x} = \lambda\mathbf{M}(\lambda)\mathbf{x} \tag{1.4}$$

in which terms of both the stiffness and the mass matrices are transcendental functions of the eigenvalue parameter λ. Provided this eigenvalue problem can be solved, exact results would be obtained for the system frequencies and mode shapes with no inherent discretization error for prismatic members. The frequency dependence of both the system matrices means that at each (linearized) step of the eigenvalue analysis, reformulation and redecomposition of a full matrix is required. Kolousek first applied this method to dynamic analysis of frames [31, 32]. This method has been studied further by Williams and Wittrick [68, 69, 71, 67], Swannell [63, 62], Richards and Leung [43], Hallauer and Liu [26], and others [3, 2, 69]. While this method provides more accurate solutions than the conventional formulation, it can be very computationally intensive and impractical for large problems.

1.2.3 Dynamic Element Method

In an effort to circumvent the computational intensity of the exact method, Gupta [21, 22] formulated a dynamic element method that uses the correction terms up to ω^4.

The corresponding eigenvalue problem takes the form

$$\left[\mathbf{K}_0 - \omega^2\mathbf{M}_0 - \omega^4(\mathbf{M}_2 - \mathbf{K}_4)\right]\mathbf{x} = 0, \tag{1.5}$$

where $\mathbf{K}_0$ and $\mathbf{M}_0$ are the conventional stiffness and mass matrices, respectively, and $\mathbf{K}_4$ and $\mathbf{M}_2$ are the corresponding correction matrices [22].

In the dynamic stiffness formulation, force-displacement relationships are used to construct the dynamic stiffness matrix from dynamic displacement fields in a manner analogous to the construction of the static stiffness matrix using static displacement fields. The dynamic stiffness formulation has the form

$$[\mathbf{D}(\omega)]\,\{\delta\} = \mathbf{P} \tag{1.6}$$

where $\{\delta\}$ and $\mathbf{P}$ are the nodal displacement and nodal force vectors, respectively. For free vibration, a nontrivial displacement solution is sought for no prescribed loads ($\mathbf{P} \equiv 0$). This results in an 'implicit' eigenvalue problem

$$\mathbf{D}(\omega)\mathbf{x} = \mathbf{0} \tag{1.7}$$

where $\mathbf{D}(\omega)$ is the dynamic stiffness matrix. Swannell [62, 63] has presented free and forced vibration analysis procedures for skeletal elastic structures using the dynamic stiffness formulation. Paz [37, 38] established that the stiffness and mass matrices (as well as the geometric matrix used for buckling analysis) obtained from the static displacement considerations used in the conventional finite element analysis are the first order terms in the expansion of the dynamic stiffness matrix.

1.2.4   Mixed Finite Element Method

The mixed formulation developed by Melosh and Smith [34] and Smith [52, 53, 54] used both the exact and polynomial displacement fields in formulating the vibration eigenproblem. In this formulation, inertial forces are computed exactly using the frequency dependent shape functions, and an equivalent load theory is used to represent the exact element inertia forces at the element nodes. The resulting eigenvalue problem is

$$[\mathbf{K} - \lambda \mathbf{M}(\lambda)] \, \mathbf{x} = \mathbf{0} \tag{1.8}$$

where $\mathbf{K} \equiv \mathbf{K_0}$, thus only the mass matrix is a frequency dependent matrix. The iterative procedure to determine a few eigenvalues and eigenvectors of Eq. (1.8) requires repeated solution of a linear system involving one of the matrices and matrix vector products with the other matrix. These computations are arranged such that the solution to the linear system involves only the frequency independent stiffness matrix, and the matrix vector product computations involve the frequency dependent mass matrix. This turns out to be a very important advantage of the mixed formulation as it requires the stiffness matrix $\mathbf{K}$ to be factored only once throughout the entire eigenvalue computation, thus lessening the computational intensity considerably [55, 56]. The mixed formulation is discussed in detail in Section 2.4.

The mixed formulation utilizes the closed form solution to the governing partial differential equations of motion as a basis for frequency dependent shape functions. Therefore, modifications are necessary in cases where a closed form solution is not available even for the simplest geometry, such as free vibration of a plate or a membrane. However, both these problems have an infinite series solution and it is possible

to reduce discretization error by using additional terms from the series solution as a basis for the finite element shape functions. Gupta [23] has presented one such example for a square cantilevered plate.

1.3 Damped Free Vibration Problem

In dynamic analysis of linear structures subject to seismic excitations, it is generally assumed that the systems has either no damping or it is classically damped, meaning the damping matrix can be diagonalized by the eigenvectors of the undamped system. It should be noted, however, that in most real structures the energy dissipation mechanism is not homogeneous; thus, the modal equations are coupled by the damping term and cannot be diagonalized using the undamped mode shapes. Such structures are said to be non-proportionally or non-classically damped systems. The differential equation of motion for a damped structure is written as

$$\mathbf{M\ddot{v}} + \mathbf{C\dot{v}} + \mathbf{Kv} = \mathbf{p} \tag{1.9}$$

in which $\mathbf{v}$ and $\mathbf{p}$ are the displacement and force vectors, respectively, and $\mathbf{M}$, $\mathbf{C}$ and $\mathbf{K}$ are the system mass, damping and stiffness matrices, respectively. For free vibration, the damping matrix coupling in Eq. (1.9) results in a quadratic eigenvalue problem of the form

$$[\hat{\lambda}^2\mathbf{M} + \hat{\lambda}\mathbf{C} + \mathbf{K}]\hat{\mathbf{x}} = \mathbf{0}. \tag{1.10}$$

where $\hat{\lambda}$ is the complex frequency and $\hat{\mathbf{x}}$ is the complex mode shape.

Clough and Mojtahed [9] presented a procedure for evaluating earthquake response of non-proportionally damped structures using a variation of direct integration of Eq. (1.9) that is commonly used for the classically damped case. Warburton and Soni [66] developed a criterion to determine when the response calculated by proportional damping assumption is unacceptably large. Igusa et al. [29] developed a modal decomposition methodology for the non-proportionally damped systems and gave closed form solutions for the the case of response to a white noise. Singh and Ghafory-Ashtiany [49] used a complex-valued modal time history analysis to compute the forced vibration response. Damped free vibration using the mixed formulation is presented in Chapter 6.

1.4 Eigensolution Techniques

The eigenvalue problems associated with the finite element models described in Section 1.2 all have the basic form

$$\mathbf{Ax} = \lambda \mathbf{Bx} \tag{1.11}$$

where $\mathbf{A}$ and $\mathbf{B}$ are, in general, large, sparse, λ-dependent, unsymmetric matrices. Specific simplifications result for individual models: for example, for the conventional finite element (and its $h-$ and $p-$refinements), after rigid body modes have been eliminated, both $\mathbf{A}$ and $\mathbf{B}$ are frequency independent, symmetric and positive definite; for the mixed formulation, while $\mathbf{A}$ is frequency independent, symmetric and positive definite, $\mathbf{B} = \mathbf{B}(\lambda)$ is frequency dependent and symmetric but not necessarily positive at arbitrary λ. However, from energy considerations, it is inferred that $\mathbf{B}(\lambda)$ is positive definite in the neighborhood of an admissible solution.

Wilkinson [70] and Parlett [36] have extensively discussed the various mathematical properties of the generalized and symmetric eigenvalue problems, respectively. See Golub and van Loan [16] for a detailed overview of various numerical techniques used to solve the symmetric and unsymmetric eigenvalue problems.

1.4.1 Linear, Symmetric Eigenproblem

The Jacobi method (circa. 1850) for the symmetric eigenvalue problem is perhaps the earliest algorithm to solve an eigenvalue problem. In this method, the 'norm' of the off-diagonal terms are systematically reduced by applying a set of Jacobi rotations. For computing only a few extreme eigenvalues, power methods are often used; in structural dynamics applications, the lowest eigenvalue (first natural frequency) is of importance and inverse power methods are used. Mathematical properties and convergence analysis of this and other related methods like QR and LR are discussed in detail in the above mentioned books by Wilkinson and Parlett and Golub and van Loan.

For a real symmetric $n \times n$ matrix $\mathbf{A}$ there is the very well recognized form of the one-sided Lanczos recursion that generates a set of column vector which form an orthogonal basis for the Krylov subspace $\{\mathbf{v}_1, \mathbf{A}\mathbf{v}_1, \mathbf{A}^2\mathbf{v}_1, \ldots, \mathbf{A}^{j-1}\mathbf{v}_1\}$. Thus, for $j = 1, 2, \ldots, m$

$$\beta_{j+1}\mathbf{v}_{j+1} = \mathbf{A}\mathbf{v}_j - \alpha_j\mathbf{v}_j - \beta_j\mathbf{v}_{j-1} \equiv \mathbf{f}_j \qquad (1.12)$$

where $\alpha_j = \mathbf{v}_j^T(\mathbf{A}\mathbf{v}_j - \beta_j\mathbf{v}_{j-1})$ and $\beta_{j+1} = \|\mathbf{f}_j\|$. The iteration is started with a randomly generated vector $\mathbf{v}_1$. The recursion in Eq. (1.12) maps a real symmetric

matrix **A** into a set of real symmetric, tridiagonal matrices

$$\mathbf{T}_j = \begin{bmatrix} \alpha_1 & \beta_2 & & & & \\ \beta_2 & \alpha_2 & \beta_3 & & & \\ & \beta_3 & \ddots & \ddots & & \\ & & & \ddots & \ddots & \beta_j \\ & & & & \beta_j & \alpha_j \end{bmatrix} \tag{1.13}$$

such that eigenvalues and eigenvectors **A** can be computed by solving for eigenvalues and eigenvectors of the reduced system. For the generalized eigenvalue problem

$$\mathbf{Ax} = \lambda \mathbf{B}(\lambda)\mathbf{x} \tag{1.14}$$

the matrix **A** in the above formulation can be replaced by $(\mathbf{A}^{-1} \cdot \mathbf{B}(\lambda))$. Since only matrix vector products of the form $\mathbf{w} \leftarrow (\mathbf{A}^{-1} \cdot \mathbf{B}(\lambda))\mathbf{x}$ are required, the matrix **A** is never inverted.

The above form of the Lanczos algorithm has been used extensively to solve large, sparse symmetric eigenvalue problems in structural dynamics. The Lanczos process may be viewed as a truncation of the complete reduction to tridiagonal form. Typically the extreme eigenvalues appear well before the reduction of matrix **A** is complete, making this method especially suitable for engineering applications where only a few extreme eigenvalues are required. Some of its main drawbacks are loss of orthogonality among the basis vectors and appearance of spurious eigenvalues. Various schemes have been proposed to overcome these problems ranging from recognizing and casting out spurious eigenvalues to selective re-orthogonalization techniques [12, 35, 36].

Block versions of the basic Lanczos recursion have been used by Gupta [23] to solve the quadratic eigenvalue problem of Eq. (1.5) associated with the dynamic finite element formulation. Cullum and co-workers [10, 11, 12, 13] investigated generalized non-symmetric Lanczos procedures for large, sparse problems. Rajkumar and Rogers [42] presented a two-sided Lanczos recursion to the unsymmetric generalized eigenvalue problem in which the recursion is performed in real arithmetic while complex arithmetic is employed only in the QR step of the transformed eigenvalue problem.

1.4.2 Nonlinear, Symmetric Eigenproblem

The eigensolution techniques mentioned in the previous section for the case when both matrices **A** and **B** are frequency independent can also be used for the frequency dependent case as the 'inner iteration' in which the nonlinear problem is solved via successive linear problems. A zero finding technique can be coupled with the linear eigensolver to function as the 'outer iteration.'

A number of researchers have presented alternate ways to solve the eigenvalue problem associated with the exact and mixed finite element formulations and the dynamic stiffness formulation. Simpson [46] presented a Newtonian procedure ro solve for eigenvalues and eigenvectors for the $\mathbf{D}(\omega)\mathbf{x} = \mathbf{0}$ formulation. An eigenvalue analysis method for large structures by component synthesis was also developed by Simpson and Tabarrok [47]. In this method, the structure is torn apart into conveniently sized subsystems whose receptance matrices are then obtained in series form by solving the subsystem eigenvalue problems [48]. Williams and Wittrick [68, 71, 67], and Williams and Kennedy [69] have presented a determinant search technique that is applicable to both the eigenvalue dependent and eigenvalue independent problems.

This method starts with a guess for the parameter λ, say λ^0, followed by the factorization of $[\mathbf{A}(\lambda^0) - \lambda^0\mathbf{B}(\lambda^0]$. The sign count (inertia) of the factored matrix as well as the value of the determinant $\det|[\mathbf{A}(\lambda^0) - \lambda^0\mathbf{B}(\lambda^0)]|$ are considered to improve the starting guess using an iteration technique such as bisection or quadratic interpolation. Gupta [24, 25] has presented a variation of the determinant search method in which the determinant search technique is used until all the eigenvalues of interest have been uniquely bounded. Afterwards, an inverse power iteration or Rayleigh quotient inverse iteration is used to converge to the desired eigenvalue.

1.4.3 Unsymmetric Eigenproblem

As discussed previously in Section 1.3, the damped free vibration analysis requires solving an eigenvalue problem of the form

$$[\hat{\lambda}^2\mathbf{M} + \hat{\lambda}\mathbf{C} + \mathbf{K}]\hat{\mathbf{x}} = \mathbf{0} \tag{1.15}$$

which is quadratic in $\hat{\lambda}$. Likewise, Gupta's dynamic element method results in a quadratic eigenvalue problem even for the undamped problem.

$$\left[\mathbf{K}_0 - \omega^2\mathbf{M}_0 - \omega^4(\mathbf{M}_2 - \mathbf{K}_4)\right]\mathbf{x} = \mathbf{0} \tag{1.16}$$

In both of these formulations, the mass matrices $\mathbf{M}$, $\mathbf{M}_0$ and $\mathbf{M}_2$ and stiffness matrices $\mathbf{K}$, $\mathbf{K}_0$ and $\mathbf{K}_4$ are real, symmetric and positive definite; the damping matrix $\mathbf{C}$ is symmetric, but not positive definite. (If any part of the structure is spinning, the Coriolis force may be significant and the damping matrix may not even be symmetric; however, this problem is not addressed in the present work.) Frequency ω is real

while the damped eigenvalue λ is, in general, complex. For computational purposes, Eqs. (1.15) and (1.16) can be represented as

$$\mathbf{Ax} + \mu\mathbf{Bx} + \mu^2\mathbf{Cx} = \mathbf{0} \tag{1.17}$$

One way to solve Eq. (1.17) is to group the matrices $\mathbf{B}$ and $\mathbf{C}$ together into a μ–dependent matrix such that

$$\mathbf{D}(\mu) = (-\mathbf{B} - \mu\mathbf{C}) $$

and rewriting Eq. (1.17) as

$$\mathbf{Ax} = \mu\mathbf{D}(\mu)\mathbf{x} \tag{1.18}$$

In this formulation, matrices $\mathbf{A}$ and $\mathbf{D}$ are still symmetric, but the latter is complex valued. Furthermore, eigenvalues μ and eigenvectors $\mathbf{x}$ are complex as well. Thus, if the solutions methods discussed in Section 1.4.2 are to be employed, all the arithmetic will have to be done in complex form, which increases computational intensity significantly. In addition, the zero finding techniques are more difficult to safeguard in the complex domain.

Another way to reduce the quadratic eigenvalue problem into a standard form is to use state-space type transformations. This technique transforms a quadratic eigenvalue problem of size N into an equivalent linear, possibly unsymmetric, eigenvalue of size $2N$. This problem can be solved using the two-sided Lanczos method which is a generalization of the Lanczos method for symmetric problems. This method has been used for both the standard and generalized unsymmetric problems [70, 13, 42].

Given an $n \times n$ unsymmetric matrix $\mathbf{A}$ and two arbitrarily chosen vectors $\mathbf{v}_1$ and $\mathbf{w}_1$ such that $\mathbf{w}_1^T \mathbf{v}_1 = 1$, two sets of Lanczos vectors $\mathbf{V}_j = \{\mathbf{v}_1, \mathbf{v}_2, \ldots, \mathbf{v}_j\}$ and $\mathbf{W}_j = \{\mathbf{w}_1, \mathbf{w}_2, \ldots, \mathbf{w}_j\}$ are generated from the right and left Krylov sequence of vectors given by $\{\mathbf{v}_1, \mathbf{A}\mathbf{v}_1, \mathbf{A}^2\mathbf{v}_1, \ldots, \mathbf{A}^{j-1}\mathbf{v}_1\}$ and $\{\mathbf{w}_1, (\mathbf{A}^T)\mathbf{w}_1, (\mathbf{A}^T)^2\mathbf{w}_1, \ldots, (\mathbf{A}^T)^{j-1}\mathbf{w}_1\}$, respectively. Together the two sets of Lanczos vectors form the biorthonormal bases for subspaces onto which the given matrix $\mathbf{A}$ is projected. These vectors are generated using the following recursive equations

$$
\begin{aligned}
\beta_{j+1}\mathbf{v}_{j+1} &= \mathbf{A}\mathbf{v}_j - \alpha_j\mathbf{v}_j - \gamma_j\mathbf{v}_{j-1} \equiv \mathbf{r}_j \\
\gamma_{j+1}\mathbf{w}_{j+1} &= \mathbf{A}^T\mathbf{w}_j - \alpha_j\mathbf{w}_j - \beta_j\mathbf{w}_{j-1} \equiv \mathbf{p}_j
\end{aligned}
\tag{1.19}
$$

for $j = 1, 2, \ldots, n$. Note that $\gamma_1\mathbf{v}_0 \equiv \beta_{n+1}\mathbf{v}_{n+1} = 0$ and $\beta_1\mathbf{w}_0 \equiv \gamma_{n+1}\mathbf{w}_{n+1} = 0$. The biorthonormality of the left and right Lanczos vectors implies that the scalars α_j, β_j and γ_j are given by

$$
\alpha_j = \mathbf{w}_j^T\mathbf{A}\mathbf{v}_j, \quad \mathbf{v}_j^T\mathbf{w}_j = 1 \quad \text{and} \quad \beta_{j+1}\gamma_{j+1} = \mathbf{r}_j^T\mathbf{p}_j
\tag{1.20}
$$

This process transforms $\mathbf{A}$ into a set of real unsymmetric, tridiagonal matrices

$$
\mathbf{T}_j =
\begin{bmatrix}
\alpha_1 & \gamma_2 & & & \\
\beta_2 & \alpha_2 & \gamma_3 & & \\
& \beta_3 & \ddots & \ddots & \\
& & \ddots & \ddots & \gamma_j \\
& & & \beta_j & \alpha_j
\end{bmatrix}
\tag{1.21}
$$

The j complex eigenvalues of the unsymmetric tridiagonal matrix $\mathbf{T}_j$ approximate j

eigenvalues of the matrix $\mathbf{A}$ at one end of spectrum. However, unlike the symmetric Lanczos recursion, the two-sided Lanczos recursion is an oblique projection and the convergence properties of $\lambda(\mathbf{T}_j)$ are poorer than that of the symmetric case.

The two-sided Lanczos recursion also suffers from some of the drawbacks of the symmetric Lanczos, such as loss of biorthonormality among the left and right Lanczos vectors and severe ill-conditioning of $\mathbf{V}$ and $\mathbf{W}$. More importantly, the two-sided Lanczos suffers from a more severe drawback: the entire recursion process needs to be halted if $\mathbf{r}_j^T \mathbf{p}_j = 0$ for some j. In such an event, the entire process is restarted with a new set of $\mathbf{v}_1$ and $\mathbf{w}_1$.

Another projection-type of method for unsymmetric eigenvalues is the Arnoldi method. It can be considered as an extension of the one-sided symmetric Lanczos recursion to an unsymmetric matrix $\mathbf{A}$. A set of Arnoldi vectors $\mathbf{V}_j = \{\mathbf{v}_1, \mathbf{v}_2, \dots, \mathbf{v}_j\}$ are generated that are the basis for the right Krylov subspace $\{\mathbf{v}_1, \mathbf{A}\mathbf{v}_1, \dots, \mathbf{A}^{j-1}\mathbf{v}_1\}$ associated with the matrix $\mathbf{A}$ and the initial random starting vector $\mathbf{v}_1$. The Arnoldi vectors are generated using the following recursion

$$\mathbf{v}_{j+1} h_{j+1,j} = \mathbf{A}\mathbf{v}_j - \sum_{i=1}^{j} h_{ij}\mathbf{v}_i \equiv \mathbf{f}_j \tag{1.22}$$

where $h_{ij} = \mathbf{v}_i^T \mathbf{A}\mathbf{v}_j$ and $h_{j+1,j} = \|\mathbf{f}_j\|$. Theoretically, each new Arnoldi vector $\mathbf{v}_{j+1}$ is orthogonal to the set of all the preceding Arnoldi vectors $\mathbf{V}_j$.

This process transforms $\mathbf{A}$ into a set of real upper Hessenberg matrices

$$
\mathbf{H}_j \;=\; \begin{bmatrix} h_{11} & h_{12} & \cdots & \cdots & & h_{1j} \\ h_{21} & h_{22} & h_{23} & \cdots & & h_{2j} \\ & h_{32} & \ddots & \ddots & & \vdots \\ & & \ddots & \ddots & & h_{(j-1),j} \\ & & & h_{j,(j-1)} & & h_{j,j} \end{bmatrix} \tag{1.23}
$$

The eigenvalues of the reduced matrices $\mathbf{H}_j$ approximate part of the spectrum of the eigenvalues of $\mathbf{A}$. Sorensen has presented an implicitly restarted $k-$step Arnoldi method to overcome the loss of orthogonality among the Arnoldi vectors associated with the above recursion scheme of Eq. (1.22). The residual vector $\mathbf{f}_j$ is recognized as a function of the starting vector $\mathbf{v}_1$ and an attempt is made to iteratively update $\mathbf{v}_1$ in such way as to force the residual vector $\mathbf{f}_j = f(\mathbf{v}_1)$ to zero. The total number of Arnoldi steps is limited to a fixed prescribed value k, usually two to three times the number of eigenvalues desired. This fixes and limits the total storage requirements.

By virtue of the fixed small number of Arnoldi vectors, it is computationally feasible to maintain full numerical orthogonality among the basis vectors. Typically one step of iterative refinement of the residual vector $\mathbf{f}_j$, at a very minimal cost, is sufficient to enforce orthogonality among the Arnoldi vectors. A set of polynomial filters are constructed and applied implicitly to cast out unwanted portions of the spectrum of eigenvalues of $\mathbf{A}$. The complete details of this process and construction leading to the proof of convergence are presented in Sorensen [58]. Application of this technique to compute complex frequencies and mode shapes for damped free vibration is presented in Chapter 6.

1.4.4   Interior Eigenproblem

In engineering analysis and design, usually only the first few eigenvalues are of interest. The solution methods outlined above are designed to take this into consideration. For example, in computing the forced response of a structure subject to seismic loading, usually only the first few modes participate in the response. However, there are many situations when there is a need to accurately solve for some set of eigenvalues that lie in the interior of the spectrum. A common application is to determine if any of the higher-order modes of a building are close to some vibrating machinery that might be inside the building, so as to avoid any possibility of resonance.

For the eigenvalue problem of the conventional finite element, a shift and invert strategy is used that transforms the eigenvalues from the interior of the spectrum to the ends of the spectrum. Specifically, for some prespecified shift σ

$$\mu \mathbf{x} = [\mathbf{K} - \sigma \mathbf{M}]^{-1} \mathbf{M} \mathbf{x} \tag{1.24}$$

where $\mu = \dfrac{1}{(\lambda - \sigma)}$. As a result of this transformation, eigenvalues λ from the interior that are in the vicinity of the shift σ are the new extreme eigenvalues in the μ spectrum. It should be noted that in the above formulation, matrix inverse is used only symbolically. In the actual implementation, a banded *LU* factorization of the matrix $[\mathbf{K} - \sigma \mathbf{M}]$ is used to solve linear system.

For the eigenvalue problem of the mixed formulation, the mass matrix is eigenvalue dependent. This necessitates an *LU* factorization of the matrix $[\mathbf{K} - \sigma \mathbf{M}(\lambda)]$ at each iteration of the solution procedure. Thus, the simple shift and invert method is computationally very intensive and inefficient for the frequency dependent case.

One way to overcome this difficulty is to decompose $\mathbf{M}(\lambda)$ into $\lambda-$independent and $\lambda-$dependent parts. Chapter 5 discusses constraints that must be imposed on any such decompositions in order to make the algorithm convergent. In this research, a decompositions of the following form for $\lambda_0 = 0$ and $\lambda_0 = \sigma$ are used.

$$\mathbf{M}(\lambda) = \mathbf{M}(\lambda_0) + \mathbf{M}_1(\lambda) \qquad (1.25)$$

1.5 Scope and Outline of Current Research

The goal of this research has been to develop an eigensolution technique that can be used for structural dynamics problems, specifically, the nonlinear eigenvalue problems associated with the free vibration analysis of trusses and frames using the mixed formulation introduced in Section 1.2, and to present a performance comparison of the mixed finite element formulation and the conventional finite element formulation with its $h-$ and $p-$refinements. Furthermore, it is desired to extend the development and implementation of the nonlinear eigensolution technique to solve the eigenvalue problem for damped free vibration analysis. This problem is quadratic, with a state-space transformation which yields a linear, but unsymmetric eigenvalue problem. Lastly, the nonlinear eigensolution technique is modified to solve for eigenvalues in the interior of the spectrum.

This dissertation is organized in seven chapters. The following chapter formulates the governing differential equations of motion for a two-dimensional Bernoulli-Euler beam. Chapter 2 also presents the spatial discretization of these equations of motion for free vibration analysis. A power series expansion is used to show the equivalence

between the eigenproblems of the mixed formulation and the dynamic stiffness method for axial vibration.

Chapter 3 presents the implicitly restarted Lanczos technique and a secant procedure that is used as the 'outer iteration' for the nonlinear eigenvalue problem. Brief details of the determinant search method are also presented here. Chapter 4 is a performance comparison study of the conventional formulation, its $h-$ and $p-$refinements and the mixed formulation. Chapters 5 and 6 describe the extension of the implicitly restarted eigensolution technique to solve the interior eigenvalue problem and damped free vibration problem, respectively. Numerical examples are presented at the end of each of Chapters 3, 4, 5 and 6. Chapter 7 presents the overall summary for this research.

The first seven chapters are supplemented by two appendices. Appendix A lists the displacement fields, shape functions and stiffness and mass matrices for all the two-dimensional finite element formulations used in this research for axial and lateral vibrations of Bernoulli-Euler beam. Appendix B shows equivalence using a series expansion between the eigenproblems of the mixed finite element formulation and the dynamic stiffness formulation for lateral vibrations.

CHAPTER 2

Dynamics of Continuous Systems

This chapter describes the continuous form of the governing partial differential equations of motion for free vibration analysis of trusses, beams and frames. In Sections 2.2–4, these equations are first decomposed into two ordinary differential equations in the space and time domains using separation of variables. The ordinary differential equation in space domain is transformed to the Galerkin form using approximate, finite element displacement fields; this discretization leads to the matrix form of the governing equations. For undamped, free vibrations these equations lead to the generalized eigenvalue problem of the form $\mathbf{Ax} = \lambda \mathbf{Bx}$. In Section 2.5 equivalence between eigenproblems of the dynamic stiffness matrix and the mixed finite element formulation is established using a series expansion in powers of ω.

2.1 Governing Equations

The governing equations for free vibration of a two-dimensional, undamped, linear, elastic, Bernoulli-Euler beam element with uniform properties can be obtained by establishing the dynamic equilibrium of a differential element dx of the beam, as shown in Figure (2.1). As shown in the figure, axial deformation occurs along the beam's x-axis and is indicated by u. Lateral vibration in the y-direction and rotation

(a)

(b)

(c)
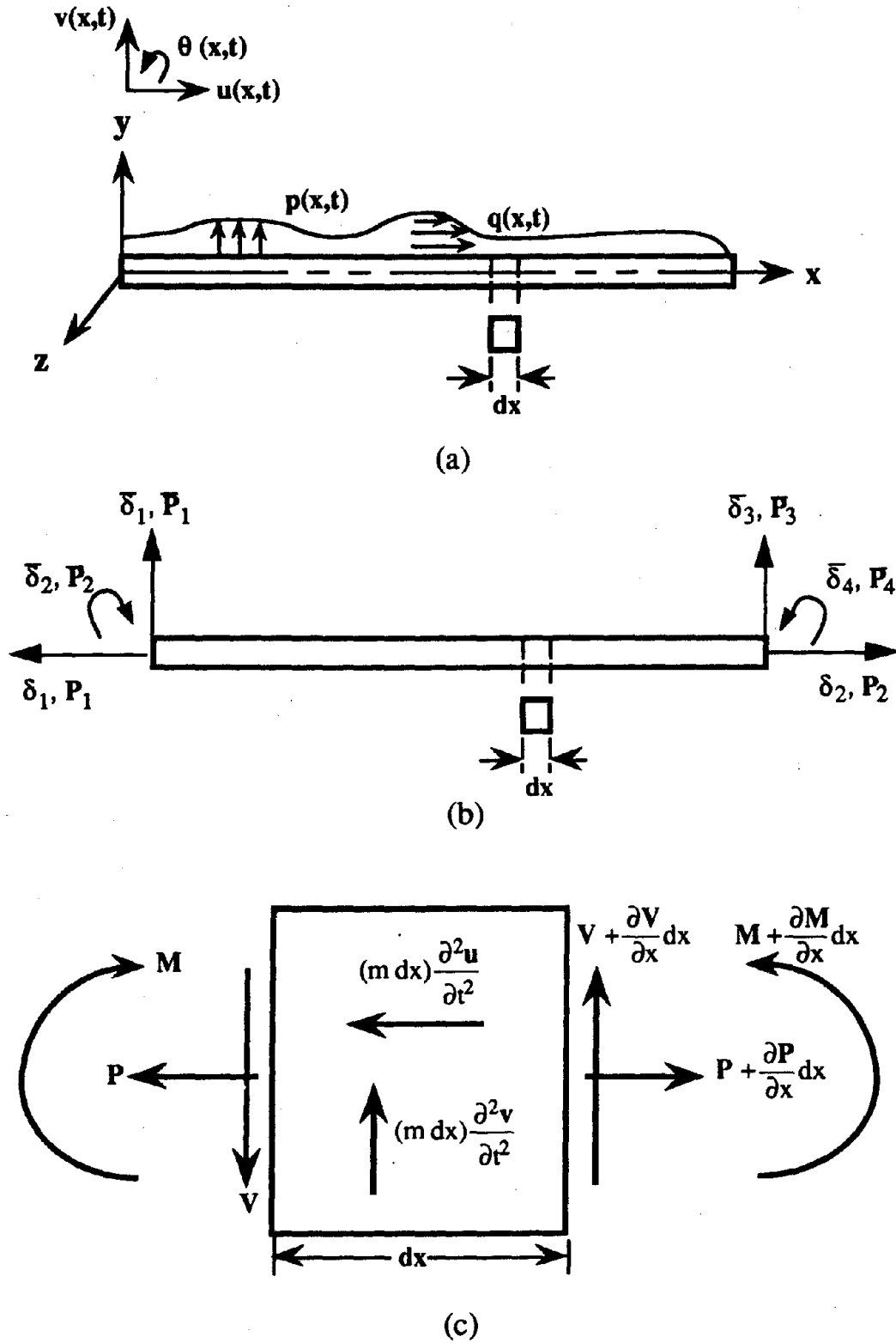
Figure 2.1: Axial and lateral vibrations of a Bernoulli-Euler beam

about the z-axis are indicated by v and θ, respectively. The equilibrium equations are found in the horizontal direction for axial vibration and in the vertical direction for lateral vibration. It is assumed that the axial and lateral vibration behaviors are independent and that no coupling takes place between u and v. Using Hooke's law and elementary beam theory, the equations governing axial and lateral vibration take the following form

$$\frac{\partial^2 u}{\partial x^2} - \frac{m}{EA}\frac{\partial^2 u}{\partial t^2} = 0 \tag{2.1}$$

$$\frac{\partial^4 v}{\partial x^4} + \frac{m}{EI}\frac{\partial^2 v}{\partial t^2} = 0 \tag{2.2}$$

where A is the cross-sectional area of the beam, m is the uniform mass distribution, E is the material modulus of elasticity, and I is the beam moment of inertia about the z-axis. It is quite easy to show that partial differential Eqs. (2.1) and (2.2) possess nontrivial solutions only if the quantities $\frac{m}{EA}$ and $\frac{m}{EI}$ are positive, which is indeed the case for structural dynamics.

For the axial vibration problem, solution of the form $u(x,t) = U(x)\sin\omega t$ will result in a harmonic motion of amplitude

$$U(x) = C_1 \cos bx + C_2 \sin bx \tag{2.3}$$

where

$$b = \sqrt{\frac{m\omega^2}{EA}} \tag{2.4}$$

and C_1 and C_2 are constants of integration.

To obtain the dynamic matrix for this problem, the following boundary conditions

are imposed

$$U(0) = \delta_1, \qquad U(l) = \delta_2$$
$$U'(0) = -\frac{P_1}{EA}, \quad U'(l) = \frac{P_2}{EA} \tag{2.5}$$

where δ_1 and δ_2 are the displacements and P_1 and P_2 are the forces, respectively, at the nodal coordinates of the beam segment as shown in Figure (2.1).

By substituting the boundary conditions of Eq. (2.5) into Eq. (2.3), solving for constants of integration, and simplifying the resulting expression, the dynamic matrix for an axially vibrating beam segment is obtained. Thus,

$$\left\{ \begin{array}{c} P_1 \\ P_2 \end{array} \right\} = EAb \left[\begin{array}{cc} \cot bl & -\csc bl \\ -\csc bl & \cot bl \end{array} \right] \left\{ \begin{array}{c} \delta_1 \\ \delta_2 \end{array} \right\} \tag{2.6}$$

subject to the condition that $\sin bl \neq 0$. The square matrix on the right hand side of Eq. (2.6) is the dynamic matrix for axial vibrations, $\mathbf{D}_a(\omega)$.

In a similar fashion, for lateral vibrations, $v(x,t) = V(x)\sin \omega t$ results in a harmonic motion of amplitude

$$V(x) = \bar{C}_1 \cos \bar{b}x + \bar{C}_2 \sin \bar{b}x + \bar{C}_3 \cosh \bar{b}x + \bar{C}_4 \sinh \bar{b} \tag{2.7}$$

where

$$\bar{b} = \left(\frac{m\omega^2}{EI} \right)^{\frac{1}{4}} \tag{2.8}$$

and $\bar{C}_1$, $\bar{C}_2$, $\bar{C}_3$ and $\bar{C}_4$ are constants of integration. To obtain the dynamic coefficients for the beam segment, displacement and force boundary conditions are imposed. The displacement boundary conditions take the form

$$V(0) = \bar{\delta}_1, \quad V(l) = \bar{\delta}_3$$

$$V'(0) = \bar{\delta}_2, \quad V'(l) = \bar{\delta}_4$$

(2.9)

and the force boundary conditions take the form

$$V'''(0) = \frac{\bar{P}_1}{EI}, \quad V'''(l) = -\frac{\bar{P}_3}{EI}$$

$$V''(0) = \frac{\bar{P}_2}{EI}, \quad V''(l) = -\frac{\bar{P}_4}{EI}$$

(2.10)

with $\bar{\delta}_1$, $\bar{\delta}_2$, $\bar{\delta}_3$ and $\bar{\delta}_4$ representing the amplitudes at the nodal coordinates and $\bar{P}_1$, $\bar{P}_2$, $\bar{P}_3$ and $\bar{P}_4$ representing the corresponding harmonic forces and moments.

Combining Eqs. (2.7), (2.9) and (2.10) in a manner analogous to the formulation of Eq. (2.6) and simplifying results in

$$\left\{ \begin{array}{c} \bar{P}_1 \\ \bar{P}_2 \\ \bar{P}_3 \\ \bar{P}_4 \end{array} \right\} = B \begin{bmatrix} \bar{b}^2(cS + sC) & & symmetric & \\ \bar{b}sS & (sC - cS) & & \\ -\bar{b}^2(s + S) & \bar{b}(c - C) & \bar{b}^2(cS + sC) & \\ -\bar{b}(c - C) & (S - s) & -\bar{b}sS & (sC - cS) \end{bmatrix} \left\{ \begin{array}{c} \bar{\delta}_1 \\ \bar{\delta}_2 \\ \bar{\delta}_3 \\ \bar{\delta}_4 \end{array} \right\}$$

(2.11)

where,

$$B = \frac{\bar{b}EI}{(1 - \cos \bar{b}l \cosh \bar{b}l)}$$

$$s = \sin \bar{b}l, \qquad S = \sinh \bar{b}l$$

$$c = \cos \bar{b}l, \qquad C = \cosh \bar{b}l$$

subject to the condition that $(1 - \cos \bar{b}l \cosh \bar{b}l) \neq 0$. The square matrix on the right

hand side of Eq. (2.11) is the dynamic matrix for flexural vibrations, $\bar{\mathbf{D}}_f(\omega)$.

2.2 Finite Element Models

In the finite element method, the element displacement field represents the solution to that element's differential equation of motion. Since the element displacement field is used to derive the shape function matrices from which the system matrices of the vibration eigenproblem are formed, the choice of this field plays a crucial role in both solution accuracy and efficiency.

There are three classes of finite element models which are capable of discretizing a structural system for dynamic analysis: the conventional finite element model, the exact displacement model, and a mixed model proposed by Melosh and Smith [34]. These models can be distinguished by the shape function utilized by the model.

As discussed in Chapter 1, shape function matrices are derived from element displacement fields and can be expressed through series expressions in ascending powers of ω, the natural circular frequency of the system [39]. Equation (1.1), repeated here for completeness, takes the form

$$\mathbf{N}(\omega) = \mathbf{N}_0 + \omega\mathbf{N}_1 + \omega^2\mathbf{N}_2 + \omega^3\mathbf{N}_3 + \cdots \tag{2.12}$$

where $\mathbf{N}(\omega)$ is the exact, frequency dependent shape function matrix based on the solution to the differential equation of motion; $\mathbf{N}_0$ is the shape function matrix based on the static displacement field; and $\mathbf{N}_1, \mathbf{N}_2, \ldots$ are the shape function matrices representing the dynamic corrections. Derivation of the dynamic correction terms for the shape function, stiffness, and mass matrices can be found in Przemieniecki [39]

and Zienkiewicz [73].

The eigenproblem resulting from the exact modeling formulation is eigenvalue dependent in the sense that the eigenproblem matrices are dependent on the natural frequencies of the system. Therefore, although fewer degrees-of-freedom are associated with the exact displacement model than with the conventional finite element model, the re-formation and re-decomposition of the matrices for each iteration of the eigenvalue analysis cause the exact model to be computationally intensive. This eigenvalue-dependent eigenproblem takes the form

$$[\mathbf{K}(\lambda) - \omega^2 \mathbf{M}(\lambda)]\mathbf{x} = \mathbf{0}. \tag{2.13}$$

Kolousek [31, 32] was the first to apply the exact displacement model to dynamic analysis of frames. This problem has been studied by Przemieniecki [39], Williams and Wittrick [68, 69, 71, 67], Swannell [63, 62], Richards and Leung [43], Hallauer and Liu [26], and others [3, 2, 69]. Bergman and McFarland [7] studied the differential equation of motion for continuous vibrating beams, but formulated the corresponding eigenvalue problem using Green's function.

Williams and Wittrick's formulation [67, 71] used Green's functions to discretize the governing differential equations; they solved the resulting nonlinear eigenvalue problem by successive determinant evaluation and interval halving. Yang [72] used a Jacobi-type method to solve a nonlinear eigenvalue problem in which the nonlinear terms are second order polynomials. However, neither of these two methods are suitable for the nonlinear eigenproblem associated with the mixed formulation due to the transcendental nature of frequency dependent shape functions, and computational

complexity of large problems, particularly when higher modes are desired.

The mixed model discussed by Melosh and Smith [34] uses both the exact and polynomial displacement fields in formulating the vibration eigenproblem [52, 53, 54]. This formulation is based on exact representation of element inertia forces and obtains exact natural modes and frequencies of vibrating systems.

The element inertia forces are found by taking the derivative of the element external work expression with respect to each degree-of-freedom. The external work expression for an element of uniform cross-section takes the form

$$W = \int_0^L \mathbf{d}^T \mathbf{F} dx \tag{2.14}$$

where W is the element external work, $\mathbf{d}$ is the vector of continuous element axial, lateral or rotational displacements and $\mathbf{F}$ is the vector of element inertia forces. The element inertia forces can be expressed as $\mathbf{F} = -m\ddot{\mathbf{d}}$ (where m is the uniform mass distribution over the element). Assuming harmonic motion, $\ddot{\mathbf{d}} = -\omega^2 \mathbf{d}$, the above equation becomes $\mathbf{F} = \omega^2 m\mathbf{d}$. Introducing the exact shape function matrix $\mathbf{N}_e$ gives

$$\mathbf{F} = \omega^2 m \mathbf{N}_e \mathbf{q}_e$$

and the external work expression becomes

$$W = \omega^2 m \int_0^L \mathbf{d}^T \mathbf{N}_e \mathbf{q}_e dx \tag{2.15}$$

where the subscript e indicates use of the exact displacement field.

The inertia forces can be expressed at the nodes without approximation using

equivalent loads. The displacement due to these inertia force equivalent loads can be represented exactly using the polynomial shape functions. Therefore, Eq. (2.15) becomes

$$W = \omega^2 m \int_0^L \mathbf{q}_p^T \mathbf{N}_p^T \mathbf{N}_e \mathbf{q}_e dx \tag{2.16}$$

where the subscript p indicates use of the polynomial displacement field.

Equivalent load theory is used to represent the exact element inertia forces; thereby, the vibrating system is modeled quasi-statically. The frequency independent stiffness matrix of the conventional finite element model is used to represent the stiffness of this quasi-static system without introducing discretization error. The eigenvalue problem of this model takes the form

$$[\mathbf{K} - \omega^2 \mathbf{M}(\lambda)]\mathbf{x} = 0. \tag{2.17}$$

Previous studies show that for vibration analysis of skeletal systems with lumped, uniform, or nonuniform mass distributions, the mixed formulation is more computationally efficient than the exact displacement and conventional finite element models particularly when accuracy requirements are high [53, 54]. These studies use the inverse power method to extract the system's first mode and frequency and orthogonality conditions to obtain the second and subsequent modes and frequencies. However, this eigensolution technique is not well suited for larger problems and higher modes.

2.3 The Matrices of the Conventional Formulation

Using separation of variables, where $u(x,t) = \tilde{u}(x)h(t)$, the equation of motion for axial vibration, Eq. (2.1), can be reduced to two ordinary differential equations. The resulting equation in the space domain is

$$\frac{d^2\tilde{u}(x)}{dx^2} + \omega^2 \frac{m}{EA}\tilde{u}(x) = 0 \tag{2.18}$$

where $\tilde{u}(x)$ is the exact axial displacement given by Eq. (2.3) in Section 2.1. The conventional finite element uses polynomial shape functions to approximate the solution to Eq. (2.18), $\tilde{u}(x)$, by a polynomial displacement field, $\tilde{u}_p(x)$. Thus,

$$
\begin{aligned}
\tilde{u}(x) &\approx \tilde{u}_p(x) \\
&= \begin{bmatrix} 1 & x \end{bmatrix} \begin{Bmatrix} \tilde{C}_1 \\ \tilde{C}_2 \end{Bmatrix} \\
&= \begin{bmatrix} 1 & x \end{bmatrix} \begin{bmatrix} 1 & 0 \\ -\frac{1}{l} & \frac{1}{l} \end{bmatrix} \begin{Bmatrix} a_1 \\ a_2 \end{Bmatrix} \\
&= \begin{bmatrix} \left(1 - \frac{x}{l}\right) & \frac{x}{l} \end{bmatrix} \begin{Bmatrix} a_1 \\ a_2 \end{Bmatrix} \\
&= \mathbf{N}_p \mathbf{a}
\end{aligned}
\tag{2.19}
$$

where $\mathbf{N}_p$ is the polynomial shape function matrix and $\mathbf{a}$ is the vector of nodal degrees-of-freedom based on the polynomial element displacement field for axial displacement.

Using the expressions for strain and kinetic energy, the above shape function matrix is related to element stiffness matrix $\mathbf{k}_p$ and element mass matrix $\mathbf{m}_p$, respectively.

Thus,

$$\mathbf{k}_p = \int_0^l EA \frac{d\mathbf{N}'_p}{dx} \frac{d\mathbf{N}_p}{dx} dx$$

$$= \frac{EA}{l} \begin{bmatrix} 1 & -1 \\ -1 & 1 \end{bmatrix} \qquad (2.20)$$

and

$$\mathbf{m}_p = \int_0^l m\mathbf{N}'_p\mathbf{N}_p dx$$

$$= \frac{ml}{6} \begin{bmatrix} 2 & 1 \\ 1 & 2 \end{bmatrix} \qquad (2.21)$$

where prime denotes transpose of a matrix. The element matrices $\mathbf{k}_p$ and $\mathbf{m}_p$ are assembled into global matrices $\mathbf{K}_p$ and $\mathbf{M}_p$ using standard finite element procedure. Therefore, the resulting eigenvalue problem for the conventional finite element case takes the form of Eq. (2.22).

$$[\mathbf{K}_p - \omega^2\mathbf{M}_p] = 0 \qquad (2.22)$$

Similarly, using separation of variables, where $v(x,t) = \tilde{v}(x)g(t)$, the equation of motion for flexural vibration, partial differential Eq. (2.2), can be reduced to two ordinary differential equations. The equation in the space domain is

$$\frac{d^4\tilde{v}(x)}{dx^4} + \omega^2 \frac{m}{EI}\tilde{v}(x) = 0 \qquad (2.23)$$

where $\tilde{v}(x)$ is the exact lateral displacement given by Eq. (2.7) in Section 2.1. Using the conventional cubic polynomial shape functions

$$\bar{\mathbf{N}}_p = [\,(1 - 3\eta^3 + 2\eta^3) \quad l\eta(1 - \eta)^2 \quad (3\eta^2 - 2\eta^3) \quad l\eta^2(\eta - 1)\,] \qquad (2.24)$$

where $\eta = \dfrac{x}{l}$, and expressions for strain and kinetic energy, the element stiffness and mass matrices for a 2-D system takes the form

$$\bar{\mathbf{k}}_p = \frac{EI}{l^3} \begin{bmatrix} 12 & 6l & -12 & 6l \\ 6l & 4l^2 & -6l & 2l^2 \\ -12 & -6l & 12 & -6l \\ 6l & 2l^2 & -6l & 4l^2 \end{bmatrix}$$ (2.25)

and

$$\bar{\mathbf{m}}_p = \frac{ml}{420} \begin{bmatrix} 156 & 22l & 54 & -13l \\ 22l & 4l^2 & 13l & -3l^2 \\ 54 & 13l & 156 & -22l \\ -13l & -3l^2 & -22l & 4l^2 \end{bmatrix}$$ (2.26)

For the lowest circular natural frequency of an axially vibrating cantilever beam, a one-element discretization results in

$$\omega_1 = \sqrt{3\frac{EA}{ml^2}}$$

compared to the exact value of

$$\omega_1 = \frac{\pi}{2}\sqrt{\frac{EA}{ml^2}}.$$

Thus, the one element approximation has over 10% error, due to the discretization process. This error reduces as the number of elements increases and the system is

modeled with more degrees-of-freedom. As the number of degrees-of-freedom approaches ∞, theoretically the discretization error will vanish. However, as the number of elements increases, the solution complexity increases by approximately $\mathcal{O}(bn^2)$, where n is the number of degrees-of-freedom and b is the bandwidth.

2.4 The Matrices of the Mixed Formulation

In this formulation, in addition to the polynomial based shape function matrix $\mathbf{N}_p$, a frequency dependent shape function matrix $\mathbf{N}_e$, based on the exact solution of Eq. (2.18) is also used. Thus, using the solution given by Eq. (2.3)

$$
\begin{aligned}
\tilde{u}(x) &= u_e(x) \\[2mm]
&= C_1 \cos bx + C_2 \sin bx \\[2mm]
&= [\cos bx \quad \sin bx] \left\{ \begin{array}{c} C_1 \\ C_2 \end{array} \right\} \\[2mm]
&= [\cos bx \quad \sin bx] \left[\begin{array}{cc} 1 & 0 \\ -\dfrac{\cos bl}{\sin bl} & \dfrac{1}{\sin bl} \end{array} \right] \left\{ \begin{array}{c} a_1 \\ a_2 \end{array} \right\} \qquad (2.27) \\[2mm]
&= \left[\left(\cos bx - \dfrac{\sin bx}{\tan bl} \right) \quad \left(\dfrac{\sin bx}{\sin bl} \right) \right] \left\{ \begin{array}{c} a_1 \\ a_2 \end{array} \right\} \\[2mm]
&= \mathbf{N}_e\, \mathbf{a}
\end{aligned}
$$

where $\mathbf{a}$ is the vector of nodal degrees-of-freedom based on the exact element displacement field for axial displacement.

Again using the virtual work principle and the procedure outlined by Melosh and Smith [54], both the shape function matrices are related to element stiffness

and mass matrices. Only the polynomial shape functions are used to compute the element stiffness matrix and hence, $\mathbf{k}_e = \mathbf{k}_p$ is same as given by Eq. (2.20). Both the polynomial and the frequency dependent exact shape functions are used to compute the element mass matrix as given below.

$$
\begin{aligned}
\mathbf{m}_e &= \int_0^l m\mathbf{N}'_p\mathbf{N}_e dx \\
&= ml \begin{bmatrix} \left(\dfrac{1}{(bl)^2} - \dfrac{\cos bl}{bl\sin bl}\right) & \left(\dfrac{1}{bl\sin bl} - \dfrac{1}{(bl)^2}\right) \\[4mm] \left(\dfrac{1}{bl\sin bl} - \dfrac{1}{(bl)^2}\right) & \left(\dfrac{1}{(bl)^2} - \dfrac{\cos bl}{bl\sin bl}\right) \end{bmatrix}
\end{aligned}
\tag{2.28}
$$

The element stiffness and mass matrices $\mathbf{k}_e$ and $\mathbf{m}_e$ are assembled into the global stiffness and mass matrices $\mathbf{K}_e$ and $\mathbf{M}_e$ using standard finite element procedure. Therefore, the resulting eigenvalue problem for the conventional finite element case takes the form

$$
[\mathbf{K}_e - \omega^2\mathbf{M}_e(\omega^2)] = 0.
\tag{2.29}
$$

For lateral vibrations the shape function matrix $\bar{\mathbf{N}}_e$, and the element stiffness and mass matrices $\bar{\mathbf{k}}_e$ and $\bar{\mathbf{m}}_e$ are derived using Eqs. (2.7) and (2.2) in a manner analogous to the above.

$$
\begin{aligned}
\tilde{v}(x) &= v_e(x) \\
&= \bar{C}_1\cos\bar{b}x + \bar{C}_2\sin\bar{b}x + \bar{C}_3\cosh\bar{b}x + \bar{C}_4\sinh\bar{b} \\
&\vdots \\
&= \bar{\mathbf{N}}_e\bar{\mathbf{a}}
\end{aligned}
\tag{2.30}
$$

Expressions for $\bar{\mathbf{N}}_e$, $\bar{\mathbf{k}}_e$ and $\bar{\mathbf{m}}_e$ are given in Appendix A.

For the axially vibrating cantilever beam of the previous section, a one element discretization using the mixed formulation to compute the lowest circular natural frequency results in

$$\frac{EA}{l} - \omega^2 \left(\frac{1}{(bl)^2} - \frac{\cos bl}{bl \sin bl} \right) = 0.$$

Substituting $bl = \omega \sqrt{\dfrac{ml^2}{EA}}$ and simplifying,

$$\frac{EA}{l} - \omega^2 (ml) \left(\frac{EA}{\omega^2 ml^2} \right) \left(1 - \frac{\omega \sqrt{\dfrac{ml^2}{EA}}}{\tan w \sqrt{\dfrac{ml^2}{EA}}} \right) = 0$$

or,

$$\frac{\omega \left(\dfrac{EA}{l} \right) \sqrt{\dfrac{ml^2}{EA}}}{\tan \omega \sqrt{\dfrac{ml^2}{EA}}} = 0$$

or,

$$\cos \omega \sqrt{\frac{ml^2}{EA}} = 0$$

or,

$$\omega_1 = \frac{\pi}{2} \sqrt{\frac{EA}{ml^2}},$$

which is the exact circular naturally frequency for the first mode. Thus, by using both the polynomial based shape functions and the frequency dependent exact shape functions, the discretization error for this problem has been completely eliminated.

2.5 Power Series Expansion of the Dynamic Matrix

As derived in Section 2.1, for an axially vibrating beam, the dynamic stiffness matrix is

$$\mathbf{D}_a = EAb \begin{bmatrix} \dfrac{1}{\tan bl} & \dfrac{-1}{\sin bl} \\ \dfrac{-1}{\sin bl} & \dfrac{1}{\tan bl} \end{bmatrix}.$$

Using the trigonometric power series for $\cot x$ and $\csc x$, and $bl = \omega\sqrt{\dfrac{ml^2}{EA}}$ results in

$$EAb \cot bl = EAb \left(\frac{1}{bl} - \frac{bl}{3} - \frac{(bl)^3}{45} - \dots \right)$$

$$= \frac{EA}{l} - \omega^2 \frac{ml}{3} - \omega^4 \frac{ml}{45} \frac{l^2}{EA} - \dots$$

and

$$-EAb \csc bl = -- EAb \left(\frac{1}{bl} + \frac{bl}{6} - \frac{7(bl)^3}{360} - \dots \right)$$

$$= \frac{-EA}{l} - \omega^2 \frac{ml}{6} - \omega^4 \frac{7}{45} ml \frac{l^2}{EA} - \dots,$$

and finally,

$$\mathbf{D}_a = EAb \begin{bmatrix} \dfrac{1}{\tan bl} & \dfrac{-1}{\sin bl} \\ \dfrac{-1}{\sin bl} & \dfrac{1}{\tan bl} \end{bmatrix}$$

$$= \frac{EA}{l} \begin{bmatrix} 1 & -1 \\ -1 & 1 \end{bmatrix} - \omega^2 \frac{ml}{6} \begin{bmatrix} 2 & 1 \\ 1 & 2 \end{bmatrix} + \mathcal{O}\left(\frac{\omega^4 ml^3}{EA} \right) \qquad (2.31)$$

$$= \mathbf{k}_p - \omega^2 \mathbf{m}_p + \mathcal{O}\left(\frac{\omega^4 m^2 l^3}{EA} \right).$$

Comparing the two sides of Eq. (2.31), it can be inferred that for larger values of

nondimensional quantity $\left(\dfrac{\omega^2 m l^2}{EA}\right)$, i.e, for higher modes and/or nonslender beams, the formulation based only on polynomial shape functions will approximate the dynamic matrix rather poorly and the results will be increasingly more inaccurate due to the neglect of nonlinear terms. On the other hand, for the formulation based on both polynomial shape function and frequency dependent exact shape function gives the following.

$$\mathbf{k}_{e11} - \omega^2 \mathbf{m}_{e11} = \frac{EA}{l} - \omega^2 m l \left(\frac{1}{(bl)^2} - \frac{\cos bl}{bl \sin bl}\right)$$

$$= EAb\left\{\frac{1}{bl} - \frac{ml}{EAb}\left[\frac{1}{(bl)^2} - \frac{\cot bl}{bl}\right]\right\}$$

$$= EAb\left\{\frac{1}{bl} - \frac{1}{bl}\frac{ml^2}{EA(bl)^2} + \frac{ml^2}{EA(bl)^2}\cot bl\right\}$$

$$= EAb\cot bl$$

$$\mathbf{k}_{e12} - \omega^2 \mathbf{m}_{e12} = -\frac{EA}{l} - \omega^2 m l \left(\frac{1}{(bl)\sin bl} - \frac{1}{(bl)^2}\right)$$

$$= -EAb\csc bl.$$

Hence $\mathbf{k}_e - \omega^2 \mathbf{m}_e = \mathbf{D}_a$; thus, the mixed formulation based on both the polynomial shape functions and frequency dependent exact shape functions does not lead to any discretization error.

For the transverse vibrations, the dynamic matrix elements are much more complicated than the above terms and, hence, a direct manipulation to show the equivalence between the eigenproblems of the mixed finite element formulation and the dynamic matrix for flexural vibrations is impossible even using symbolic manipulation tools. In Appendix B, the equivalence between $\bar{\mathbf{D}}_f$ and $\bar{\mathbf{k}}_e - \omega^2 \bar{\mathbf{m}}_e$ is established using a

Taylor series expansion about $\omega = 0$ and matching the terms with like powers of ω in the two series expressions.

CHAPTER 3

Eigensolution Techniques for Nonlinear

Eigenproblems

The linear, positive definite, symmetric eigenvalue problem can be solved for the system natural frequencies and modes using conventional eigensolution techniques. However, the eigenproblem of Eq. (2.17) is needed if exact solutions are sought which are free of discretization error. This chapter describes two eigensolvers for obtaining the natural frequencies and modes of Eq. (2.17). The first solution technique is based upon a variant of Lanczos method that has been derived from the more general implicitly restarted Arnoldi method developed by Sorensen [58]. The second method is the determinant search method using qualified parabolic interpolation as proposed by Williams and Kennedy [69], with some modifications to solve the nonlinear eigenproblem.

3.1 Conventional Lanczos Methods

Lanczos methods have been used extensively to solve large, sparse symmetric eigenvalue problems $\mathbf{A}\mathbf{x} = \lambda\mathbf{x}$. In its most basic form, using exact arithmetic, the Lanczos process is a scheme to tridiagonalize a symmetric $\mathbf{A} \in \Re^{n \times n}$. After j steps of the

Lanczos process, an orthonormal $n \times j$ matrix $\mathbf{V}_j$ and a symmetric tridiagonal matrix $\mathbf{T}_j$ are produced such that

$$\mathbf{A}\mathbf{V}_j = \mathbf{V}_j\mathbf{T}_j + \mathbf{f}_j\mathbf{e}_j^T \tag{3.1}$$

where $\mathbf{f}_j$ is a vector of length n and $\mathbf{e}_j$ is the *jth* co-ordinate vector of length j with $\mathbf{V}_j^T\mathbf{f}_j = 0$. This is easily shown to be a truncation of the complete orthogonal reduction of $\mathbf{A}$ to tridiagonal form that typically precedes the implicitly shifted tridiagonal QR iteration.

The eigenvalues of $\mathbf{T}_j$ approximate a subset of eigenvalues of $\mathbf{A}$. If $(\mu, \mathbf{y})$ is an eigenpair for $\mathbf{T}_j$ (i.e., $\mathbf{T}_j\mathbf{y} = \mathbf{y}\mu$) then $(\mu, \mathbf{x} = \mathbf{V}_j\mathbf{y})$ is an approximate eigen-pair for $\mathbf{A}$ and the error of approximation is given by

$$\|\mathbf{A}\mathbf{x} - \mathbf{x}\mu\| = \|\mathbf{f}_j\| |\mathbf{e}_j^T\mathbf{y}| \tag{3.2}$$

In particular, the approximation is exact when $\mathbf{f}_j = 0$. Eigenvalues and eigenvectors of the symmetric tridiagonal matrix $\mathbf{T}_j$ are determined using either the symmetric QR method or by bisection.

The Lanczos process has been used to solve engineering dynamics problems for two main reasons: the Lanczos process only requires matrix vector products involving $\mathbf{A}$ together with a few vectors of storage in main memory, and the largest and the smallest eigenvalues tend to emerge well before the tridiagonalization is complete making this method especially useful for structural dynamics problems where usually only a few of the smallest eigenvalues are desired.

Unfortunately, the Lanczos process also has some drawbacks: In its original form, roundoff errors severely affect the iteration, resulting in loss of orthogonality among

the Lanczos vectors produced while tridiagonalizing the matrix $\mathbf{A}$ and the appearance of spurious eigenvalues in the spectrum of $\mathbf{T}$. Various schemes have been proposed to overcome these problems ranging from recognizing and casting out spurious eigenvalues to selective re-orthogonalization techniques [12, 36]. Another problem is that in order to recover the eigenvectors corresponding to the computed approximate eigenvalues, it may be necessary to store a very large dense matrix on an auxiliary device because all of the Lanczos basis vectors are required to compute an approximate eigenvector.

3.2 The Implicitly Restarted Lanczos Method

The method outlined in Sorensen [58] addresses the drawbacks of the Lanczos process listed in the previous section. The underlying idea is to recognize that the residual vector at any step of the Lanczos process is a function of the initial starting vector (i.e., the first column of $\mathbf{V}_j$). The total number of Lanczos steps is limited to a fixed prescribed value k and the starting vector is iteratively updated in a way that forces the norm of the residual vector $\mathbf{f}_k$ to converge to zero. This limits storage requirements and allows full numerical orthogonality of the Lanczos basis vectors to be enforced due to the limited computational costs.

The iteration involves repeated application of 'polynomial filters' to the starting vector and an in-place updating of the k-step Lanczos factorization. The filters are designed to purge undesirable eigenvector components from the starting vector forcing it into an invariant subspace. The construction and application of these filters, how to update in-place, and other related mathematical details are explained in Ref. [58].

The technique is analogous to the implicitly shifted QR iteration for dense matrices and shares most of the important numerical properties associated with that process. Thus, this approach has the following inherent advantages.

- **Fixed space:** In this scheme, the number of Lanczos basis vectors is never larger than a pre-specified number that is proportional to the number of eigen-values sought. Because of this, peripheral storage of basis vectors is not required. Moreover, as in the basic Lanczos process, only matrix vectors products are required with **A**.

- **Orthogonal eigenvectors:** By virtue of the fixed modest number of Lanczos vectors, it is computationally feasible to maintain full numerical orthogonality among the basis vectors. The maintenance of orthogonality ensures that no spurious eigenvalues are computed.

- **Convergence:** As demonstrated in Ref. [58], convergence is guaranteed for the linear eigenproblem $\mathbf{Ax} = \lambda\mathbf{Bx}$.

This general approach has been used successfully by Sorensen [58] to solve large eigenproblems arising from discretization of convection-diffusion problems, linearized Navier-Stokes problems and a composite membrane problem up to the order of 10,000 degrees-of-freedom on a number of different computer architectures. In a subsequent study, Sorensen, Vu and Tomasic [60] used the $k-$step Arnoldi on a structural analysis problem with 250,000 degrees-of-freedom.

3.3   Solving the Nonlinear Eigenproblem

The features described above lend themselves naturally to an effective solution scheme for the nonlinear problem. With this new scheme it is possible to evaluate a specified subset of the eigenvalues of a matrix function $\mathbf{F}(\lambda)$ and to treat these as individual scalar functions of λ. Applying a simple zero finding technique to each of these in turn provides solutions to the nonlinear problem, where information from a converged eigenvalue may be used to initialize the iteration for the next one. Moreover, as shown below, the stiffness matrix is only factored once and only matrix vector products are required of the frequency dependent mass matrix.

The nonlinear eigenproblem has been approached in the past through linearization via Taylor series and solving through various forms of of Newton's method [30, 44, 72] applied directly to this system through a subspace iteration closely related to the QR method.

Only one of the matrices in Eq. (2.17) has a dependence on λ which leads to eigenvalue dependent problems problems of the form

$$\mathbf{F}(\lambda) = \mathbf{A} - \lambda\mathbf{B}(\lambda) \tag{3.3}$$

where $\mathbf{A}$ is a fixed symmetric positive definite matrix and $\mathbf{B}(\lambda)$ is symmetric. The goal is to compute a few of the algebraically smallest roots λ. Our approach will be to use the variant of the Lanczos method described above to track the eigenvalues of $\mathbf{F}(\lambda)$ as functions of the parameter λ and solve a scalar nonlinear equation for each of the nonlinear eigenvalues of interest. The new variant of the Lanczos process is well suited to this approach.

To take this approach, it is much better to cast this problem in the form

$$\mathbf{B}(\lambda)\mathbf{x} = \frac{1}{\lambda}\mathbf{A}\mathbf{x} \qquad (3.4)$$

In this formulation, the factorization becomes

$$\mathbf{B}(\lambda)\mathbf{V} = \mathbf{A}\mathbf{V}\mathbf{T}(\lambda) + \mathbf{f}\mathbf{e}_k{}^T \qquad (3.5)$$

with the columns of $\mathbf{V}$ being $\mathbf{A}$−orthogonal, and $\mathbf{T}$ tridiagonal. Subscripts on $\mathbf{V}, \mathbf{T}$ and $\mathbf{f}$ and the λ−dependence of $\mathbf{V}$ and $\mathbf{f}$ have been suppressed for simplicity. Let $\mu_1(\lambda)$ be the algebraically largest eigenvalue of $\mathbf{T}$ and let $\mathbf{y}_1$ be the corresponding eigenvector. An approximate solution to Eq. (3.4) is obtained when

$$\mu_1(\lambda) = \frac{1}{\lambda} \quad , \text{ under the condition } \quad \|\mathbf{f}\|\|\mathbf{e}_k{}^T\mathbf{y}_1\| < \epsilon\mu_1. \qquad (3.6)$$

The implicitly restarted Lanczos technique provides the ability to satisfy the side condition, viz., $\|\mathbf{f}\|\|\mathbf{e}_k{}^T\mathbf{y}_1\| < \epsilon\mu_1$. Moreover, the convergence of this inner iteration is expected to be very rapid since the eigenvalues of interest in the spectrum of the transformed problem are well separated and at the large end. This is the ideal situation with respect to convergence of the Lanczos method. Finally, the stiffness matrix $\mathbf{K}$ need only be factored once, throughout the entire nonlinear iteration. Only matrix vector products are required of the frequency dependent mass matrix $\mathbf{M}$.

It is readily seen that $\mu_1(\lambda)$ is a root of a polynomial whose coefficients are rational functions of the matrix elements of $\mathbf{B}(\lambda)$ and $\mathbf{A}$, and the components of the first column of $\mathbf{V}$. Thus, the function $\mu_1(\lambda)$ typically will inherit the smoothness of

the elements of $\mathbf{B}(\lambda)$ near a solution, even though certain difficult cases cannot be ruled out. Technically, any appropriate root finding technique may be applied to the solution of Eq. (3.6).

In this research, a safeguarded secant method is used to solve Eq. (3.6). Before describing the iteration, it is helpful to consider the graph in Figure 3.1. This graph shows three $\mu_j(\lambda)$ curves plotted as a function of the parameter λ for axial vibrations of a representative cantilever beam. The solutions to the nonlinear problem of Eq. (3.4) are those values of λ at which the curves $\mu_j(\lambda)$ intersect the curve $\frac{1}{\lambda}$. Note that these curves are nearly linear in the neighborhood of interest. Moreover, these functions are strictly increasing in this region. Thus, it is likely that a secant type of method should work well.

The secant method that is used may be described as follows: first, the linear eigenproblem at $\lambda_0 = 0$ is solved and then λ_1 is set equal to $\frac{1}{\mu_1(0)}$. The mass matrix $\mathbf{M}(\lambda_1)$ is formed and a new linear eigenproblem is solved to calculate $\mu_1(\lambda_1)$. A linear interpolation between these two successive points will intersect the curve $\frac{1}{\lambda}$ at a point λ_2 due to the increasing of the μ curve and the convexity and decreasing of the curve $\frac{1}{\lambda}$. Again the mass matrix is re-evaluated and a linear eigenproblem is solved to evaluate $\mu_1(\lambda_2)$ where another linear interpolation is made between the points $(\lambda_1, \mu_1(\lambda_1))$ and $(\lambda_2, \mu_2(\lambda_2))$. Once this pattern has been set, the technique continues to form these secant approximations using the latest two λ points. This strategy has been quite successful for the structural dynamics problems. It typically converges to ten digit accuracy within four iterations. If the μ-curves behave as shown in Figure 3.1 this simple secant method is guaranteed to converge to the solution.

Each iteration of the zero finder requires a determination of $\mu_1(\lambda)$ such that
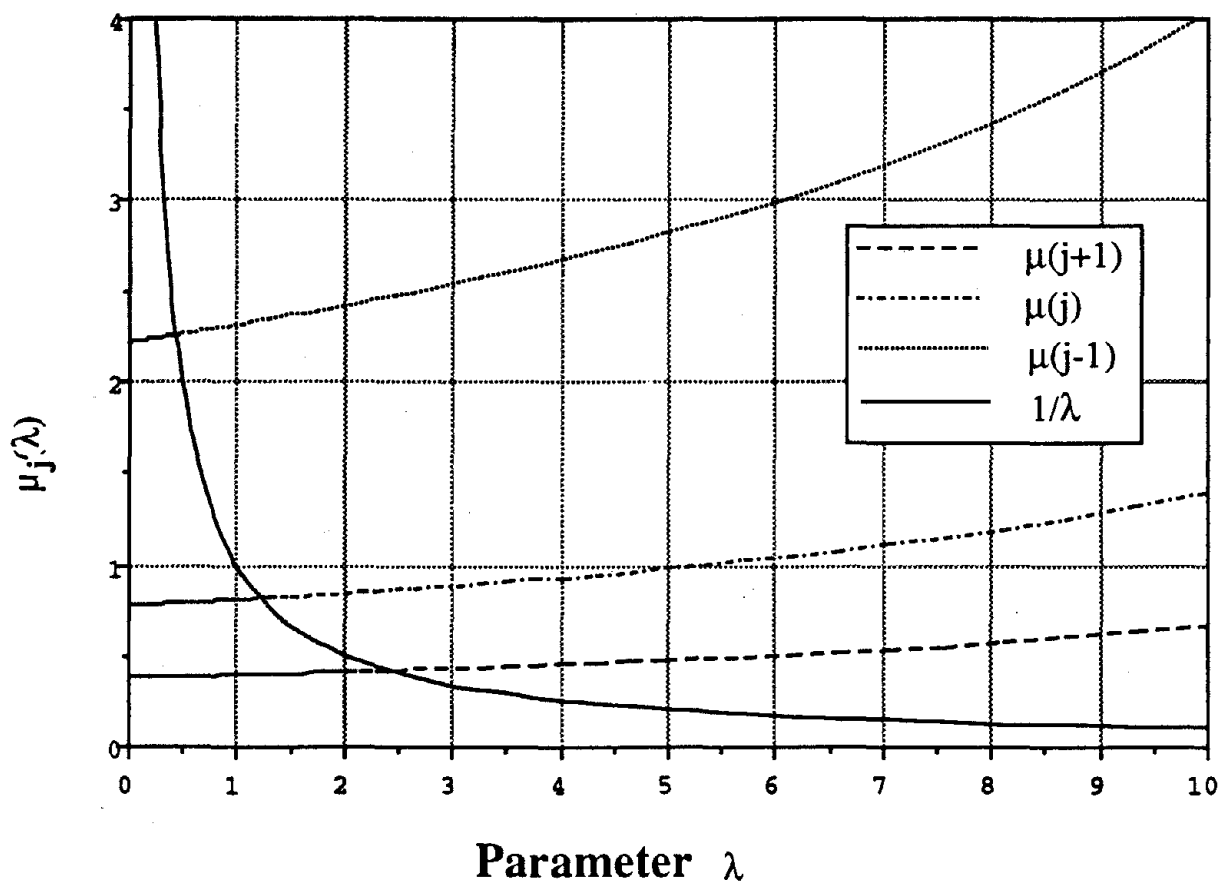
Figure 3.1: Eigenvalue curves — $\mu_j(\lambda)$ versus λ

$\|\mathbf{f}\|\|\mathbf{e}_k{}^T\mathbf{y}_1\| < \epsilon\mu_1$ through the implicitly restarted Lanczos process. Hence, this may be regarded as an inner iteration to the root finding technique. Once the value of λ is updated within the root finder, the next evaluation of μ_1 may use the first column of $\mathbf{V}$ to begin the new restarted Lanczos process. Note that for two-dimensional skeletal systems, after the rigid body modes have been eliminated, there are no repeated eigenvalues problems and thus the $\mu_j(\lambda)$ curves never intersect each other. This lends to an easy safeguarding of the iterative zero finding process. (Theoretically, if the plan of a three-dimensional structure is completely symmetric about two mutually perpendicular axes then there could be modal beating and the $\mu_j(\lambda)$ might intersect each other.)

This process may be repeated using the existing k-step Lanczos factorization from the previous step to great advantage. Once a solution λ_j to the jth nonlinear problem

$$\mu_j(\lambda) = \frac{1}{\lambda} \quad , \text{ under the condition } \quad \|\mathbf{f}\|\|\mathbf{e}_k{}^T\mathbf{y}_j\| < \epsilon\mu_j \qquad (3.7)$$

has been found, the entire k-step Lanczos factorization that is in place from the final iterative step to solve the jth problem may be used to initiate the $(j+1)$st problem. This provides an excellent starting guess to begin the zero finding iterations for λ_{j+1}. The accuracy of the solutions to the linear subproblems is assured by the implicitly restarted Lanczos iteration. Accuracy and consistency of the computed solutions to the nonlinear problem can be checked by the extension of Sturm sequence for nonlinear eigenvalue problems [17].

3.4 Determinant Search Method

Determinant search method is one of a family of nonlinear eigensolution techniques that are generally referred to as 'frequency scanning' methods. The simplest of these methods determines the eigenvalues of interest by looking at a plot of the characteristic polynomial versus the eigenvalue parameter λ. This involves evaluating and plotting the $\det |[\mathbf{A} - \lambda\mathbf{B}]|$ at fine intervals of λ. The jth zero-crossing on the plot, counting from the origin, is the jth eigenvalue. In addition to being computationally very intensive, this method also suffers from numerical scaling difficulties as the determinant of a matrix is generally a very fast varying function. This method fails if poles are present near the desired eigenvalues, or if eigenvalues are clustered close to each other.

Williams and Kennedy [69] combined the determinant evaluation with a sign count (inertia) of the matrix, and an update technique (bisection or quadratic interpolation) to improve upon the basic method outlined above. This method consists of several stages outlined below for the case when extreme eigenvalues are desired.

The first stage, called overall bounding stage, establishes global lower and upper bounds on the set of eigenvalues required. It is assumed that a consecutive set of eigenvalues $\lambda_1, \lambda_2, \ldots, \lambda_m$ are required. The global lower bound is established by computing the sign count of the matrix

$$
\begin{aligned}
\mathbf{D}(\lambda) &= [\mathbf{A} - \lambda\mathbf{B}(\lambda)] \\
&= \mathbf{L}\hat{\mathbf{D}}\mathbf{L}^T
\end{aligned}
\tag{3.8}
$$

using a symmetric factorization. Number of negative diagonals of the matrix $\hat{\mathbf{D}}$ is

the same as number of negative eigenvalues of the matrix $\mathbf{D}(\lambda)$, the latter being the sign count of the matrix $\mathbf{D}(\lambda)$. The current bound is updated as $\lambda^l \leftarrow \dfrac{\lambda^l}{\sigma}$, where $\sigma \in (1, 2)$ is a prespecified scaling factor, until $\mathbf{sign}(\mathbf{D}(\lambda^l)) = 0$. Similarly, the global upper bound is established by successively updating $\lambda^u \leftarrow (\lambda^u \cdot \sigma)$ until $\mathbf{sign}(\mathbf{D}(\lambda)) = \mathbf{sign}(\hat{\mathbf{D}}) \geq m$. In the second stage, local lower and upper bounds are established for each eigenvalue of interest. A hashed table is used to store and retrieve the previously computed $(\mathbf{sign}(\mathbf{D}(\lambda)), \lambda)$ pairs. Using bisection and table lookup, a set of λ_i^l and λ_i^u are determined such that the following set of inequalities hold.

$$\lambda^l \leq \cdots \leq \lambda_{i-1}^u \leq \lambda_i^l \leq \lambda_i \leq \lambda_i^u \leq \lambda_{i+1}^l \leq \cdots \leq \lambda^u$$

The third stage is called qualified parabolic interpolation and its objective is to use $\mathbf{sign}(\mathbf{D}(\lambda))$ and $|\mathbf{D}(\lambda)|$ at the current lower bound λ_i^l and at the current and previous upper bounds, λ_i^u and λ_i^{uu} to converge on λ_i more rapidly than would bisection alone between points λ_i^l and λ_i^u. To avoid the disastrous possibility of using quadratic interpolation in case there is a pole between the current lower and upper bounds, Williams and Kennedy's method uses a heuristic approach. Define the parameters α, β and γ as

$$\alpha = \max \left\{ \begin{array}{c} \text{distance} \\ \forall \lambda_i^* \in [\lambda_i^l, \lambda_i^u] \end{array} \{ \, |\mathbf{D}(\lambda_i^*)| - \text{chord}(\, |\mathbf{D}(\lambda_i^u)|, \, |\mathbf{D}(\lambda_i^{uu})| \,) \, \} \right\}$$

$$\beta = \text{distance} \{ \, (\, |\mathbf{D}(\lambda_i^u)| - |\mathbf{D}(\lambda_i^u)| \,) \, \}$$

$$\gamma = |\tfrac{\alpha}{\beta}|$$

then a pole is assumed to lie between the current lower and upper bounds if $\gamma > \gamma^*$

for some specified $\gamma^* < 1$. This method also monitors convergence rate and reverts back to bisection method if the convergence rate is slower than a specified value θ. One major drawback of this method is that there is no systematic way of choosing the parameters σ, γ^* and θ. In addition, the symmetric factorization may require pivoting, in which case, $\mathbf{PD}(\lambda)\mathbf{P}^T = \mathbf{L}\hat{\mathbf{D}}\mathbf{L}^T$ destroys the banded nature of the problem.

3.5 Implementation Details

The finite element formulations and eigensolution techniques described in Chapters 2, 3 and 4 have been implemented in Fortran 77 on a DEC 5000 workstation with MIPS compiler and Ultrix 4.2 operating system. To maintain scalability, portability and modular nature of all computations, linear algebra subroutines from BLAS [33] levels 1, 2 and 3, LAPACK [1] and ARPACK [59] libraries have been used wherever possible. Noting that in Fortran two-dimensional arrays are stored in a column-wise format, whenever possible, various algorithmic details of the finite element modeling and eigensolution technique have been restructured to perform SDOT() and SAXPY() type of operations, and to access storage sequentially with unit stride. All matrix computations were performed in banded form and in order to keep the programs portable, system specific calls and vendor specific language extensions have been avoided.

The program can perform undamped or damped, extreme or interior, free vibration analysis of two- and three-dimensional trusses, beams and frames. The structure can be discretized using one or more of the following finite element formulations: the conventional formulation, three levels of the $h-$ and $p-$formulations and the

frequency dependent mixed formulation. Three different choices are available for solving linear and nonlinear eigenproblems: the implicitly restarted Lanczos/Arnoldi method, the determinant search method and, for small problems, dense eigensolvers from LAPACK. The program can use a modal superposition analysis to compute forced vibration response as well.

3.6 Numerical Results

This section presents examples where the lowest few natural frequencies of two-dimensional frame-type structures are determined. In the first example, solutions obtained using the mixed finite element model of Eq. (2.17) are compared on the basis of accuracy with solutions obtained using the conventional finite element model. The eigenvalue problems of both models are solved using the implicitly restarted Lanczos method presented in the previous section. Section 3.6.2 compares the computational efficiency of the implicitly restarted Lanczos eigensolver with the multiple determinant parabolic interpolation method developed by Williams and Kennedy [69] for solving frequency dependent vibration eigenproblems.

3.6.1 Comparison of the Mixed and Conventional Formulations

In this example, the first ten natural frequencies are found for a four story plane frame with 36 unconstrained degrees-of-freedom shown in Figure 3.2. Simpson [46] reports these frequencies obtained both experimentally and numerically using a variation of the exact model with Kron's eigenvalue procedure [48].

Kron's procedure is a method for piecewise eigenvalue analysis of dynamic systems. The original system matrix is successively 'torn' into a multiplicity of smaller subsystems, each of which is analyzed by standard eigensolution methods. The sub-matrices are transformed such that the eigenvalues of the composite system can be determined via a frequency scanning process. However, this method requires inverting a matrix (of size equal to the number of physical connections between subsystems) at each stage of frequency scanning. Thus, it becomes quite unwieldy even for a moderately sized problem.

Table 3.1 summarizes the results from Simpson [46] and compares them with results obtained using the conventional model and the mixed model. As shown, the conventional finite element model shows large error particularly for the higher modes. The sharp increase in error for the fifth frequency for the first discretization pattern is due to the inability of the conventional finite element model to represent higher-order member deformation when discretized with only one element per member. This problem is eliminated when two elements per member are used. The mixed model and the model used by Simpson use one element per structural member. The relative tolerance for eigenvalue convergence was specified as 10^{-9}.

The mixed model results are nearly exact when compared to the results reported by Simpson. The apparent difference between the experimental results and analytical results is due to inaccuracies inherent in modeling the exact material and sectional properties of the test specimen. Notably, the mixed model with the new nonlinear eigensolver gives superior results for higher and clustered frequencies.
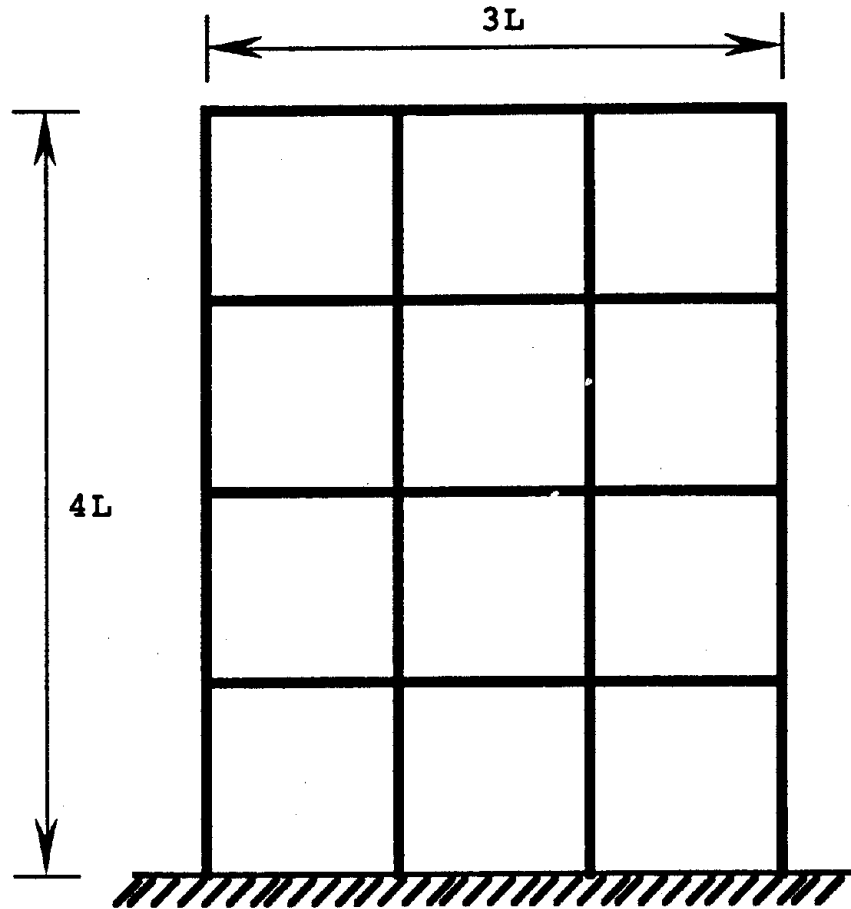
$a = 0.50$ in.

$b = 0.125$ in.

$L = 10.0$ in.

$E = 30 \times 10^6$ psi (Young's modulus)

$m = 7.619 \times 10^{-4}$ lbm/in.^{3} (mass per unit volume)
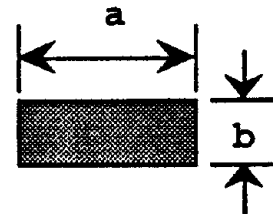
Figure 3.2: Four story plane frame

Table 3.1: First 10 frequencies for four story plane frame

Frequency	Finite Element Results (Hz)			Reference [46] Results (Hz)	
Number	Conv[1]	Conv[2]	Mixed	Kron's Method	Experimental
1	7.86	7.86	7.86	7.88	8.18
2	24.8	24.8	24.8	24.9	25.7
3	44.2	44.1	44.0	44.2	45.9
4	62.7	62.5	62.5	62.6	65.6
5	128.3	115.5	115.0	115.5	118.3
6	148.8	130.0	129.3	130.0	133.6
7	153.9	133.3	132.6	133.0	136.5
8	180.6	150.1	149.1	150.0	154.2
9	192.3	156.5	155.4	155.3	163.1
10	194.7	157.9	156.7	156.5	163.1

[1] One element per structural member
[2] Two elements per structural member

3.6.2 Comparison of Implicitly Restarted Lanczos and Determinant Search Techniques

In these examples, seven frame-type structures involving 48, 75, 162, 270, 330, 585, and 960 unconstrained degrees-of-freedom are modeled for free vibration analysis using the frequency dependent mixed finite element formulation. The first ten natural frequencies and modes of each system are obtained using the Lanczos-based technique with secant interpolation presented here and a determinant search technique used by Williams and Kennedy [69]. The purpose of these examples is to illustrate the computational efficiency of the implicitly restarted Lanczos technique for large-order problems and to compare the method with the determinant search eigenvalue techniques used most frequently in exact vibration analyses.

The multiple determinant parabolic interpolation eigenvalue technique was developed for use with exact finite element models where both **K** and **M** are comprised of frequency dependent transcendental functions. This method uses the number of eigenvalues lying between zero and a trial value together with eigenvalue curve plotting and interpolation techniques to successively improve bounds on the desired eigenvalue. As described previously in Section 3.4, an interpolation criterion decides whether the subsequent trial value should be obtained by bisection or parabolic interpolation. This method uses parabolic interpolation by default. However, if the determinant of the dynamic stiffness matrix $[\mathbf{K} - \lambda\mathbf{M}]$ evaluated at the newly interpolated value of λ differs significantly from the chord joining the upper and lower eigenvalue bounds, the presence of a pole is suspected and the bisection technique is used. Use of a

qualified parabolic interpolation procedure offers significant computational improvement over bisection techniques used in traditional determinant search methods especially for higher accuracy requirements. Results from Williams and Kennedy show a 10% decrease in computational intensity when compared with Simpson's Newtonian method [46]. However, the multiple determinant parabolic interpolation eigenvalue technique is primarily intended for nonlinear eigenproblems and is not well-suited for conventional frequency independent free vibration analyses. In addition, for large nonlinear eigenproblems computing the determinant of the dynamic stiffness matrix is impractical due to the computational intensity of evaluation and also due to the potential erratic behavior of the determinant function. In contrast, the $\mu(\lambda) - \lambda$ curves in Figure 3.1 exhibit a very mild behavior of the functions $\mu_j(\lambda)$ appearing in Eq. (3.7) for the Lanczos-based method.

Figures 3.3 and 3.4 graphically depict the total computational time needed to obtain ten natural frequencies as a function of problem size. Figure 3.3 illustrates that for smaller problems (with fewer than approximately 120 degrees-of-freedom), the multiple determinant parabolic interpolation technique is competitive with the Lanczos-based nonlinear eigenvalue technique using secant interpolation. However, as the problem size increases, the Lanczos-based technique becomes increasingly more efficient as shown in Figure 3.4. In particular, for problems approaching 1000 degrees-of-freedom, the computational time needed by the determinant search technique is more than one order of magnitude greater than the time needed by the implicitly restarted Lanczos method.
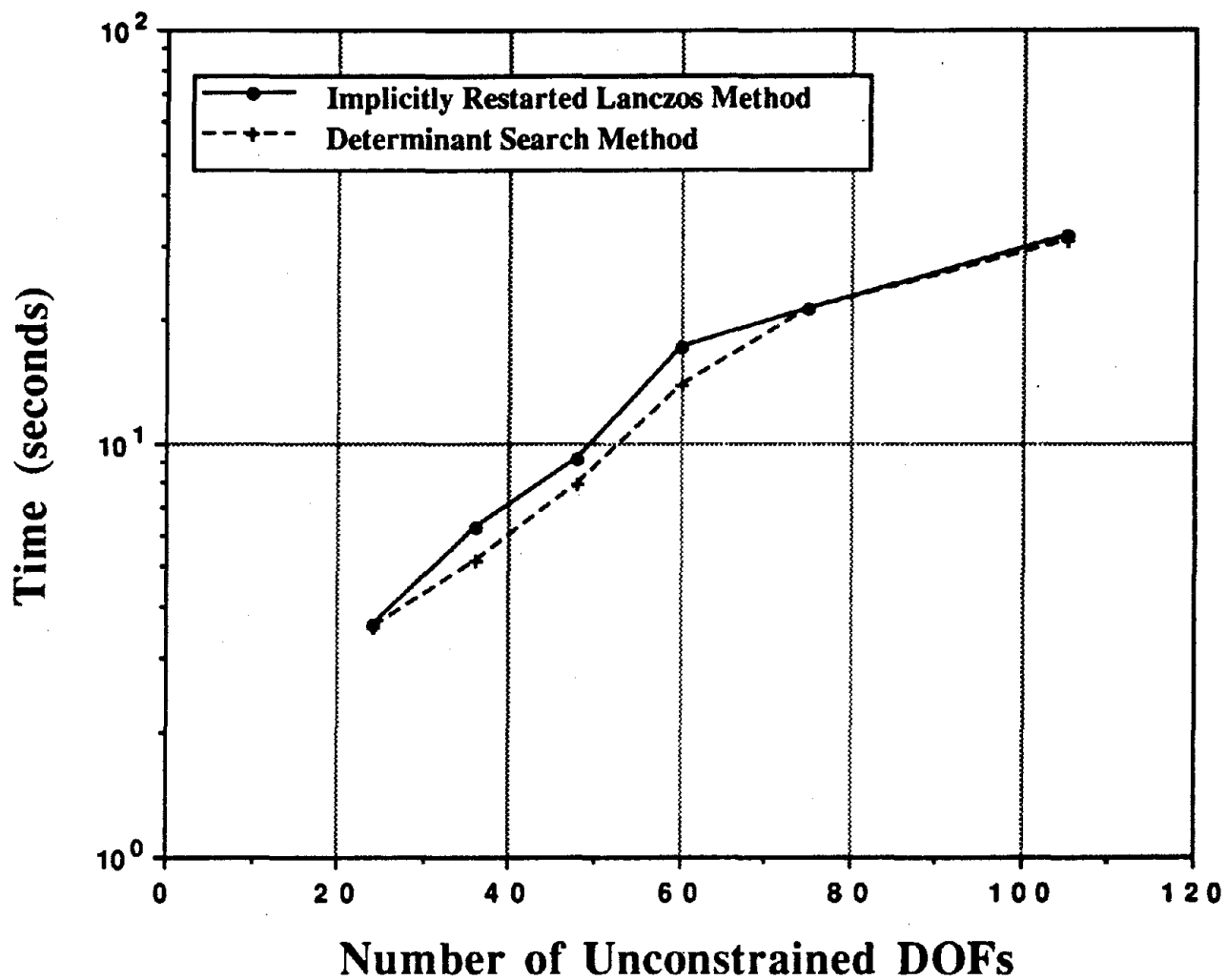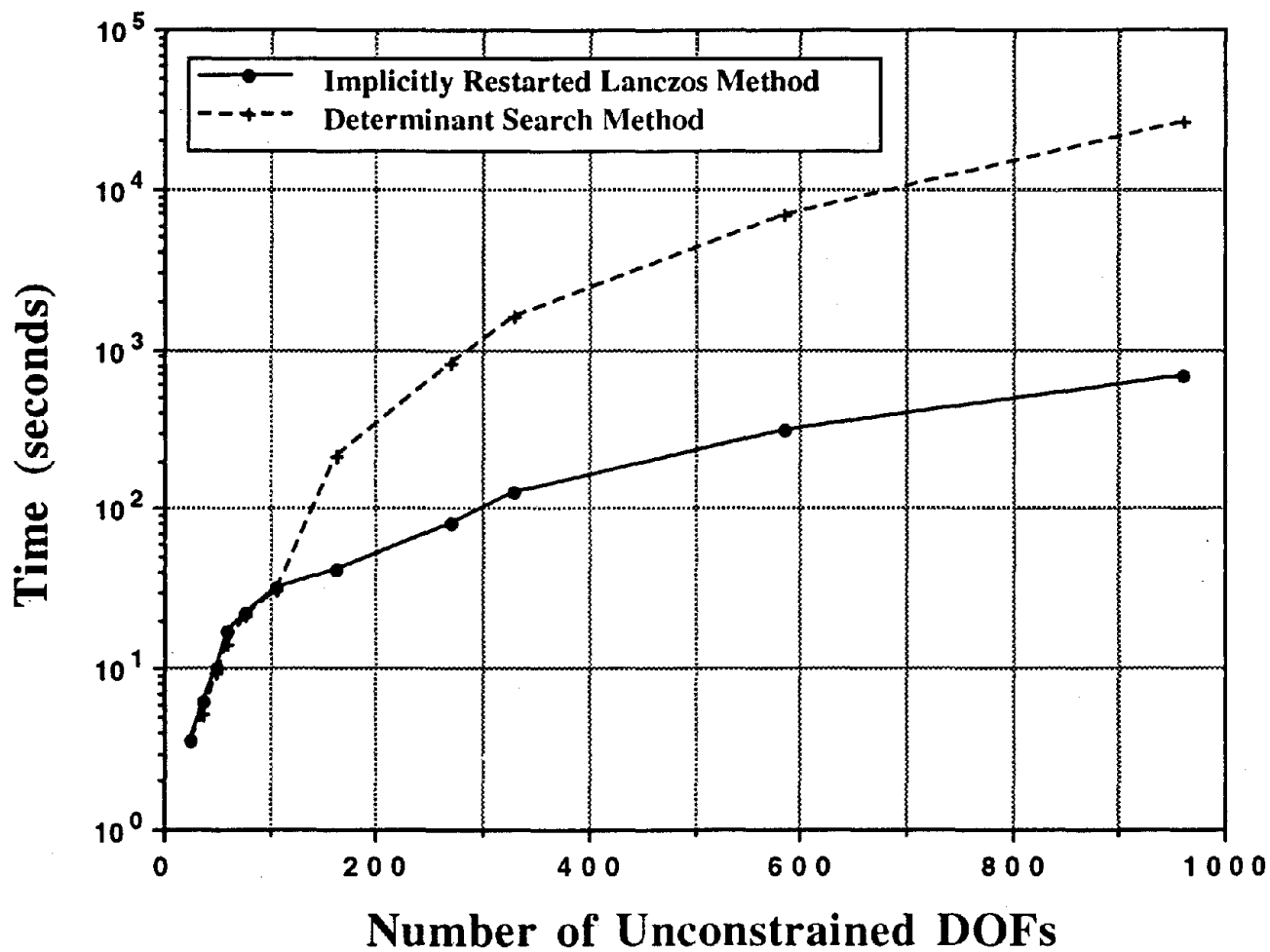
Figure 3.3: Computation time comparisons – I

Figure 3.4: Computation time comparisons – II

3.6.3 Discussion of Results

As illustrated in the first example presented here and in previous publications [34, 52], the mixed finite element formulation which involves a frequency independent **K** and a frequency dependent **M** obtains exact natural modes and frequencies of frame and truss-type structures. This method presents advantages over the computationally intensive exact vibration model where both **K** and **M** are frequency dependent and the conventional finite element model which involves spatial discretization error.

The nonlinear eigensolution technique presented here exploits the unique form of the eigenproblem of Eq. (2.17) associated with the mixed finite element model. In general, the Lanczos-based method is well suited to this class of nonlinear eigenvalue problems on several counts and has clear advantages in the large scale setting over determinant search methods. One advantage seems to be that the parameterized eigenvalue curves are much better behaved in the solution region than the parameterized determinant curves that are associated with the determinant search methods. Moreover, the determinant search method requires a factorization of the entire matrix to evaluate the determinant (or its sign) at each step of the search (i.e., at each successive guess to the solution). In contrast, the Lanczos-based technique only requires matrix vector products to evaluate the eigenvalue curves at each iteration and the number of matrix vector products required is nearly independent of problem size. Finally, reliable error estimates for the quality of the approximate solutions to the discrete problem are readily available.

The implicitly restarted Lanczos method also has been compared with a state of the art block Lanczos code from the Boeing Computing Services Library [18]. The tests included a number of problems from the Harwell-Boeing test set and also three

problems from automotive and aerospace modeling. All of these arise from structural vibration analysis applications with problem sizes ranging from 800 to over 250,000 degrees-of-freedom. Several of these problems involved significant clustering of eigenvalues. One such problem is BCSSTK25/BCSSTM25, which has 15,439 degrees-of-freedom and 3 clusters of 64 eigenvalues involving multiple roots. These eigenvalues were computed without difficulty when the stiffness matrix was factored just once and used in regular inverse mode as described earlier. The new method was comparable to the block Lanczos code on all of the problems and excelled considerably in the large scale cases involving over 50,000 degrees-of-freedom. This method outperforms the block Lanczos method in these large scale cases because the latter needs to factor large matrices several times [60]. This example further emphasizes the advantages of the k−step Arnoldi method for eigenproblems in structural dynamics.

Performance Comparison of the Mixed, $h-$ and $p-$Formulations

This chapter presents a performance comparison study of the frequency-dependent mixed finite element formulation with the conventional finite element method using $h-$ and $p-$formulations for free vibration analysis. Performance is defined through a detailed study of accuracy and computational efficiency in obtaining the natural frequencies and modes of skeletal systems. The accuracy of the conventional finite element method, which results in discretization error through use of the approximate shape functions, is increased using two formulations: the $h-$formulation, where the structural model is improved by increasing the model degrees-of-freedom; and the $p-$formulation, where the order of polynomial shape functions are increased to better define element deformation.

4.1 Finite Element Formulations

For the conventional finite element formulations, the polynomial shape functions used to discretize the continuous problem are derived from the approximate solution to the governing equations of motion. For the Bernoulli-Euler beam theory, the shape

functions describing bending behavior are derived from a 3rd order polynomial displacement field of the form

$$v^h_{p_c} = a_0 + a_1 x + a_2 x^2 + a_3 x^3 \tag{4.1}$$

where the superscript h denotes approximation and subscript p_c denotes (conventional) polynomial basis. Shape functions thus obtained are the Hermite polynomials given by Eq. (2.24). This discretization process results in the element stiffness and mass matrices of Eqs. (2.25) and (2.26).

For axial vibrations, the conventional formulation uses a linear displacement field of the form

$$u^h_{p_c} = \bar{a}_0 + \bar{a}_1 x \tag{4.2}$$

and the corresponding shape functions and element stiffness and mass matrices are given by Eqs. (2.19), (2.20) and (2.21). For a general frame element, the bending and the axial degrees-of-freedom are combined together to give 6×6 element stiffness and mass matrices which are assembled following the standard finite element process to get the overall system matrices. This results in the following generalized eigenvalue problem

$$\mathbf{Kx} = \lambda \mathbf{Mx} \tag{4.3}$$

where $\mathbf{K}$ is the system stiffness matrix and $\mathbf{M}$ is the system mass matrix. Complete derivation of the matrices of the conventional formulation is presented in Section 2.3.

In this formulation, stiffness and mass matrices are both frequency independent, symmetric and positive definite, provided rigid body modes have been eliminated.

However, as shown in Section 2.3, use of polynomial shape functions inherits discretization error and the system frequencies are overestimated. This error is particularly severe for higher-order modes. Exact accuracy is obtained in the conventional formulation only as the number of degrees-of-freedom approaches infinity, leading to computational intensity when high accuracy solutions are sought.

In the h−formulation, the discretization error is reduced by successively using an increasing number of degrees-of-freedom in defining the system. For the present investigation, discretization is done such that all finite elements modeling any structural member are of the same length. Thus, in the local coordinate system, all the finite elements in any one structural member have the same stiffness and mass matrices. Furthermore, the form of element matrices remains the same as given by Eqs. (2.25) and (2.26), except for the change in the element length. The first three levels of additional discretization, referred to as H_1, H_2 and H_3, correspond to 2, 3 and 4 elements per member, respectively.

In the p−formulation, the finite element approximation is enriched by using higher-order displacement approximations, by introducing internal nodes. Thus, the conventional polynomial basis given by Eq. (4.1) can be thought of as a p−formulation with zero internal nodes. For the present investigation, three different levels of enrichments are studied with 1, 2 and 3 internal nodes, referred to as P_1, P_2 and P_3, respectively.

In the P_1 formulation, the finite element has one additional node at the mid-point, in addition to the two end nodes; thus, a total of 3 axial and 6 bending degrees-of-freedom are associated. The axial displacement in a finite element is represented by

a 2nd order polynomial of the form

$$u^h_{p_1} = \bar{b}_0 + \bar{b}_1 x + \bar{b}_2 x^2 \tag{4.4}$$

and the corresponding bending displacement is represented by a 5th order polynomial of the form

$$v^h_{p_1} = b_0 + b_1 x + b_2 x^2 + b_3 x^3 + b_4 x^4 + b_5 x^5 \tag{4.5}$$

Combining the axial and bending degrees-of-freedom results in a 9×9 element stiffness and mass matrices.

Analogous to the above, the P_2 formulations has two internal nodes at $\frac{1}{3}$ points from the element ends and uses 3rd and 7th order polynomials to represent the axial and bending displacements, respectively. The element stiffness and mass matrices for a general frame element are of order 12×12. Finally, the P_3 formulation has three internal nodes and uses 4th and 9th order polynomials to represent the axial and bending displacements, respectively. Complete details of all three formulations P_1, P_2 and P_3 are given in the Appendix A.

For the exact finite element formulation, the shape functions used to discretize the continuous problem are derived from the exact, frequency dependent solution to the governing differential equations of motion. Both the system stiffness and mass matrices derived from this formulation are frequency dependent and the resulting eigenvalue problem

$$\mathbf{K}(\lambda)\mathbf{x} = \lambda\mathbf{M}(\lambda)\mathbf{x} \tag{4.6}$$

cannot be solved using conventional numerical techniques. As mentioned before in

Section 2.2, it is computationally very intensive to evaluate the natural frequencies and mode shapes from this formulation since a matrix decomposition has to be performed at each iteration of the eigenvalue analysis.

The mixed formulation uses both the exact and the conventional polynomial shape functions, v_e^h and $v_{p_c}^h$, in formulating the vibration eigenproblem. This formulation is based on a quasi-static representation of element inertia forces. Exact element inertia forces are represented using the frequency dependent shape functions; however, the quasi-static representation based on equivalent load theory allows the displacement due to the inertia force equivalent loads to be represented using the polynomial shape function. The resulting eigenproblem

$$\mathbf{K}\mathbf{x} = \lambda \mathbf{M}(\lambda)\mathbf{x} \qquad (4.7)$$

while still nonlinear, is computationally much easier to solve than Eq. (4.6) where both the system matrices are frequency dependent. Derivation of the matrices of the mixed formulation is presented in Section 2.4.

Although the preceding paragraphs describe the details of approximating the transverse displacement v, a completely analogous procedure is used to approximate the axial deformation u.

4.2 Eigensolution Techniques

Equation (4.3) is a linear, positive definite, symmetric eigenvalue problem which can be solved for the system natural frequencies and modes using conventional eigensolution techniques such as the Lanczos method. However, the eigenproblem of Eq. (4.7)

has to be solved if exact solutions are sought which are free of discretization error. In the present study, the frequency dependent eigenproblem is linearized and solved using a variant of the Lanczos method that has been derived from the more general implicitly restarted Arnoldi method developed by Sorensen [58]. The solution to the linearized eigenproblem is iteratively updated using a secant based zero finding technique.

The Lanczos methods works well in engineering dynamics problems for two primary reasons: only matrix vector products of the system matrices are required, and the largest and smallest eigenvalues tend to emerge prior to completion of the tridiagonalization (which is particularly useful in structural dynamics applications where typically only the smallest few natural frequencies are desired). The implicit restarted Lanczos method treats the residual vector at any step of the Lanczos process as a function of the initial starting vector and iteratively updates the starting vector in a way that forces the norm of the residual vector to converge to zero.

Mathematical and implementation details of the conventional Lanczos method, the implicitly restarted k—step Arnoldi method and the secant based zero finder are presented in Chapter 3.

4.3   Numerical Results

In this section two examples are presented to evaluate the efficiency of the frequency dependent mixed formulation, the dynamic element method, and the h— and p—formulations of the conventional finite element method. In the first example, a simple cantilever beam problem is studied to assess the solution accuracy of the

formulations. An eight story portal frame example is studied later to evaluate more thoroughly both the solution accuracy and computation efficiency of the formulations.

4.3.1   Cantilever Beam Example

A cantilever beam was analyzed using a varying number of finite elements to study the solution convergence for the various formulations. The eigenvalues obtained are then compared to the exact theoretical solution. Rotary inertia effects were included for the elemental mass matrix for the conventional and $h-$formulations only. Material and geometric properties of the cantilever beam are: length, $l = 24$ in; cross-sectional area, $A = 0.5$ in^2; modulus of elasticity, $E = 30 \times 10^6$ lb/in^2; moment of inertia, $I = 0.260417 \times 10^{-2}$ in^4; and mass density, $\rho = 0.724637 \times 10^{-3}$ lb/in^3. Results obtained by Gupta [21] using the DEM formulation, with rotary inertia effects included, are also presented.

Based on these structural properties and the closed-form solution for natural frequency, the exact theoretical frequencies for this cantilever beam are

$$\left. \begin{aligned} \omega_n &= \frac{(2n-1)}{2}\pi\sqrt{\frac{EI}{ml^2}} \\ &= \{13317.1, \ 39951.2, \ 66585.4, \ \cdots\} \ rad/sec \end{aligned} \right\} (axial), \qquad (4.8)$$

and

$$\left. \begin{aligned} \omega_n &= \alpha_n^2\sqrt{\frac{EI}{ml^4}} \\ &= \{89.6351, \ 561.734, \ 1572.87, \ 3082.20 \\ &\quad 5095.10, \ 7611.19, \ 10630.5, \ 14153.0, \ \cdots\} \ rad/sec \end{aligned} \right\} (bending), \qquad (4.9)$$

where α_n is the nth solution to the transcendental equation $(1 + \cos\alpha \cdot \cosh\alpha) = 0$.

Table 4.1: Natural frequencies for the cantilever beam

Freq.	h—formulation	p—formulation	DEM [21]	Mixed
1	89.641	89.635	89.636	89.635
2	563.480	561.742	561.672	561.734
3	1591.90	1573.36	1573.78	1572.87
4	3583.95	3273.08	3200.20	3082.20
5	6741.77	5699.08	5801.82	5095.10

Looking at the frequency distribution of Eqs. (4.8) and (4.9), it is apparent that the seven lowest modes of vibration are all flexural modes, and the first axial mode corresponds to the eighth system mode. Thus, to define uniquely the *contiguous* set of the lowest five mode shapes, a minimum of five bending degrees-of-freedom (or three finite elements) are needed and used for all analyses here. Table 4.1 presents the results of the free vibration analyses using the different finite element formulations. The natural frequencies for the first five modes are computed for a problem size $N = 9$ for each formulation. As shown in Table 4.1, the p—formulations gives more accurate results than the h—formulations, even when rotary inertia effects have not been included in the former. While the DEM formulation performs better than the h—formulation, it is less accurate than the mixed formulation, especially for the higher modes.

Figure 4.1 graphically compares the error percentage for each of the five modes. The accuracy of the mixed formulation results is clearly greater than that obtained by the other three formulations.
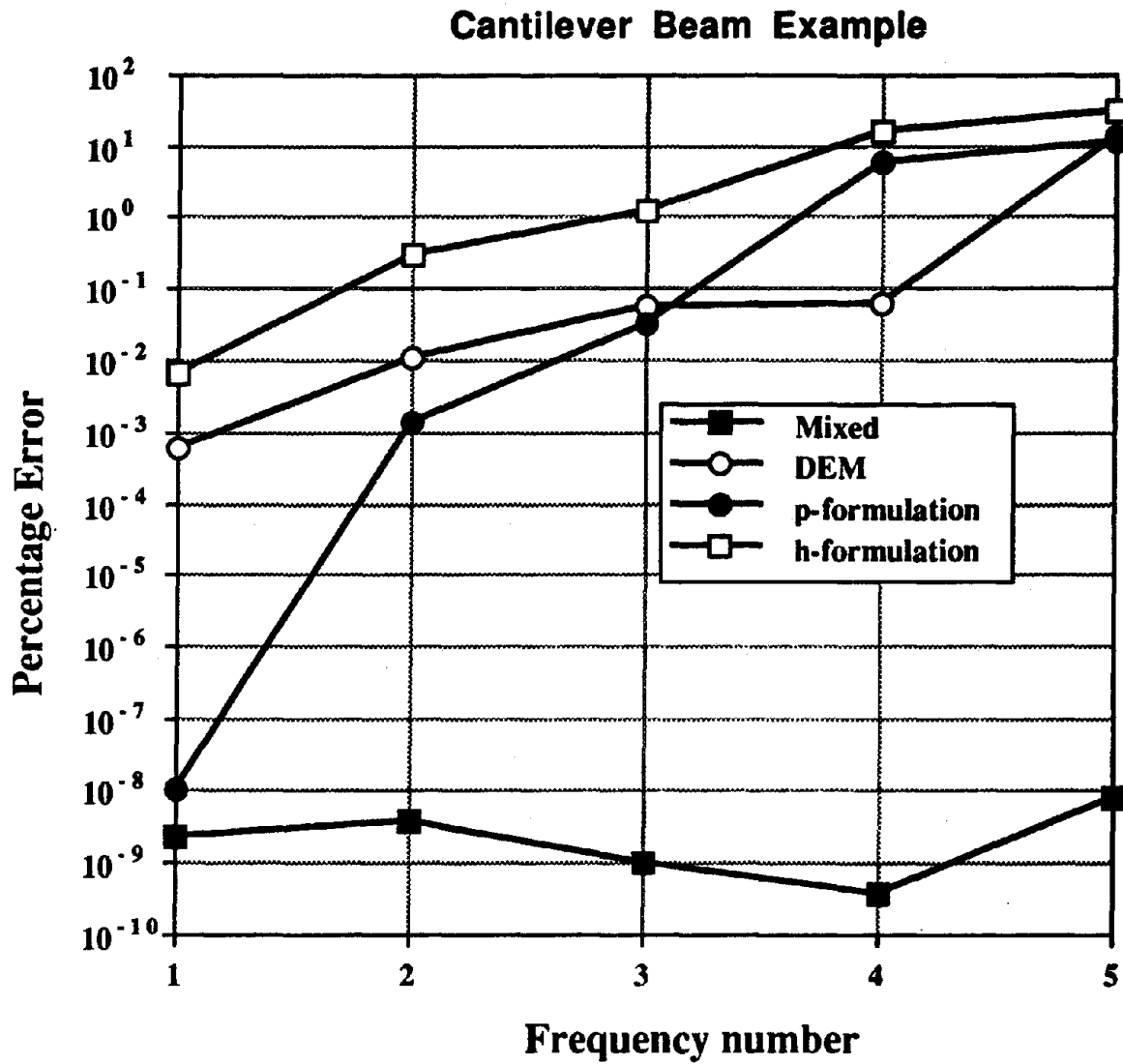
Figure 4.1: Percentage error for different modes

4.3.2 Portal Frame Example

Numerical results for a three bay, eight story portal frame originally studied by reference [27] and shown in Figure 4.2 are presented. The first fifteen natural frequencies are tabulated in Table 4.2 for the conventional, mixed, h−formulation and p−formulations along with the solutions obtained from reference [27] which is based on the exact finite element formulation. For the conventional and the mixed formulations, the minimum number of finite elements needed to define the geometry is used (i.e., one element per member) leading to a 96 degree-of-freedom model. In the h−formulation, three different discretization patterns are used: H_1, with 2 elements per structural member leading to a 264 degree-of-freedom model; H_2 with 3 elements per member leading to a 432 degree-of-freedom model; and H_3 with 4 elements per structural member leading to a 600 degree-of-freedom model. The p−formulation uses 1 element per member, but P_1, P_2, and P_3 contain 1, 2, and 3 internal nodes, respectively; thus, H_i and P_i have the same number of degrees-of-freedom. Due to use of higher-order interpolations, the p−formulation requires internal nodes to represent the higher-order displacement fields and leads to system matrices with larger bandwidths.

Referring to Table 4.2, it is seen that, as expected, the conventional formulation results are an upper bound to the exact results of the mixed formulation and that of the reference [27]. Furthermore, the higher modes have much larger errors indicating that the conventional formulation is unable to adequately represent higher-order element deformations. The mixed formulation solutions agree with the results of
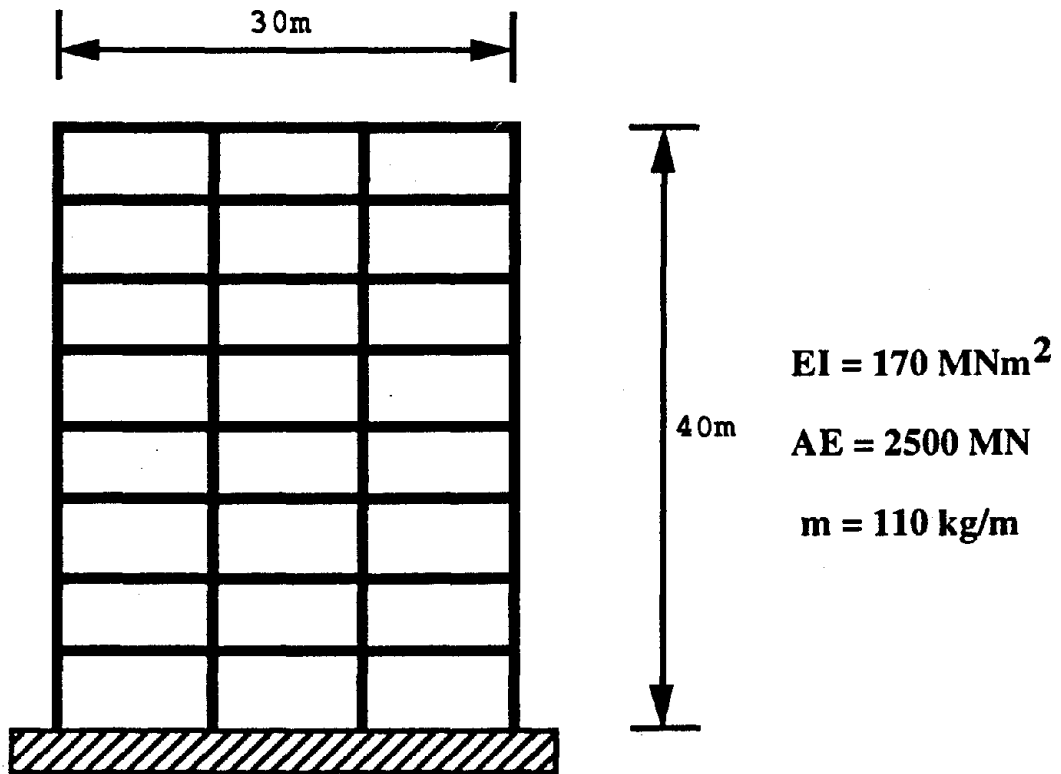
Figure 4.2: Three bay, eight story portal frame

Table 4.2: First 15 frequencies (rad/sec) for eight story portal frame

| Freq.	Conv	Mixed	P_1	P_2	P_3	H_1	H_2	H_3	Ref. [27]
N	96	96	264	432	600	264	432	600	96
1	11.21	11.21	11.21	11.21	11.21	11.21	11.21	11.21	11.21
2	34.80	34.79	34.79	34.79	34.79	34.79	34.79	34.79	34.79
3	61.79	61.74	61.74	61.74	61.74	61.74	61.74	61.74	61.74
4	92.58	92.41	92.41	92.41	92.41	92.44	92.42	92.41	92.41
5	108.29	104.39	104.39	104.39	104.39	104.62	104.43	104.40	104.39
6	123.01	118.07	118.07	118.07	118.07	118.38	118.13	118.09	118.07
7	127.63	127.16	127.16	127.16	127.16	127.24	127.19	127.17	127.16
8	147.89	142.08	142.09	142.08	142.08	142.55	142.18	142.11	142.08
9	161.45	160.33	160.33	160.33	160.33	160.80	160.43	160.37	160.33
10	165.85	164.77	164.77	164.77	164.77	165.00	164.84	164.80	164.77
11	202.57	176.58	176.71	176.58	176.58	177.88	176.86	176.67	176.58
12	220.90	187.23	187.40	187.23	187.23	188.79	187.57	187.34	187.23
13	231.85	194.76	194.95	194.76	194.76	196.51	195.14	194.88	194.76
14	243.85	198.18	198.27	198.18	198.18	199.12	198.43	198.28	198.18
15	262.42	203.43	203.65	203.43	203.43	204.95	203.84	203.57	203.43
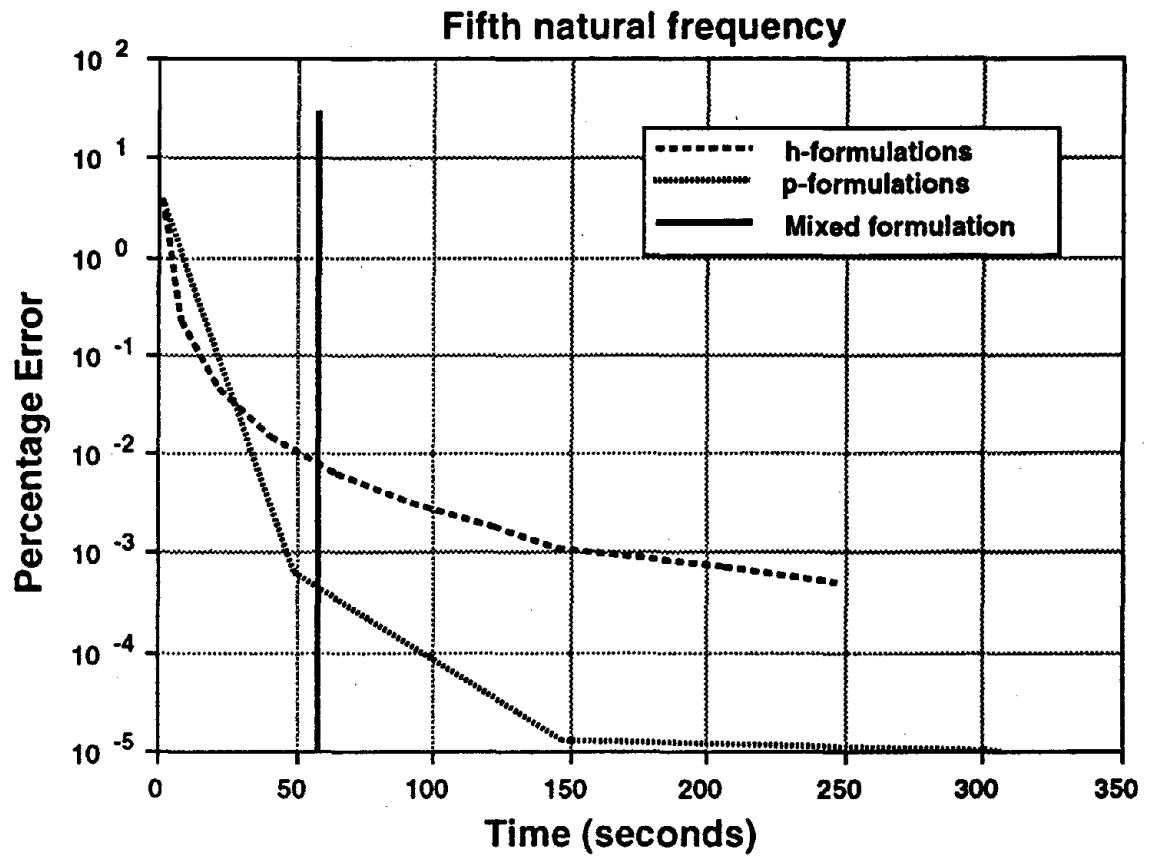
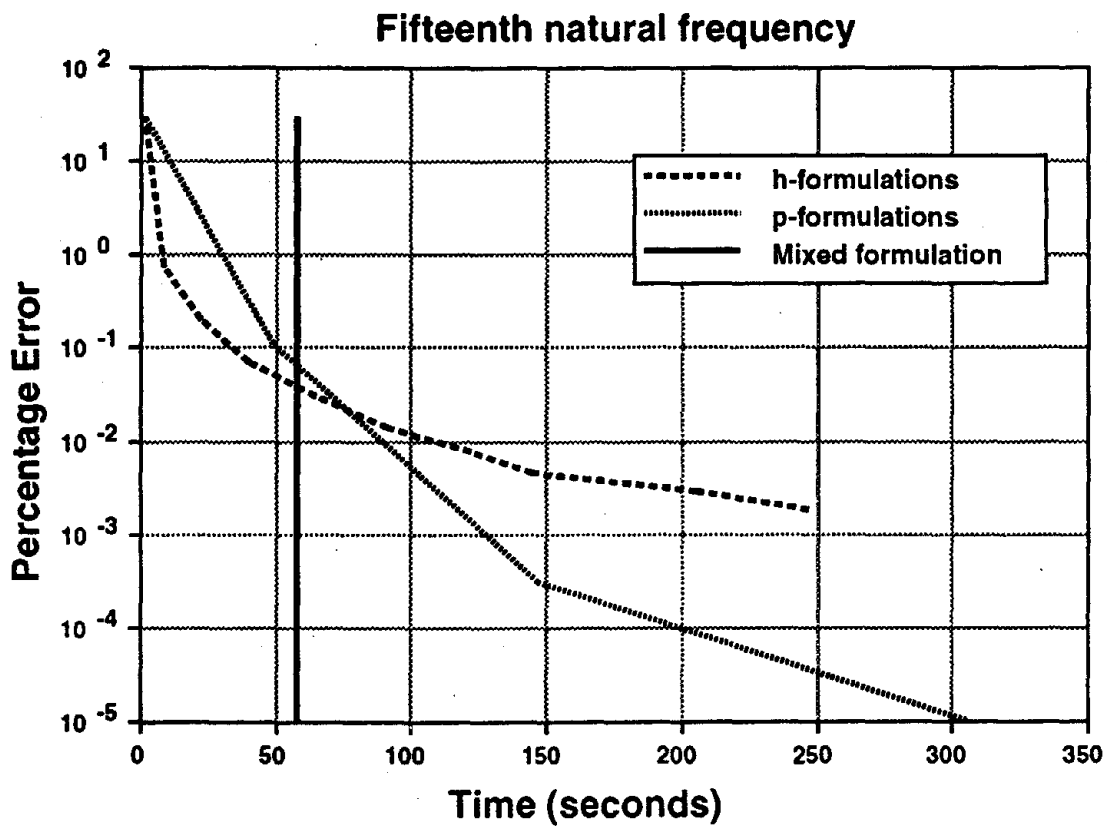Figure 4.3: Percentage error versus computational time – I

Figure 4.4: Percentage error versus computational time – II

reference [27] for all fifteen frequencies. The $h-$ and $p-$formulation results are progressively better than the conventional formulation results and approach the exact results as the total number of degrees-of-freedom in the model increases.

Figures 4.3 and 4.4 illustrates the performance comparison between the finite element formulations in terms of computational time and percent error for the 5th and 15th modes. Comparing h and p curves for both the plots, it is seen that for relatively low precision requirements (error $\leq 0.3 - 0.5\%$), the $h-$formulation performs better than the $p-$formulation. This is primarily due to the larger bandwidth associated with the latter formulation. However, as indicated by the slope of the p curves, the rate of convergence for the $p-$formulation is much greater than that for the $h-$formulation. This is due to the use of the higher-order polynomial shape functions in the $p-$formulation. Furthermore, comparing the $h-$formulation curves in the two plots of Figures 4.3 and 4.4, shows that the two curves are nearly identical except for the initial shift. This indicates that the asymptotic rate of convergence is similar for both low and high frequency modes.

The mixed formulation, with frequency dependent mass matrix, is computationally more intensive and, therefore, uncompetitive when accuracy requirements are low. However, for moderate and high accuracy requirements, it outperforms all the other formulations. This method is particularly very cost effective in obtaining higher modes. For the 15th frequency, the mixed formulation is about 6 times less intensive than the $p-$formulation and more than an order of magnitude less intensive than $h-$formulation.

4.3.3   Discussion of Results

Results and conclusions of the previous section show that the conventional formulation inherits discretization error, unacceptably large for higher modes. The h−formulation attempts to reduce these discretization errors by introducing more degrees-of-freedom; whereas, the p−formulation uses higher-order polynomials to approximate the displacement field in addition to introducing more degrees-of-freedom. For moderate accuracy requirements, the h−formulation is more efficient than the p−formulation due to the increased bandwidth associated with the internal nodes of the p−formulation. However, for high accuracy requirements, the p−formulation, despite its high bandwidth, performs superior to the h−formulation. When very accurate results are required, the mixed formulation out performs both the h− and p−formulations. Numerical results are presented for a three bay, eight story frame to to support these conclusions.

Interior Eigenvalue Problem

This chapter discusses application of the implicitly shifted Arnoldi-based eigensolver for computing the eigenvalues from the interior of the spectrum. In most structural dynamics analyses, where a structure is subject to natural loadings such as wind or earthquakes, usually only the lowest few vibrating modes are of interest. The frequency content of these natural loadings is usually in a range such that the higher order structural modes cannot be excited. However, there are situations when there is a need to accurately solve for some set of frequencies that lie in the interior of the eigenvalue spectrum. A common application is to determine if any of the higher-order modes of a building are close to some vibrating machinery that might be inside the building, so as to avoid any possibility of resonance.

5.1   Conventional Formulation

In its simplest form, the interior eigenvalue problem involves determining a set of eigenvalues λ_j and eigenvectors $\mathbf{x}_j$ of

$$\mathbf{K}\mathbf{x}_j = \lambda_j \mathbf{M}\mathbf{x}_j \tag{5.1}$$

for $j = 1, 2, \cdots, m$ such that all the λ_j's are greater than a specified threshold σ.

Omitting the subscript j for simplicity, and rewriting Eq. (5.1) in terms of the inverse of the eigenvalue, results in the standard eigenvalue problem discussed in Chapter 3 which is repeated here for clarity

$$\mu(\lambda)\mathbf{x} = \mathbf{K}^{-1}\mathbf{M}(\lambda)\mathbf{x} \qquad (5.2)$$

For the eigenvalue problem of the conventional finite element, a shift and invert strategy is used that transforms the eigenvalues from the interior of the spectrum to the ends of the spectrum. Specifically, for some prespecified shift σ, subtracting $\sigma\mathbf{Mx}$ from both sides of Eq. (5.1) gives

$$[\mathbf{K} - \sigma\mathbf{M}]\mathbf{x} = (\lambda - \sigma)\mathbf{Mx} \qquad (5.3)$$

or,

$$\hat{\mu}\mathbf{x} = [\mathbf{K} - \sigma\mathbf{M}]^{-1}\mathbf{Mx} \qquad (5.4)$$

where $\hat{\mu} = \dfrac{1}{(\lambda - \sigma)}$. As a result of this transformation, eigenvalues from the interior that are in the vicinity of the shift σ are the new extreme eigenvalues in the μ spectrum. It should be noted that in the above formulation, the matrix inverse is used only symbolically. In the numerical implementation, banded matrix factorization and banded matrix vector multiplication is used in place of inversion.

The shifted stiffness matrix $\hat{\mathbf{K}} = [\mathbf{K} - \sigma\mathbf{M}]$ may no longer be positive definite and, thus, the Cholesky factorization cannot be used. Pivoting is required during factorization to avoid large error growth. The drawback is that pivoting increases the

bandwidth of the shifted stiffness matrix and the resulting *LU* factors require three times as much storage space as the unshifted stiffness matrix, even when factorization is done in-place.

5.2   Mixed Formulation

For the eigenvalue problem of the mixed formulation the mass matrix is frequency dependent and, hence, the shifted stiffness matrix, $\hat{\mathbf{K}}(\lambda)$ is also frequency dependent. This necessitates an *LU* factorization of the matrix $\hat{\mathbf{K}}(\lambda)$ at each iteration of the solution procedure. Thus, the simple shift and invert strategy used for the linear interior eigenvalue problem is computationally very intensive and inefficient for the nonlinear interior eigenvalue problem associated with the mixed finite element formulation.

An alternate approach is to factor the unshifted stiffness matrix $\mathbf{K}$ and shift the mass matrix. Subtracting $\bar{\sigma}\mathbf{K}\mathbf{x}$ from both sides of the inverse eigenvalue problem

$$\mu(\lambda)\mathbf{K}\mathbf{x} = \mathbf{M}(\lambda)\mathbf{x} \tag{5.5}$$

results in

$$(\mu(\lambda) - \bar{\sigma})\mathbf{K}\mathbf{x} = [\mathbf{M}(\lambda) - \bar{\sigma}\mathbf{K}]\mathbf{x} \tag{5.6}$$

Defining $\bar{\mu}(\lambda) = \mu(\lambda) - \bar{\sigma}$ and $\bar{\mathbf{M}}(\lambda) = \mathbf{M}(\lambda) - \sigma\mathbf{K}$ results in the shifted eigenproblem in the form

$$\bar{\mu}(\lambda)\mathbf{K}\mathbf{x} = \bar{\mathbf{M}}(\lambda)\mathbf{x} \tag{5.7}$$

which is similar to the extreme eigenvalue problem. From an implementation viewpoint, we need factor $\mathbf{K}$ only once, just as in the case of extreme eigenvalue computation. Furthermore, since the unshifted stiffness matrix is positive definite, a Cholesky decomposition, $\mathbf{K} = \mathbf{L}\mathbf{L}^T$, can be used and, thus, Eq. (5.7) can be transformed into an equivalent symmetric standard eigenvalue problem. However, in engineering problems, it is natural to specify a shift value σ in the λ spectrum, whereas the transformed eigenproblem above requires a shift $\bar{\sigma}$ in the μ spectrum. A simple substitution like $\bar{\sigma} = \dfrac{1}{\sigma}$ often does not work. In other words, this shift technique does not change the separation of the eigenvalue spectrum and exhibits poor convergence properties when used with ARPACK [59].

Another way to overcome this difficulty is to decompose $\mathbf{M}(\lambda)$ into $\lambda-$independent and $\lambda-$dependent parts. In this research, a decomposition of the form

$$\mathbf{M}(\lambda) = \mathbf{M}(\lambda_0) + \mathbf{M}_1(\lambda) \tag{5.8}$$

is used for $\lambda_0 = 0$ and $\lambda_0 = \sigma$. Substituting Eq. (5.8) into Eq. (5.1) gives

$$\mathbf{K}\mathbf{x} = \lambda[\mathbf{M}_0 + \mathbf{M}_1(\lambda)]\mathbf{x} \tag{5.9}$$

where $\mathbf{M}_0 = \mathbf{M}(\lambda_0)$. Applying a shift at $\lambda = \sigma$,

$$[\mathbf{K} - \sigma\mathbf{M}_0]\mathbf{x} = \lambda\left[\left(1 - \frac{\sigma}{\lambda}\right)\mathbf{M}_0 + \mathbf{M}_1(\lambda)\right]\mathbf{x} \tag{5.10}$$

or,

$$\mu(\lambda)\mathbf{x} = \hat{\mathbf{K}}^{-1} \cdot \tilde{\mathbf{M}}(\lambda)\mathbf{x} \tag{5.11}$$

where

$$\hat{\mathbf{K}} = [\mathbf{K} - \sigma\mathbf{M}_0]$$
$$\tilde{\mathbf{M}}(\lambda) = \left[\left(1 - \frac{\sigma}{\lambda}\right)\mathbf{M}_0 + \mathbf{M}_1(\lambda)\right] \tag{5.12}$$

The above equation avoids the need for an *LU* factorization at each step of the iteration, and satisfactory results are obtained for a number of eigenvalues close to the shift value σ. A slight variation in the above allows a considerable speed up in convergence for this problem. Defining

$$\hat{\mu} = \frac{1}{(\mu^{-1} - \sigma)} \tag{5.13}$$

and rewriting Eq. (5.10) results in

$$\begin{aligned}
[\mathbf{K} - \sigma\mathbf{M}_0]\mathbf{x} &= \lambda\left[\left(1 - \frac{\sigma}{\lambda}\right)\mathbf{M}_0 + \mathbf{M}_1(\lambda)\right]\mathbf{x} \\
&= (\lambda - \sigma)\left[\mathbf{M}_0 + \frac{\lambda}{(\lambda - \sigma)}\mathbf{M}_1(\lambda)\right]\mathbf{x} \\
&= (\lambda - \sigma)\left[\frac{\lambda}{(\lambda - \sigma)}\mathbf{M}(\lambda) - \frac{\sigma}{(\lambda - \sigma)}\mathbf{M}_0\right]\mathbf{x}
\end{aligned} \tag{5.14}$$

or,

$$\hat{\mu}(\lambda)\mathbf{x} = \hat{\mathbf{K}}^{-1} \cdot \hat{\mathbf{M}}(\lambda)\mathbf{x} \tag{5.15}$$

where $\hat{\mathbf{M}}(\lambda)$ is the shifted frequency dependent mass matrix given by the bracketed expression on the right hand side of Eq. (5.14). As before, the eigenvalue problem of Eq. (5.15) requires only one factorization. This property is exploited to make the zero finder converge very quickly to the intersection of curves $\hat{\mu}(\lambda)$ and $\frac{1}{(\lambda - \sigma)}$.

Figures 5.1 shows the plots of the inverse eigenvalues $\mu_j(\lambda)$ versus the parameter

λ for axial vibration of a cantilevered rod. Eigenvalues of the frequency dependent problem correspond to the intersection points of these curves with the $\dfrac{1}{\lambda}$ curve. These points are marked as 'A', 'B', 'C' and 'D' on the graph and correspond to the first through fourth eigenvalues, respectively, of the unshifted eigenproblem given by Eq. (5.5). For the same cantilevered rod problem, Figure 5.2 shows the plots of the $\hat{\mu}_j(\lambda)$ curves which are solution to the shifted eigenvalue problem given by Eq. (5.15). The parameter λ is varied in the range $0 < \lambda < 1.6$ which includes the entire range of interest for the first four eigenvalues for both the unshifted and shifted cases. The shift value of $\sigma = 0.4$ lies between the second and third eigenvalues. Note that the shifted problem is singular at the shift point (i.e., $\hat{\mu}_j(\lambda)$ curves have a pole at $\lambda = \sigma$). The intersection of the $\hat{\mu}_j(\lambda)$ curves with $\dfrac{1}{(\lambda - \sigma)}$ correspond to the eigenvalues of the shifted problem and are marked by points 'E' and 'F' in Figure 5.2. It should be noted that points 'E' and 'F' for the shifted problem correspond to the points 'C' and 'D' for the unshifted problem, respectively.

5.3   Numerical Results

This section presents an example where eigenvalues from the interior of the spectrum for a two-dimensional frame are computed using the shifted formulation. First a large contiguous set of natural frequencies of the structure is determined using the standard eigenvalue formulations presented in Chapter 3 with one finite element per structural member. For the same finite element model eight different shifts are used to formulate the interior eigenvalue problems. In each shifted case, ten eigenvalues higher than the specified shift are computed. In all cases, the mixed finite element
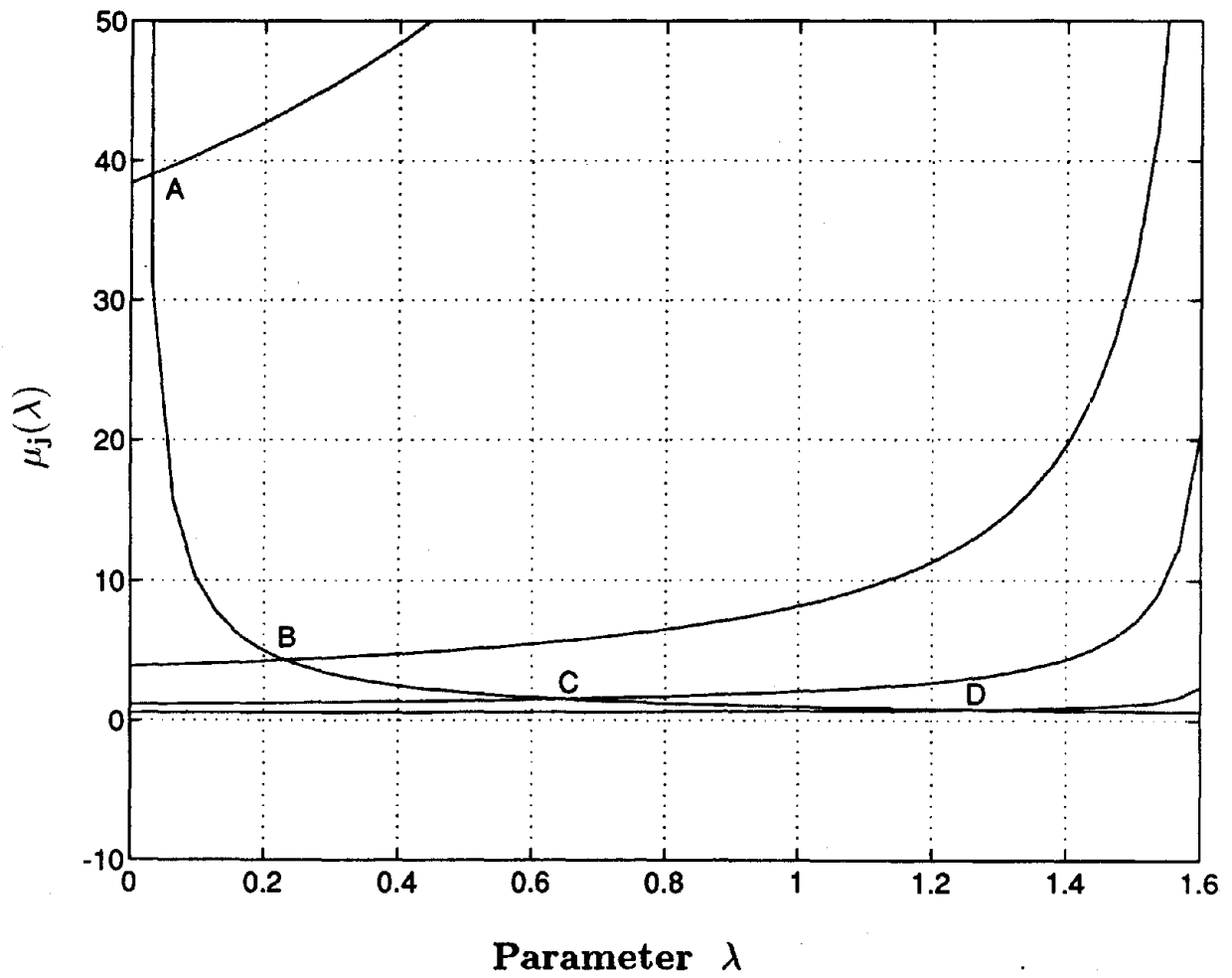
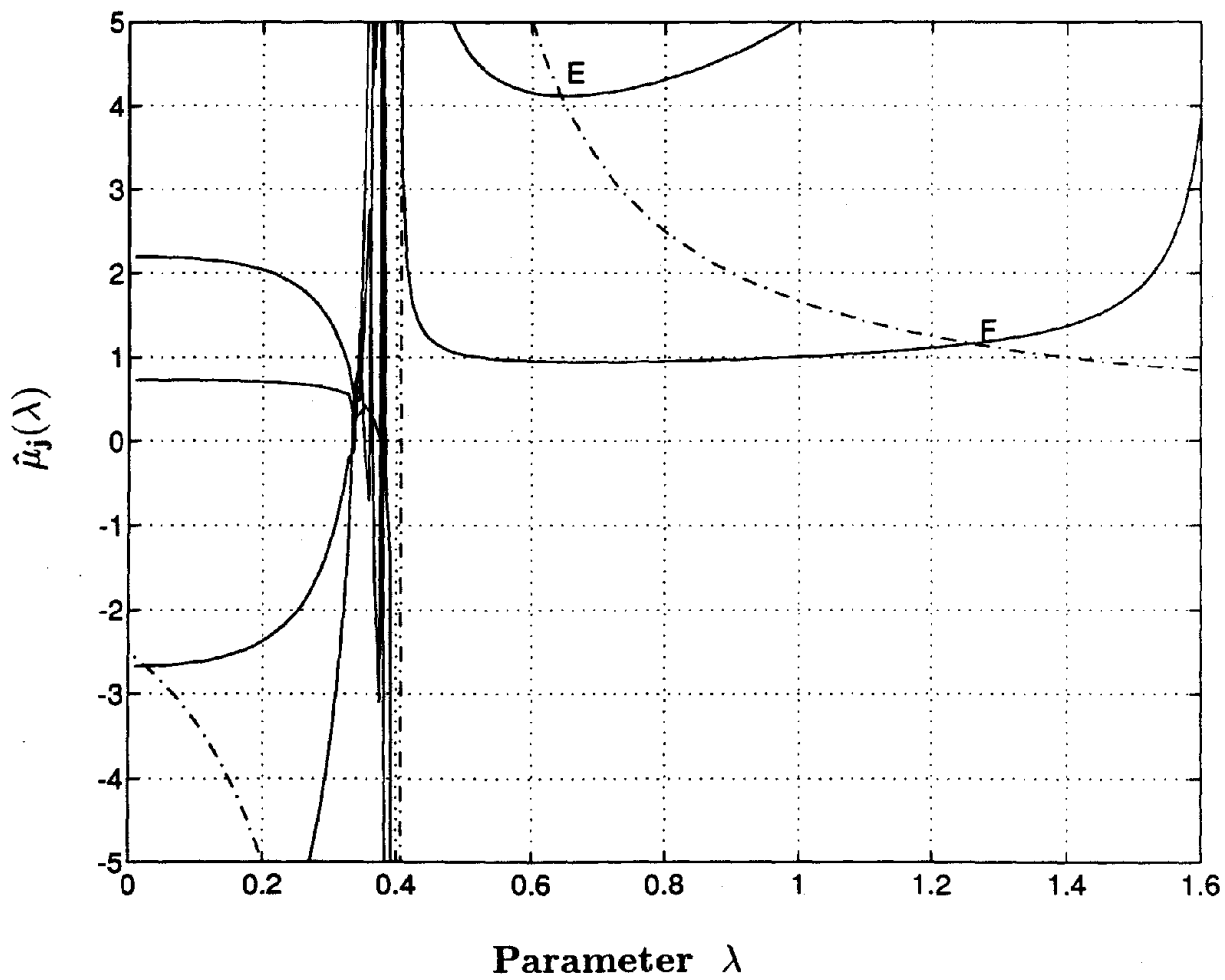Figure 5.1: $\mu_j(\lambda)$ and $\dfrac{1}{\lambda}$ curves for a representative problem

Figure 5.2: $\hat{\mu}_j(\lambda)$ and $\dfrac{1}{(\lambda - \sigma)}$ curves for a representative problem

formulation and implicitly shifted Arnoldi method are used. The solution method is implemented on a DEC 5000 workstation using the libraries and in the environment described in Section 3.5.

5.3.1 Santa Clara County Building

The Santa Clara County Office Building, designed in 1972 and constructed by 1976, is a nearly square thirteen story structure consisting of a steel moment resisting frame with members encased in fire proofing and plaster. The building stands 188 feet in height with sides each measuring 147.5 feet. This structure has been instrumented for strong motions since its construction in 1976. Through conventional system identification techniques the building's natural modes of vibration have been identified from its response to several earthquakes. Using the building's blueprints, a two-dimensional finite element model of the frame number 12, shown in Figure 5.3, was generated.

The two-dimensional model has 140 nodes and 247 general frame elements with various material and geometric properties. After eliminating the boundary conditions, the building has 390 degrees-of-freedom. In this study, first the lowest 50 eigenvalues are determined using the unshifted formulation. Next, a set of eight shifted problems are solved such that

$$\lambda_{(i*5)-1} < \sigma_i < \lambda_{(i*5)}$$

where $i = 1, 2, \cdots, 8$ (i.e., $\lambda_4 < \sigma_1 < \lambda_5$; $\lambda_9 < \sigma_2 < \lambda_{10}$, etc.). In each shifted case, all the eigenvalues greater than the shift value and up to the 50th eigenvalue were computed. Figure 5.4 shows solution times for each of these cases, with curve 1 referring to the shift value σ_1, curve 2 referring to the shift value σ_2, etc. The solution
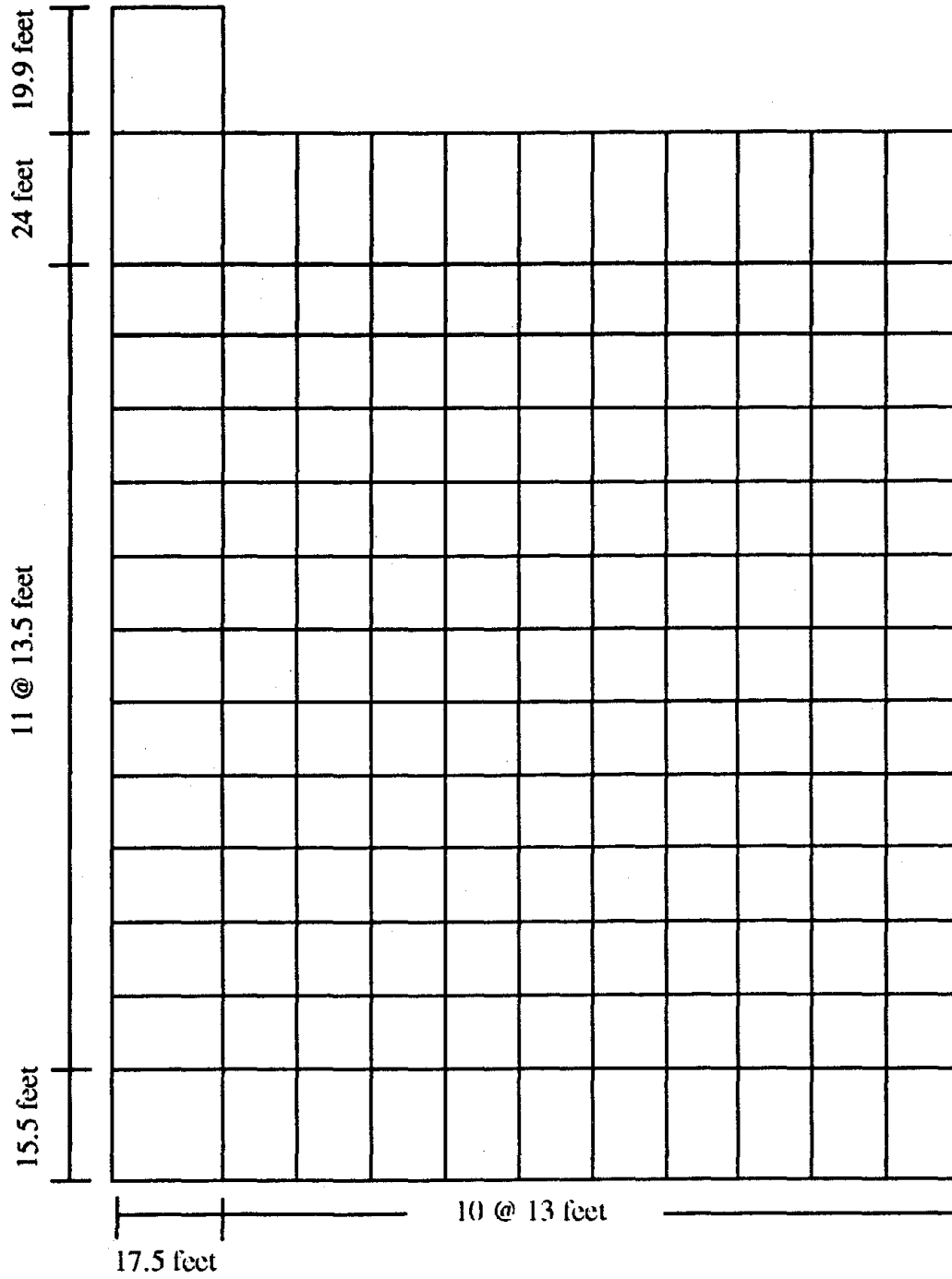
Figure 5.3: Two-dimensional model of the Santa Clara County Building
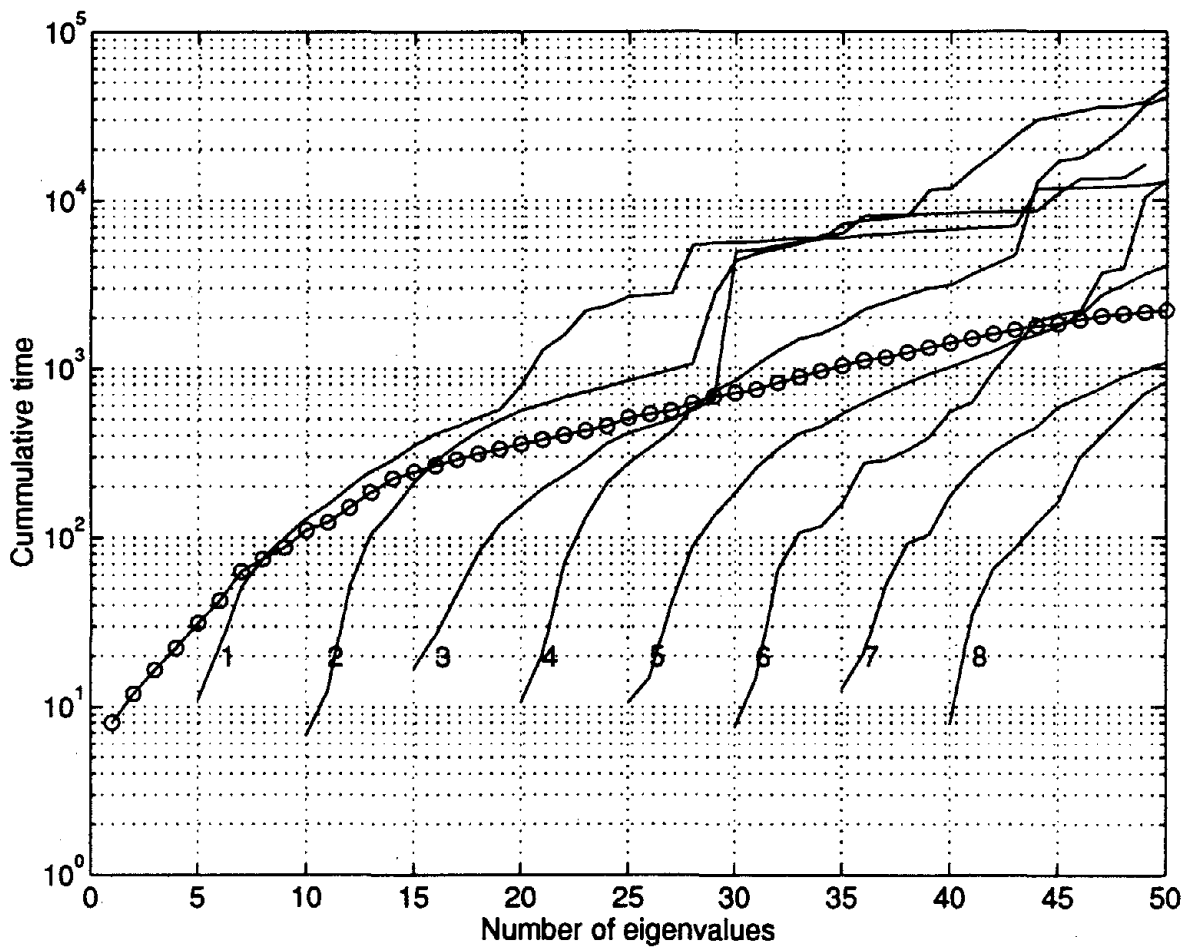
Figure 5.4: Computation time for the interior eigenvalue problem

times for the unshifted problem is denoted by the curve marked with 'o' points.

5.3.2 Discussion of Results

Referring to Figure 5.4, the curves associated with the shifted analyses have a larger slope (particularly, early in the analysis) than the 'o' marked curve associated with the unshifted analysis. This is due to the additional computational costs associated with factoring the non-positive definite shifted stiffness matrix $\hat{\mathbf{K}}$ and solving triangular system with larger bandwidth. However, if only a few eigenvalues close to the shift are required, the shifted analyses are more computationally efficient than the unshifted analysis. When the σ_0 (i.e., unshifted analysis) curve crosses the shifted analyses curves, it becomes more efficient to extract a contiguous set of eigenvalues using the unshifted formulation. This threshold where the curves cross becomes larger for higher-order modes, which is as expected given the time devoted to obtaining the undesired lower eigenvalues of the unshifted formulation. For example, it is preferable to compute all of the first 10 or 15 eigenvalues using the unshifted formulation of Chapter 3, rather than λ_{10} through λ_{15} using the shifted formulation with σ_2. Alternately, for σ_5, computing eigenvalues in the range $\lambda_{25}, \cdots, \lambda_{30}$ requires up to 4 times less time than using the unshifted formulation and computing all the eigenvalues up to λ_{30}.

This threshold, however, is most likely problem dependent, where the slopes of these curves and their intersection with the unshifted curve may change depending on eigenvalue clustering. It should be noted that if a shift is sufficiently close to an eigenvalue, then the solution point, which is the intersection of curves $\hat{\mu}_j(\lambda)$ and $\dfrac{1}{(\lambda - \sigma)}$, may lie in a region where $\hat{\mu}_j(\lambda)$ is not monotonically increasing (see Figure 5.2). In

addition, in some instances the safeguarded secant method converges very slowly for the shifted problem. Therefore, for this example, it is advantageous to use multiple shifts and compute only a few eigenvalues with each shift.
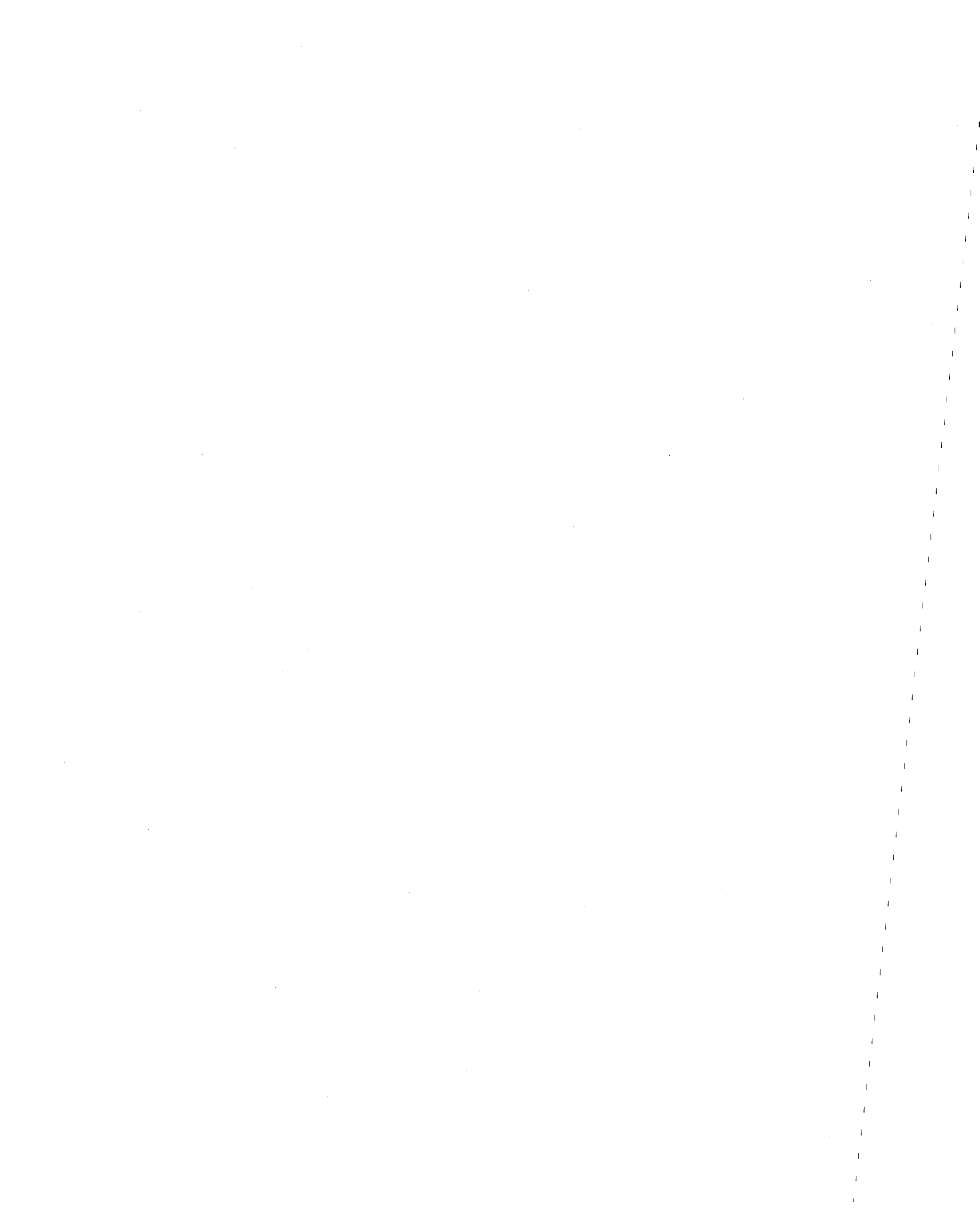
CHAPTER 6

Damped Eigenvalue Problem

The dynamic response of linear systems, such as elastic structures subject to seismic loading, generally is determined using the modal superposition method which is based on uncoupling the equations of motion for an N order multi-degree-of-freedom system into an N set of single degree-of-freedom equations. By performing a free vibration analysis on a classically damped system, the modal orthogonality properties are used to uncouple the system of equations. If the structural model cannot be assumed classically damped, where the damping matrix is represented as a function of the mass and stiffness matrices, this uncoupling of the multi-degree-of-freedom equations of motion cannot be performed.

In finite element analysis, the stiffness and mass matrices are derived based on the expressions for potential and kinetic energy, respectively, where individual element matrices are assembled to form the system matrices after appropriate coordinate transformations are performed. However, due to lack of knowledge concerning damping mechanisms which induce nonconservative forces, it generally is not possible to derive the damping matrix in a similar way. Most often estimates are made of the damping ratios associated with the first few lower modes, where these ratios are specified as a percentage of critical modal damping. If this approach is followed, it is

possible to construct a damping matrix as a function of the stiffness and mass matrices (referred to as proportional damping) such that its use would result in uncoupled equations when eigenvector orthogonality is considered.

6.1 Introduction

This assumption of proportional damping requires that the damping matrix be orthogonal to the free vibration eigenvectors of the structure. In physical terms, this means that the energy loss mechanism is homogeneous throughout the structure. For several applications in civil engineering, such as analyses of soil-structure systems, this assumption is not reasonable and, consequently, the system must be analyzed as nonclassically damped. In addition, it is possible that the damping matrix is proportional for various substructures of a model, where the proportionality constants vary from substructure to substructure. Specifically, individual elements may be modeled as possessing proportional damping that is a function of the element's stiffness and mass matrices. However, since the proportionality constants vary from one structural member to another, upon completion of the assembly process the system damping matrix is no longer proportional to the system stiffness and mass matrices.

Clough and Mojtahedi [9] presented a procedure for evaluating earthquake response of nonproportionally damped structures using a variation of direct integration of the coupled equations of motions, analogous to the classically damped case. Warburton and Soni [66] developed a criterion to determine when the response calculated by proportional damping assumption is unacceptably large. Igusa et al. [29] developed a modal decomposition methodology for the nonproportionally damped systems

and gave closed form solutions for the the case of response to a white noise. Singh and Ghafory-Ashtiany [49] used a complex-valued modal time history analysis to compute the forced vibration response. Gupta and Jaw [19, 20] presented a response spectrum method for nonproportionally damped coupled systems.

For a proportionally damped system, the eigenvectors governing the free vibration response of the undamped system diagonalize the equation of motion governing the damped system. However, for nonproportionally damped systems, decoupling of the damped equation of motion requires use of the (complex) eigenvectors associated with the damped problem; thus, demanding solution of the nonproportionally damped free vibration problem. Solutions to the nonproportionally damped free vibration problem usually involve transforming the original quadratic eigenproblem of order N into an eigenproblem of order $2N$. This eigenproblem is nonsymmetric and cannot be solved using the conventional Lanczos methods.

6.2   Proportional Damping

In finite element analysis, the system stiffness and mass matrices are assembled from the element stiffness and mass matrices. The element matrices are derived using the finite element shape functions and using virtual work principles. However, it is generally not possible to build the element damping matrix in a similar way. Most often estimates are made of the damping ratios associated with the first few lower modes, based on previous experience or experimental results. These ratios are specified as a percentage of critical modal damping. If this approach is followed, it is possible to construct a damping matrix as a function of the stiffness and mass matrices such

that its use would result in uncoupled equations in the following way.

Consider a $N-$ degrees-of-freedom finite element discretization of a structure. The undamped eigenvalue problem has the form

$$\mathbf{Kx}_i = \lambda_i^2 \mathbf{Mx}_i \tag{6.1}$$

where $\lambda_i^2, \mathbf{x}_i$ for $i = i, 2, \ldots, N$ are the eigenvalues and mass-orthonormalized eigenvectors, respectively. By definition, the mass-orthonormality relation gives

$$\mathbf{x}_j^T \mathbf{Mx}_i = \begin{cases} 0 & i \neq j \\ 1 & i = j \end{cases} \tag{6.2}$$

Premultiplying both sides of Eq. (6.1) by $\mathbf{x}_j^T \mathbf{KM}^{-1}$ gives

$$
\begin{aligned}
\mathbf{x}_j^T \mathbf{KM}^{-1} \mathbf{Kx}_i &= \lambda_i (\mathbf{x}_j^T \mathbf{KM}^{-1}) \mathbf{Mx}_i \\
&= \lambda_i^2 \mathbf{x}_j^T \mathbf{Kx}_i \\
&= \begin{cases} 0 & i \neq j \\ \lambda_i^4 & i = j \end{cases}
\end{aligned} \tag{6.3}
$$

The left hand side in Eq. (6.3) can be rewritten as

$$
\begin{aligned}
\mathbf{x}_j^T \mathbf{KM}^{-1} \mathbf{Kx}_i &= \mathbf{x}_j^T (\mathbf{MM}^{-1}) \mathbf{KM}^{-1} \mathbf{Kx}_i \\
&= \mathbf{x}_j^T \mathbf{M} (\mathbf{M}^{-1} \mathbf{K})^2 \mathbf{x}_i
\end{aligned} \tag{6.4}
$$

Substituting Eq. (6.3) into Eq. (6.4) and repeatedly premultiplying Eq. (6.3) by $\mathbf{x}_j^T \mathbf{KM}^{-1}$, the following family of generalized orthogonality relationships are obtained

for $m = 0, \pm 1, \pm 2, \ldots, \pm \infty$.

$$\mathbf{x}_j^T \mathbf{M} (\mathbf{M}^{-1} \mathbf{K})^m \mathbf{x}_i = \begin{cases} 0 & i \neq j \\ (\lambda_i^2)^m & i = j \end{cases} \tag{6.5}$$

A detailed derivation of Eq. (6.5) is presented in Humar [28].

The above generalized orthogonality relationship can be used to construct a damping matrix in such a way that the modal equations are uncoupled. The simplest case is mass proportional damping given by

$$\mathbf{C} = \alpha_0 \mathbf{M} \tag{6.6}$$

where α_0 is the constant of proportionality. It is easily verified that

$$
\begin{aligned}
\mathbf{x}_j^T \mathbf{C} \mathbf{x}_i &= \alpha_0 \mathbf{x}_j^T \mathbf{M} \mathbf{x}_i \\
&= \begin{cases} 0 & i \neq j \\ \alpha_0 & i = j \end{cases} \\
&= \begin{cases} 0 & i \neq j \\ 2\xi_i \omega_i & i = j \end{cases}
\end{aligned} \tag{6.7}
$$

where ξ_i and ω_i are the modal damping and natural frequency for the ith mode. In the form given by Eq. (6.7), there is one free parameter α_0 which can be selected so as to obtain a desired modal damping in any one mode. Damping in all other modes is inversely proportional to the undamped free vibration frequencies. Thus, if the damping is fixed is at 5% in the first mode, then $\alpha_0 = 2(0.05)\omega_1$ and $\xi_j = 0.05 \left(\frac{\omega_1}{\omega_j}\right)$ for $j = 2, 3, \cdots, n$. A second form of proportional damping, called stiffness proportional

damping, is given by

$$\mathbf{C} = \alpha_1 \mathbf{K} \tag{6.8}$$

in which the damping matrix $\mathbf{C}$ is orthogonal to the eigenvectors $\mathbf{x}_i$'s. In this case also, the one free parameter α_1 can be selected so as to obtain a desired modal damping in any one mode. Damping in any other mode is proportional to the natural frequency for that mode.

Using the generalized orthogonality relationship given by Eq. (6.5), desired modal damping can be specified in p modes using the following proportional damping matrix

$$
\begin{aligned}
\mathbf{C} &= \sum_{j=0}^{p} \alpha_j \mathbf{M} (\mathbf{M}^{-1} K)^j \\
&= \alpha_0 \mathbf{M} + \alpha_1 \mathbf{K} + \alpha_2 \mathbf{K} \mathbf{M}^{-1} \mathbf{K} + \cdots
\end{aligned}
\tag{6.9}
$$

The Rayleigh damping corresponds to truncating the above series at $j = 2$, thus including the effects of both the mass proportional and stiffness proportional damping.

6.3   Nonproportional Damping

The energy loss mechanisms which are operative in the response of a structure to transient loads such as seismic excitations are not well defined, and it is often difficult to evaluate them precisely. Nevertheless, it is evident that damping has a major influence on the amplitude of response which may be developed and, thus, damping must be included in the finite element model of a structure.

In order for the proportional damping assumptions of the previous section to be valid, it is necessary that the energy loss mechanism be homogeneous throughout

the structure. In many structures there is a significant variation between energy absorption rates of materials in different parts of the structure. For example, beam-column structures in seismic zones are detailed such that plastic hinges are formed in beams and avoided in columns. This causes the distribution of damping forces to be quite different from that of the elastic and inertial forces, since a large part of energy dissipation is provided by formation of plastic hinges and yielding. For a finite element discretization, this means that the damping matrix C is not proportional to the stiffness and mass matrices $\mathbf{K}$ and $\mathbf{M}$, even in the generalized sense of Eq. (6.9). It is also possible that the damping matrix is proportional for various substructures of a model, but the proportionality constants vary from substructure to substructure.

Another important class of problems to which the concept of nonproportional damping applies is the coupled primary-secondary systems. Typically, the primary systems (structures) have higher damping values than the secondary systems (interior substructures). Even if the individual systems are assumed to be proportionally damped, when they are coupled together, the overall system no longer has proportional damping.

The eigenvalue problem associated with damped free vibration is given by

$$\lambda^2 \mathbf{M}\mathbf{x} + \lambda \mathbf{C}\mathbf{x} + \mathbf{K}\mathbf{x} = 0 \qquad (6.10)$$

Iterative procedures like the Lanczos and Arnoldi methods converge to eigenvalues in the part of the eigenvalue spectrum with the largest relative gap. For most structural dynamics problems the eigenvalue spectrum is such that the part with the largest relative gap also corresponds to the part with the largest magnitude. However, for

engineering analyses and design, typically the first few eigenvalues with the smallest magnitude are of greater interest. Thus, it is advantageous to compute the reciprocal of the eigenvalues. Substituting $\mu = \dfrac{1}{\lambda}$ into Eq. (6.10) the equivalent eigenvalue problem is

$$\mathbf{Mx} + \mu\mathbf{Cx} + \mu^2\mathbf{Kx} = 0 \qquad (6.11)$$

Eq. (6.11) is a quadratic eigenvalue problem of size N. Defining

$$\mathbf{Mx} = \mu\mathbf{y} \qquad (6.12)$$

and substituting it into left hand side of Eq. (6.11) gives

$$
\begin{aligned}
\mathbf{Mx} + \mu\mathbf{Cx} + \mu^2\mathbf{Kx} &= \mu\mathbf{y} + \mu\mathbf{Cx} + \mu^2\mathbf{Kx} \\
&= \mu\left(\mathbf{y} + \mathbf{Cx} + \mu\mathbf{Kx}\right) \\
&= 0
\end{aligned}
\qquad (6.13)
$$

$$\text{or,} \quad -\mathbf{Cx} - \mathbf{y} = \mu\mathbf{Kx} \quad \mu \neq 0$$

Equations (6.12) and (6.13) can be combined to give a generalized eigenvalue problem of size $2N$

$$
\begin{bmatrix} -\mathbf{C} & -\mathbf{I} \\ \mathbf{M} & \mathbf{O} \end{bmatrix}
\begin{pmatrix} \mathbf{x} \\ \mathbf{y} \end{pmatrix}
= \mu
\begin{bmatrix} \mathbf{K} & \mathbf{O} \\ \mathbf{O} & \mathbf{I} \end{bmatrix}
\begin{pmatrix} \mathbf{x} \\ \mathbf{y} \end{pmatrix}
\qquad (6.14)
$$

where $\mathbf{I}$ and $\mathbf{O}$ are $N \times N$ identity and zero matrices, respectively. The stiffness matrix $\mathbf{K}$ is symmetric and positive definite. Therefore, the eigenvalue problem of

Eq. (6.14) is equivalent to

$$\mathbf{A}\mathbf{v} = \mu\mathbf{v} \tag{6.15}$$

where

$$\mathbf{A} = \begin{bmatrix} -\mathbf{K}^{-1}\mathbf{C} & -\mathbf{K}^{-1} \\ \mathbf{M} & \mathbf{O} \end{bmatrix} \tag{6.16}$$

and

$$\mathbf{v} = \begin{pmatrix} \mathbf{x} \\ \mathbf{y} \end{pmatrix} \tag{6.17}$$

Matrix $\mathbf{A}$ is real but unsymmetric and, therefore, its eigenvalues μ and eigenvectors $\mathbf{v}$ will occur in complex conjugate pairs. The implicitly shifted Arnoldi method can be used to compute the desired eigenvalues.

6.4 Eigensolution Technique

As described briefly in Chapter 1, the basic Arnoldi factorization can be viewed as a truncated reduction of a matrix $A \in \Re^{n \times n}$ to an upper Hessenberg form, such that the desired part of the eigenvalue spectrum is contained in the reduced matrix. After j steps of this process, the factorization is given by

$$\begin{aligned} \mathbf{A}\mathbf{V}_j &= \mathbf{V}_j\mathbf{H}_j + \mathbf{f}_j\mathbf{e}_j^T \\ \mathbf{V}_j^T\mathbf{f}_j &= 0 \end{aligned} \tag{6.18}$$

where $\mathbf{V}_j \in \Re^{n \times j}$, $\mathbf{V}_j^T \cdot \mathbf{V}_j = \mathbf{I}_j$, $\mathbf{H} \in \Re^{j \times j}$ is the upper Hessenberg matrix, and $\mathbf{f}_j \in \Re^n$ is the residual vector. Equation (6.18) can be alternately written as

$$\mathbf{AV}_j = (\mathbf{V}_j \quad \mathbf{v_j}) \begin{pmatrix} \mathbf{H}_j \\ \beta \mathbf{e}_j^T \end{pmatrix} \tag{6.19}$$

where

$$\beta = \|\mathbf{f}_j\| \quad \text{and} \quad \mathbf{v}_j = \frac{1}{\beta}\mathbf{f}_j. \tag{6.20}$$

From this representation, it can be seen that Eq. (6.19) is just a truncation of the complete reduction

$$\mathbf{A}(\mathbf{V}_j \quad \hat{\mathbf{V}}_j) = (\mathbf{V}_j \quad \hat{\mathbf{V}}_j) \begin{pmatrix} \mathbf{H}_j & \mathbf{G}_j \\ \beta \mathbf{e}_1 \mathbf{e}_j^T & \hat{\mathbf{H}}_j \end{pmatrix} \tag{6.21}$$

where $(\mathbf{V}_j \quad \hat{\mathbf{V}}_j)$ is an orthogonal $n \times n$ matrix and $\hat{\mathbf{H}}_j$ is an $(n-j) \times (n-j)$ upper Hessenberg matrix. The Arnoldi factorization (6.18) can be advanced one step through sequential application of the following recursive formulas.

$$\beta = \|\mathbf{f}_j\|, \quad \mathbf{v}_j = \frac{1}{\beta}\mathbf{f}_j \tag{6.22}$$

$$\mathbf{V}_{j+1} = (\mathbf{V}_j \quad \mathbf{v}_j) \tag{6.23}$$

$$\mathbf{w}_j = \mathbf{A}\mathbf{v}_j, \quad \begin{pmatrix} \gamma \\ \alpha \end{pmatrix} = \mathbf{V}_{j+1}\mathbf{w}_j \tag{6.24}$$

$$\mathbf{H}_{j+1} = \begin{pmatrix} \mathbf{H}_j & \gamma \\ \beta \mathbf{e}_j^T & \alpha \end{pmatrix} \tag{6.25}$$

$$\mathbf{f}_{j+1} = \mathbf{w}_j - \mathbf{V}_{j+1} \begin{pmatrix} \gamma \\ \alpha \end{pmatrix}$$

$$= \left(\mathbf{I} - \mathbf{V}_{j+1} V_{j+1}^T \right) \mathbf{w}_j \tag{6.26}$$

From this development it is seen that

$$\mathbf{A}\mathbf{V}_{j+1} = \mathbf{V}_{j+1}\mathbf{H}_{j+1} + \mathbf{f}_{j+1}\mathbf{e}_{j+1}^T$$

$$\mathbf{V}_{j+1}^T\mathbf{f}_{j+1} = 0 \tag{6.27}$$

Eigenvalues and eigenvectors of the reduced system are computed by the *HQR* method. It should be noted that the above procedure requires repeated formation of matrix vector product of the form $\mathbf{w} = \mathbf{A}\mathbf{v}$. This product is formed as outlined below:

1. Decompose $\mathbf{v}$ into $\mathbf{v}_1 = \mathbf{v}(1:n)$ and $\mathbf{v}_2 = \mathbf{v}(n+1:2n)$

2. Use banded matrix multiplication and banded Cholesky factorization to solve
   $$\mathbf{K}\mathbf{w}_1 = -(\mathbf{C}\mathbf{v}_1 + \mathbf{v}_2)$$

3. Use banded matrix multiplication to form $\mathbf{w}_2 = \mathbf{M}\mathbf{v}_2$

4. Recompose $\mathbf{w}_1$ and $\mathbf{w}_2$ into $\mathbf{w}$ as $\mathbf{w}(1:2n) = [\mathbf{w}_1(1:n), \mathbf{w}_2(1:n)]$

6.5 Mixed Formulation

In the previous section, all the equations were presented for the conventional formulation where both the stiffness and the mass matrices are frequency independent. At

the element level, the damping matrix is formed from the stiffness and mass matrices using specified proportionality constants. The assembled system damping matrix remains frequency independent too.

As discussed in Chapter 3, in the mixed formulation, both polynomial basis and the frequency dependent exact basis are used, and hence the mass matrix is frequency dependent. This allows for representing inertia forces exactly and eliminates the discretization error associated with the conventional formulation. For damped free vibrations, the eigenvalues (frequencies) are complex. Let the complex frequency be $\lambda = \lambda_r + j\lambda_i$, where $j = \sqrt{-1}$, then the pseudo undamped natural frequency and pseudo modal damping are defined as

$$
\begin{aligned}
\hat{\omega} &= (\lambda_r^2 + \lambda_i^2)^{\frac{1}{2}} \\
\hat{\xi} &= \frac{\lambda_r}{\hat{\omega}}
\end{aligned}
\tag{6.28}
$$

The frequency dependent shape functions derived in Chapter 2 are used for the damped free vibration problem with the parameter ω replaced by $\hat{\omega}$. Thus, the parameter b and $\bar{b}$ in Eqs. (2.4) and (2.8) are given as

$$
b = \sqrt{\frac{m\hat{\omega}^2}{EA}}
\tag{6.29}
$$

and

$$
\bar{b} = \left(\frac{m\hat{\omega}^2}{EI}\right)^{\frac{1}{4}}
\tag{6.30}
$$

The frequency dependent mass matrix $\mathbf{M}(\hat{\omega})$ is assembled using the new definition of the parameters b and $\bar{b}$. In the mixed formulation for damped free vibration, the

damping matrix is also frequency dependent and a function of the pseudo undamped natural frequency. The rest of the assembly process for matrices $\mathbf{M}(\hat{\omega})$ and $\mathbf{C}(\hat{\omega})$ remains unchanged. The resulting eigenproblem is given by

$$\mathbf{A}(\lambda)\mathbf{v}(\lambda) = \mu(\lambda)\mathbf{v}(\lambda) \tag{6.31}$$

where

$$\mathbf{A}(\lambda) = \begin{bmatrix} -\mathbf{K}^{-1}\mathbf{C}(\hat{\omega}) & -\mathbf{K}^{-1} \\ \mathbf{M}(\hat{\omega}) & \mathbf{O} \end{bmatrix} \tag{6.32}$$

The secant zero finder is used in conjunction with the implicitly restarted Arnoldi method to compute the eigenvalues and eigenvectors of the nonlinear eigenproblem given by Eq. (6.32). The secant iteration is carried out using the procedure described in Chapter 3, with the exception that $|\mu_j(\lambda)| = \dfrac{1}{\hat{\omega}}$. The iteration process stops when the values of $\hat{\omega}$ used to formulate $\mathbf{M}(\hat{\omega})$ and obtained at the end of the Arnoldi process are within the prescribed tolerance.

6.6 Numerical Results

This section presents examples where the lowest few damped free vibration frequencies are determined. In the first example, a shear building with a damper is analyzed and the solution accuracy is verified with the results presented by Veletsos [65]. This example demonstrates the effect of nonproportional damping. The second example compares the solution accuracy of the mixed formulation to three different levels of discretization using the conventional formulation.

6.6.1   Lumped Parameter Shear Building

A three story building frame with a damper in the bottom story (case 1) and top story (case 2) is presented. The structure is modeled as shear building with uniform story stiffnesses, k, and with floor masses m, m and $\dfrac{m}{2}$ on floors 1, 2 and 3 respectively. The damping coefficient c of the dashpot is expressed as $c = \alpha\,(k\,m)^{\frac{1}{2}}$. The stiffness, mass and damping matrices are as given below.

$$\mathbf{K} = k \begin{bmatrix} 2 & -1 & 0 \\ -1 & 2 & -1 \\ 0 & -1 & 1 \end{bmatrix} \quad \mathbf{M} = m \begin{bmatrix} 1 & & \\ & 1 & \\ & & \frac{1}{2} \end{bmatrix} \tag{6.33}$$

$$\mathbf{C}_{case1} = \alpha\,(k\,m)^{\frac{1}{2}} \begin{bmatrix} 1 & & \\ & 0 & \\ & & 0 \end{bmatrix} \quad \mathbf{C}_{case2} = \alpha\,(k\,m)^{\frac{1}{2}} \begin{bmatrix} 0 & & \\ & 0 & \\ & & 1 \end{bmatrix} \tag{6.34}$$

Table (6.1) lists the complex eigenvalues and modal damping factors for two different levels of damping, $\alpha = 0.5$ and 1.0 for each of the two configurations, where ξ is the percentage modal damping obtained from the damped free vibration analysis. This example was studied by Veletsos [65] as part of a forced vibration analysis. Results presented in Table (6.1) match exactly with the results obtained by Veletsos using library routines from EISPACK. As expected, higher modal damping is obtained when the dashpot is at the top story. Equivalent modal damping in each of the three modes for both cases are shown in Figures 6.1 and 6.2.
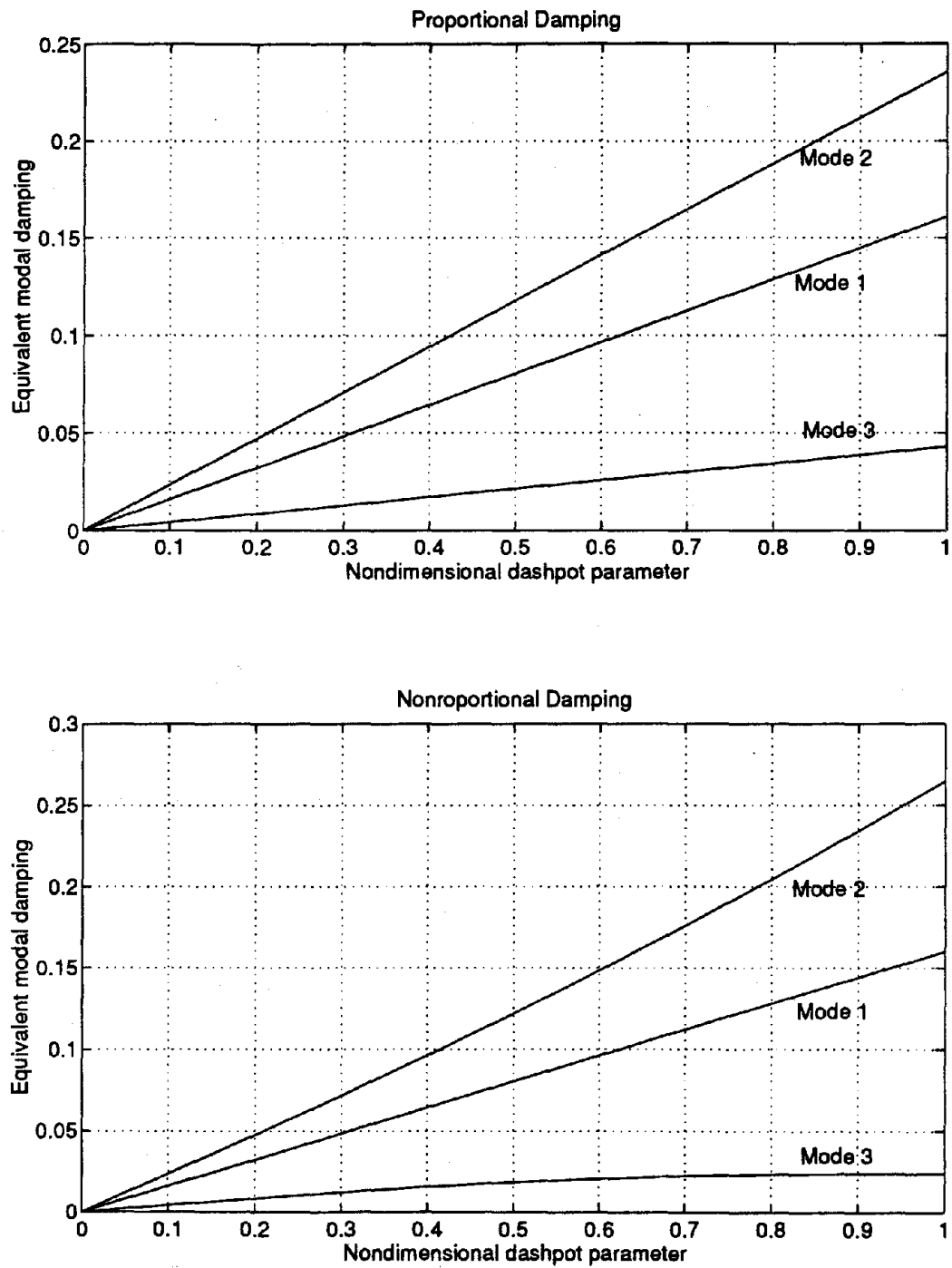
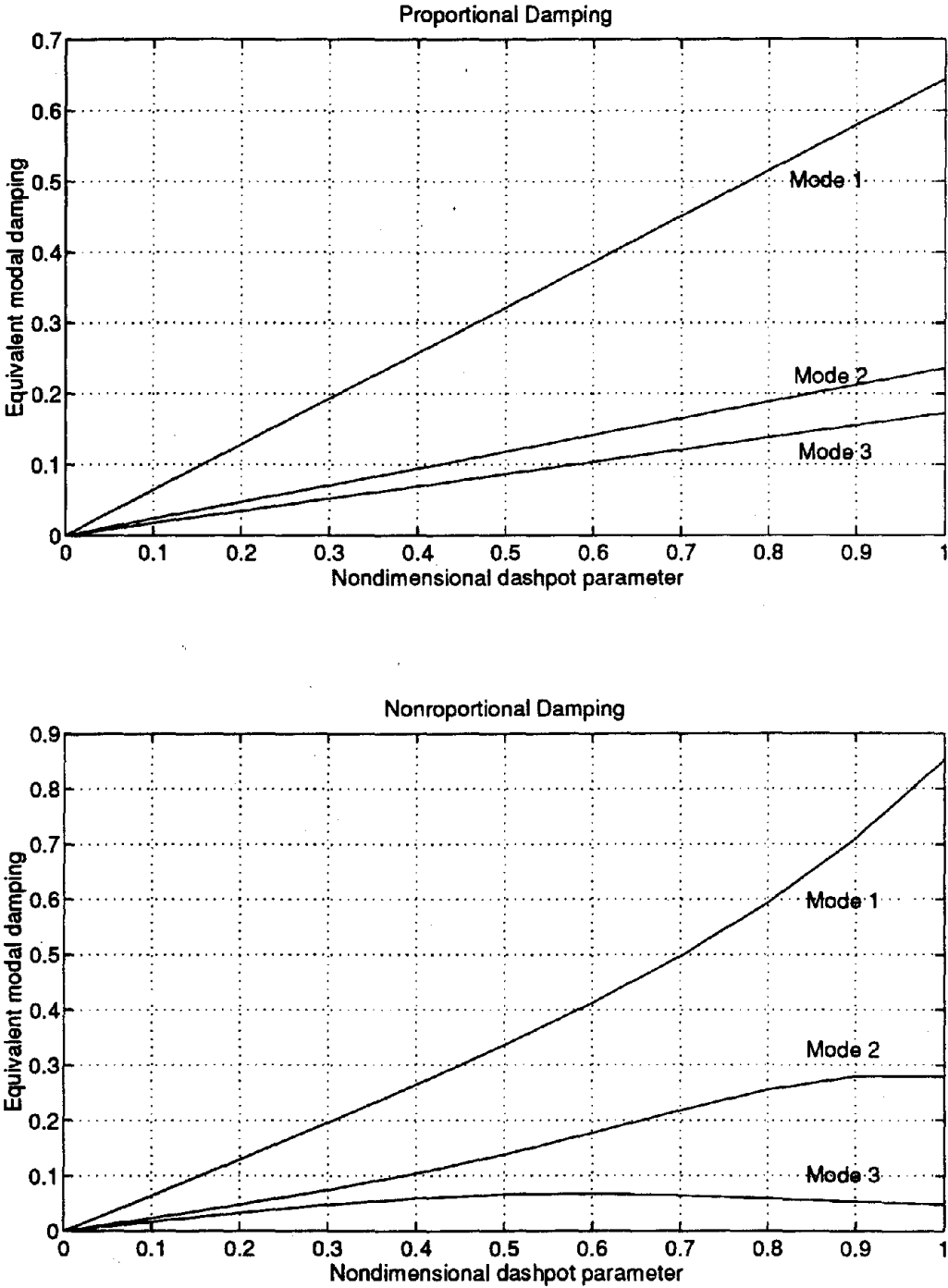Figure 6.1: Equivalent modal damping for the damped shear building – case 1

Figure 6.2: Equivalent modal damping for the damped shear building – case 2

Table 6.1: Comparison of modal damping factors

α	Mode	Case 1		Case 2	
		λ_i	ξ_i	λ_i	ξ_i
0.5	1	$-0.0420 + 0.5207i$	0.081	$-0.1836 + 0.5143i$	0.336
	2	$-0.1724 + 1.4022i$	0.122	$-0.1940 + 1.3901i$	0.138
	3	$-0.0356 + 1.9159i$	0.019	$-0.1224 + 1.8410i$	0.066
1.0	1	$-0.0861 + 0.5313i$	0.159	$-0.5893 + 0.3619i$	0.852
	2	$-0.3685 + 1.3425i$	0.265	$-0.3252 + 1.1173i$	0.279
	3	$-0.0454 + 1.8870i$	0.024	$-0.0855 + 1.7553i$	0.049

6.6.2 Eight Story Frame Building

In this section damped free vibration of the three bay, eight story portal frame shown in Figure 4.2 is considered. This problem was originally studied by Hooper et al. [27] using the exact finite element formulation for undamped free vibration. The first ten complex eigenvalues are tabulated in Table 6.2 for the conventional, mixed and $h-$formulations, and compared in terms of solution accuracy. For the conventional and the mixed formulations, the minimum number of finite elements needed to define the geometry is used (i.e., one element per member) leading to a 96 degrees-of-freedom model. In the $h-$formulation, three different discretization patterns are used: H_1 with 2 elements per structural member leading to a 264 degrees-of-freedom model; H_2 with 3 elements per member leading to a 432 degrees-of-freedom model; and H_3 with 4 elements per structural member leading to a 600 degrees-of-freedom model.

As expected, the conventional formulation results are an upper bound to the

Table 6.2: First 10 complex frequencies for eight story portal frame

Mode	Conventional formulation $N = 96$	Mixed formulation $N = 96$	h−formulations		
			H_1 $N = 264$	H_2 $N = 432$	H_3 $N = 600$
1	-0.203 + 11.204 i	-0.203 + 11.204 i	-0.203 + 11.204 i	-0.203 + 11.204 i	-0.203 + 11.204 i
2	-1.053 + 34.784 i	-1.053 + 34.775 i	-1.053 + 34.777 i	-1.053 + 34.776 i	-1.053 + 34.775 i
3	-2.963 + 61.735 i	-2.958 + 61.684 i	-2.959 + 61.693 i	-2.958 + 61.688 i	-2.958 + 61.686 i
4	-6.095 + 92.435 i	-6.072 + 92.264 i	-6.078 + 92.295 i	-6.077 + 92.276 i	-6.076 + 92.270 i
5	-6.058 + 108.121 i	-5.634 + 104.238 i	-6.042 + 104.489 i	-6.039 + 104.303 i	-6.038 + 104.271 i
6	-8.150 + 122.757 i	-7.490 + 117.841 i	-8.068 + 118.180 i	-8.061 + 117.929 i	-8.060 + 117.886 i
7	-10.667 + 127.305 i	-10.592 + 126.836 i	-10.622 + 126.922 i	-10.618 + 126.869 i	-10.616 + 126.854 i
8	-12.189 + 147.421 i	-11.286 + 141.659 i	-12.156 + 142.176 i	-12.144 + 141.814 i	-12.142 + 141.750 i
9	-15.910 + 160.709 i	-15.757 + 159.604 i	-15.904 + 160.081 i	-15.889 + 159.721 i	-15.886 + 159.654 i
10	-16.715 + 165.184 i	-16.497 + 164.103 i	-16.643 + 164.337 i	-16.622 + 164.185 i	-16.618 + 164.148 i

exact results of the mixed formulation, and the results obtained from the H_1 and H_2 formulations. Furthermore, the higher modes have much larger discretization error indicating that the conventional formulation is unable to adequately represent higher-order element deformations.

6.6.3 Discussion of Results

Results show that the Arnoldi-based eigensolver can be used effectively to solve the eigenvalue problem associated with the nonproportionally damped system. A full reduction of the system, which is computationally very intensive, is not required. In addition, the unsymmetric version of the implicitly restarted Arnoldi method avoids use of complex arithmetic, even though the eigenproblem is unsymmetric and the frequencies and mode shapes are complex. Therefore, this method requires less storage space and still avoids use of costly complex arithmetic.

It should be noted that for damped free vibration, even the mixed formulation results are only approximate. For undamped free vibration the frequency dependent shape functions derived from the exact solution to the governing differential equations of motion are able to represent the inertia forces exactly. However, that is no longer the case for the damped free vibration problem due to the presence of the damping term in the equations of motion. Even with this limitation, the results of the mixed formulation are more accurate than the conventional formulation, or h−refinements which involve more degrees of freedom than the mixed formulation. This improvement is due to the frequency dependence of the mass and damping matrices. The advantages of the frequency dependent mass matrix in being able to represent inertia forces has been enumerated previously. The new damping matrix $C(\hat{\omega})$ used here

helps improve the solution accuracy due to its ability to represent varying amounts of energy dissipated in a finite element. In physical terms, a frequency dependent damping matrix means that the energy dissipated in each finite element varies with frequency. This is useful for civil engineering structures as it is believed that more energy is dissipated at higher frequencies.

CHAPTER 7

Summary and Conclusions

Analysis of civil structures subject to transient loads such as wind forces or earthquake excitations is a very important part of the overall design process. For frame and truss structures, the governing partial differential equations of motion are usually derived based on Bernoulli-Euler beam theory. These equations cannot be solved continuously in all but some very simple cases. Numerical solution to this problem involves deriving a mathematical model of the physical system and solving for the characteristics of this model that are needed in the design process. A free vibration analysis usually is the first step in the dynamic analysis.

The finite element method is a very valuable and much used technique to formulate mathematical models of structures. This method uses locally defined shape functions that are approximate solutions to the governing differential equations, and establishes the number of equations of motion needed to accurately define the behavior of the vibrating system. A numerical algorithm is used to solve for frequencies and mode shapes (eigenvalues and eigenvectors) for free vibration. Thus, the development of accurate, efficient dynamic models and eigensolution techniques is crucial to free vibration analysis.

The conventional finite element formulation uses polynomial shape functions and

111

introduces discretization error that gets progressively worse for higher-order modes. As a result of this, the mathematical model is stiffer than the physical model, and computed eigenvalues are too high. The discretization error is reduced by h—refinement, where the number of degrees-of-freedom used to model the structure is increased, and by p—refinement where higher-order shape functions are used. Once the rigid body modes have been eliminated, the eigenproblems of the conventional formulation and h— and p—refinements are linear and the matrices are symmetric and positive definite.

The exact model uses the (frequency dependent) exact element displacement fields and, therefore, obtains exact frequencies and modes. Both the stiffness and mass matrices derived from this formulation are frequency dependent and the resulting eigenvalue problem is computationally very intensive. The quadratic model a is modification of this method in that it expands the frequency dependent stiffness and mass matrices in a Taylor series and retains the terms up to the order of ω^4. This process increases the problem size two fold.

The mixed formulation uses both the polynomial shape functions and the frequency dependent exact shape functions and models the vibrating system quasi-statically. Inertia forces are represented exactly and the equivalent load theory is used to compute displacements due to these forces. In this formulation only the mass matrix is frequency dependent. It is shown that this formulation provides exact free vibration frequencies and mode shapes for truss and frame type structures. For the mixed formulation, the eigenvalue problem is nonlinear and requires use of iterative zero finding technique in addition to a linear eigensolver to extract the system frequencies and mode shapes.

Mathematically, eigenvalues are roots of the characteristic polynomial, and eigenvectors generate a subspace that is invariant with respect to multiplication by the system matrix. Eigenvalue computation involves reducing down the given problem into a collection of smaller eigenvalue problems via a set of similarity transformations. In engineering applications typically only a few eigenvalues, often the lowest few, are of interest and, thus, a full, dense reduction of the system matrices is not desirable. Lanczos methods have been used extensively to solve large, sparse symmetric eigenvalue problems. It reduces a given (large) matrix into much smaller tridiagonal system whose eigenvalues approximate the eigenvalues of the original system. This process also has a few drawbacks like appearance of spurious eigenvalues and the loss of orthogonality among the basis vectors.

The implicitly restarted k—step Arnoldi method eliminates the major drawbacks of the conventional Lanczos method such as loss of orthogonality among basis vectors and appearance of spurious eigenvalues, by recognizing that the residual vector at any step of the Lanczos process is a function of the initial starting vector. The starting vector is iteratively updated using polynomial filters such that the residual vector converges to zero. This method forms the inner iteration for extracting the frequencies and mode shapes from the nonlinear eigenproblem of mixed formulation. A safeguarded secant method is used as the zero finder in the outer iteration to advance the eigenvalue computation one step further, until convergence.

Numerical examples have been presented to demonstrate the implementation and advantages of this method. The mixed formulation models the physical system accurately with a minimum number of finite elements, and the nonlinear eigensolution

technique takes advantage of the unique form of the eigenproblem of this formulation. The eigensolution technique presented is well suited to this class of nonlinear eigenvalue problems on several counts and has clear advantages in the large scale setting over the determinant search methods traditionally used. The parameterized eigenvalue curves are much better behaved in the solution region than the parameterized determinant curves that are associated with the determinant search methods. It is demonstrated that for large problems, the present method requires solution times that are over an order of magnitude less than the time required by the determinant search methods. Reliable error estimates for the quality of the approximate solutions to the discrete problem are readily available.

The mixed formulation is extended to model nonproportionally damped structures for damped free vibration, and the eigensolution technique is modified to solve for the complex frequencies and mode shapes associated with this model. It is shown that the mixed formulation, with a minimum number of finite elements, models the vibrating system more accurately than the conventional formulation and h−refinements.

Finally, the eigensolution technique is modified to extract the frequencies for a set of higher-order modes from the interior of the eigenvalue spectrum without solving for all the eigenvalues below a given threshold, the shift value. The usual shift and invert procedure is not very efficient for the eigenproblem associated with the mixed formulation due to the frequency dependence of the mass matrix, which causes the shifted stiffness matrix to become frequency dependent as well. A decomposition approach is used to reformulate the problem in such a way as to render the shifted stiffness matrix frequency independent. This eliminates the need to factor a large non-positive matrix at each step of eigenvalue computation. Results show that the

modified solution technique can extract eigenvalues from the interior of spectrum of the nonlinear eigenproblem in an efficient manner.

The research presented in this dissertation shows that mixed formulation effectively models the structure, and the Arnoldi-based eigensolution technique, coupled with a safeguarded secant zero finder, extracts the desired frequencies and mode shapes for undamped and damped free vibration efficiently, requiring much less time than the methods conventionally used. Together this model and solver provide a powerful analysis tool for determining the free vibration behavior (involving low-order and higher-order modes) of undamped, proportionally damped, and nonproportionally damped skeletal structures.

Bibliography

[1] Anderson, E., Bai, Z., Bischof, C., Demmel, J., Dongarra, J., Du Croz, J., Greenbaim, A., Hammerling, S., McKennedy, A., Ostrouchov, S. and Sorensen, D. C., [1992], *LAPACK Users' Guide,* Siam Publications, Philadelphia, Pennsylvania.

[2] Anderson, M. S. and Williams, F. W., [1986], "Natural Vibration and Buckling of General Periodic Lattice Structures," *AIAA Journal,* Vol. 24, pp. 163–169.

[3] Anderson, M. S. and Williams, F. W., [1987], "BUNVIS-RG: Exact Frame Buckling and Vibration Program, with Repetitive Geometry and Substructuring," *Journal Spacecraft,* Vol. 24, pp. 353–361.

[4] Arnoldi, W. E., [1951], "The Principle of Minimized Iterations in the Solution of the Matrix Eigenvalue Problem", *Quart. Appl. Math.,* Vol. 9, pp. 17–29.

[5] Babuska, I. and Dorr, M. R., [1981] "Error Estimates for the Combined h and p Versions of the Finite Element Method," *Numerische Mathematics,* Vol. 37, pp. 257–277.

[6] Babuska, I. and Guo, B., [1988] "The $h-p$ Version of the Finite Element Method," *SIAM Journal of Numerical Analysis* Vol. 25, pp. 837–861.

[7] Bergman, L. A. and McFarland, D. M., [1988], "On the Vibration of Point-Supported Linear Distributed System," *Journal of Vibration, Stress, and Reliability in Design,* Vol. 110, pp. 485–492.

116

[8] Chatelin, F. and Ho, D., [1990], "Arnoldi–Tchebychev Procedure for Large Scale Nonsymmetric Matrices," *Mathematical Modeling and Numerical Analysis,* Vol. 24, pp. 53–65.

[9] Clough, R. W. and Mojtahedi, S., [1976], "Earthquake Response Analysis Considering Non-proportional Damping," *Earthquake Engineering and Structural Dynamics,* Vol. 4, pp. 489–496.

[10] Cullum J. and Donath, W. E., [1974], "A block Lanczos Algorithm for Computing the q Algebraically Largest Eigenvalues and a Corresponding Eigenspace for Large, Sparse Symmetric Matrices," in *Proc. 1974 IEEE Conference on Decision and Control,* IEEE Press, New York, pp. 505–509.

[11] Cullum, J., [1978], "The Simultaneous Computation of a Few of the Algebraically Largest and Smallest Eigenvalues of a Large, Symmetric, Sparse Matrix," *BIT* Vol. 18, pp. 265–275.

[12] Cullum, J. and Wiloughby, R. A., Lanczos, [1985], *Algorithms for Large Symmetric Eigenvalue Computations, Vol. I Theory,* Birkhauser Boston, Inc.

[13] Cullum, J., Kerner, W. and Willoughby, R., [1989], "A Generalized Nonsymmetric Lanczos Procedure," *Computer Physics Communications,* Vol. 53, pp. 19–48.

[14] Daniel, J., Gragg, W.B., Kaufman, L., and Stewart, G. W., [1976], "Reorthogonalization and Stable Algorithms for Updating the Gram–Schmidt QR Factorization," *Math. Comp.,* Vol. 30, pp. 772–795.

[15] Francis, J. G. F., [1961], "The QR transformation: A Unitary Analogue to the LR Transformation, Parts I and II," *Comp. J.,* Vol. 4, pp. 265–272, 332–345.

[16] Golub, G. H. and van Loan, C. F., [1989], *Matrix Computations,* 2nd edition, The Johns Hopkins University Press, Baltimore, Maryland.

[17] Greenberg, L., [1989], "Sturm Sequences for Nonlinear Eigenvalue Problems," *SIAM Journal of Mathematical Analysis,* Vol. 20, pp. 182–199.

[18] Grimes, R. G., Lewis, J. G. and Simon, H. D., [1986], "The Implementation of a Block Shifted and Inverted Lanczos Algorithm for Eigenvalue Problems in Structural Engineering," *Boeing Computer Services,* ETA–TR–39, Seattle, Washington.

[19] Gupta, A. K. and Jaw, J.-W., [1986], "Seismic Response of Nonclassically Damped Systems," *Nuclear Engineering and Design* Vol. 91, pp. 153–159.

[20] Gupta, A. K. and Jaw, J.-W., [1986], "Response Spectrum Method for Nonclassically Damped Systems," *Nuclear Engineering and Design* Vol. 91, pp. 161–169.

[21] Gupta, K. K., [1976], "On a Finite Dynamic Element Method for Free Vibration Analysis of Structures," *Computational Methods in Applied Mechanics and Engineering,* Vol. 9, pp. 105–120.

[22] Gupta, K. K., [1978] "Development of a Finite Dynamic Element for Free Vibration Analysis of Two-dimensional Structures," *International Journal for Numerical Methods in Engineering,* Vol. 12, pp. 1311–1327.

[23] Gupta, K. K., Lawson, C. L. and Ahmadi, A. R., [1992] "On Development of a Finite Dynamic Element and Solution of Associated Eigenproblem by a Block Lanczos Procedure," *International Journal for Numerical Methods in Engineering,* Vol. 33, pp. 1611–1623.

[24] Gupta, K. K., [1973], "Eigenproblem Solution Based on a Combined Sturm Sequence and Inversion Iteration Technique," *International Journal for Numerical Methods in Engineering,* Vol. 7, pp. 17–42.

[25] Gupta, K. K., [1981], "Development of a Unified Numerical Procedure for Free Vibration Analysis of Structures," *International Journal for Numerical Methods in Engineering,* Vol. 17, pp. 187–198.

[26] Hallauer, W. L. and Liu R. Y. L., [1982], "Beam Bending–Torsion Dynamic Stiffness Method for Calculation of Exact Vibration Modes," *Journal of Sound and Vibration* , Vol. 85, pp. 105–113.

[27] Hooper, C. T., Simpson, A., and Williams, F. W., [1980], "A Study of the Bounds on Eigenvalues of a Transcendental Dynamic Stiffness Matrix Provided by a Simply Derived Linear Matrix Pencil," *Journal of Structural Mechanics,* Vol. 8(4), pp. 365–422.

[28] Humar, J. L., [1990], *Dynamics of Structures,* Prentice Hall International Series, Englewood Cliffs, New Jersey.

[29] Igusa, T., der Kiureghian, A. and Sackman, J. L., [1984], "Modal Decomposition Method for Stationary Response of Non-classically Damped Systems," *Earthquake Engineering and Structural Dynamics,* Vol. 12, pp. 121–136.

[30] Jain, N. K., Singhal, K., and Huseyin, K., [1983], "On Roots of Functional Lambda Matrices," *Computers Methods in Applied Mechanics and Engineering,* Vol. 40, pp. 277–292.

[31] Kolousek, V., [1941], "Anwendung des Gesetzes der virtuellen Vershchiebun-gen und des Reziprozitatssatzes in der Stabwerksdynamic," *Ingenieur Archiv*, Vol. 12, pp. 363-370.

[32] Kolousek, V., [1973], *Dynamics in Engineering Structures*, Halsted Press, New York, New York.

[33] Lawson, C., Hanson, R., Kincaid, D. and Krogh, F., [1979], "Basic Linear Al-gebra Subprograms for Fortran Usage," *ACM Transactions on Mathematical Software*, Vol. 5, pp. 308-323.

[34] Melosh, R. J. and Smith, H. A., [1989], "New Formulation for Vibration Analy-sis," *Journal of Engineering Mechanics*, Vol. 115, No. 3, pp. 543-554.

[35] Parlett, B. N., [1979], "The Lanczos Algorithm with Selective Orthogonaliza-tion," *Math. Comp.*, Vol. 33, 217-238.

[36] Parlett, B. N., [1980], *The Symmetric Eigenvalue Problem*, Prentice Hall, Engle-wood Cliffs, New Jersey.

[37] Paz, M. and Dung, L., [1975], "Power Series Expansion of the General Stiffness Matrix for Beam Elements," *International Journal for Numerical Methods in Engineering*, Vol. 9, pp. 449-459.

[38] Paz, M., [1985], *Structural Dynamics, Theory and Computation*, 2nd edition, Van Nostrand Reihhold Company, New York, New York.

[39] Przemieniecki, J. S., [1968], *Theory of Matrix Structural Analysis*, McGraw Hill Book Company, New York, New York.

[40] Rachowicz, W., Oden, J. T. and Demkowicz, L., [1989], "Towards a Universal $h-p$ Adaptive Finite Element Strategy: Part 3. Design of $h-p$ Meshes," *Computer Methods in Applied Mechanics and Engineering,* Vol. 77, pp. 181–212.

[41] Rachowicz, W., Oden, J. T. and Demkowicz, L., [1989], "Towards a Universal $h-p$ Adaptive Finite Element Strategy: Part 2. A Posteriori Error Estimate," *Computer Methods in Applied Mechanics and Engineering,* Vol. 77, pp. 131–180.

[42] Rajkumar, C. and Rogers, C. R., [1991], "The Lanczos Algorithm Applied to Unsymmetric Generalized Eigenvalue Problem," *International Journal for Numerical Methods in Engineering,* Vol. 32, pp. 1009–1026.

[43] Richards, T. H. and Leung, Y. T., [1977], "An Accurate Method in Structural Vibration Analysis," *Journal of Sound and Vibration,* Vol. 55, pp. 363–376.

[44] Ruhe, A., [1973], "Algorithms for the Nonlinear Eigenvalue Problem ," *SIAM J. Numer. Anal.* Vol. 10, pp. 674–689.

[45] Saad, Y., [1984], "Chebyshev Acceleration Techniques for Solving Nonsymmetric Eigenvalue Problems," *Math. Comp.,* Vol. 42, pp. 567–588.

[46] Simpson, A., [1978], "On the Solution of $S(\omega)x = 0$ by a Newtonian Procedure," *Journal of Sound and Vibration,* Vol. 97, pp. 153–164.

[47] Simpson, A. and Tabarrok, B., [1967], "On Kron's Eigenvalue Procedure and Related Methods of Frequency Analysis," *Quarterly Journal of Mechanics and Applied Mathematics,* Vol. XXI, Pt. I, pp. 1–36.

[48] Simpson, A., [1980], "The Kron Methodology and Practical Algorithms for Eigenvalue Sensitivity and Response Analyses of Large Scale Structural Systems," *Aeronautical Journal*, December, pp. 417–433.

[49] Singh, M. P. and Ghafory-Ashtiany, M., [1986], "Modal Time History Analysis of Non-classically Damped Structures for Seismic Motions," *Earthquake Engineering and Structural Dynamics*, Vol. 14, pp. 133–146.

[50] Singh, R. K. and Smith, H. A., [1993], "Comparison of Computational Effectiveness of the Finite Element Formulations in Free Vibration Analysis," accepted for publication in the *Computers and Structures*.

[51] Singh, R. K. and Smith, H. A., [1993] "Performance Comparison of the Mixed, $h-$ and $p-$formulations of the Finite Element Method for Vibration Analysis," *Proceedings of the 34th Structures, Structural Dynamics, and Materials Conference*, La Jolla, California, pp. 103–109.

[52] Smith, H. A. and Melosh, R. J., [1990], "The Unsymmetric Formulation for Vibration Analysis of Frames," *Computers and Structures*, Vol. 36, pp. 531–537.

[53] Smith, H. A. and Melosh, R. J., [1990], "Dynamic Modeling of Skeletal Systems with Arbitrary Mass Distributions," *International Journal for Numerical Methods in Engineering*, Vol. 29, pp. 1219–1228.

[54] Smith, H. A., [1989]. *Dynamic Modeling of Trusses and Frames with Arbitrary Stiffness and Mass Using the Unsymmetric Exact Formulation*, a dissertation presented to Duke University in partial fulfillment of the requirements for the degree Doctor of Philosophy, Durham, North Carolina.

[55] Smith, H. A., Sorensen, D. C., and Singh, R. K., [1992], "A Nonlinear Eigensolver for Exact Vibration Analysis," *Proceedings of the Ninth Conference on Engineering Mechanics, ASCE,* Texas A & M University, pp. 920–923.

[56] Smith, H. A., Sorensen, D. C., and Singh, R. K. [1993], "A Lanczos-based Eigensolution Technique for Exact Vibration Analysis," *International Journal for Numerical Methods in Engineering,* Vol. 36, pp. 1987–2000.

[57] Sorensen, D. C., [1990], "The k–step Arnoldi Process," Chapter 14 , *Large–scale Numerical Optimization,* T. F. Coleman and Y. Li eds., SIAM Publications, Philadelphia, pp. 228–237.

[58] Sorensen, D. C., [1992], "Implicit application of polynomial filters in a k–step Arnoldi Method," *SIAM Journal on Matrix Analysis and Applications,* Vol. 13(1), pp. 357–385.

[59] Sorensen, D. C. and Vu, P., [1991-3], *ARPACK: A Library of Eigenvalue Solution Routines,* available from sorensen@rice.edu.

[60] Sorensen, D. C., Vu, P. A. and Tomasic, Z., [1993], "Algorithms and Software for Large Scale Eigenproblems on High Performance Computers," *High Performance Computing 1993 — Grand Challenges in Computer Simulation* Adrian Tentner, ed., Proceedings of the 1993 Simulation Multiconference, Society for Computer Simulation, pp. 149–154.

[61] Stewart, G. W., [1973], *Introduction to Matrix Computations,* Academic Press, New York.

[62] Swannell, P., [1973], "Automatic Computation of the Natural Frequencies of Structural Frames Using an Exact Matrix Technique," *Theory and Practice in Finite Element Structural Analysis,* University of Tokyo Press, Tokyo, Japan, pp. 289–303.

[63] Swannell, P. and Tranberg, C. H., [1978], "Procedures for the Forced, Damped Vibration Analysis of Structural Frames Using Distributed Parameter Model," *Computer Methods in Applied Mechanics and Engineering,* Vol. 16, pp. 291–302.

[64] Thurston, G. A., [1978], "Roots of Lambda Matrices," *Journal of Applied Mechanics,* Vol. 45, pp. 859–863.

[65] Veletsos, A. S. and Ventura, C. E., [1986], "Modal Analysis of Non-classically Damped Linear Systems," *Earthquake Engineering and Structural Dynamics,* Vol. 14, pp. 217–243.

[66] Warburton, G. B. and Soni, S. R., [1977], "Errors in Response Calculations for Non-classically Damped Structures," *Earthquake Engineering and Structural Dynamics,* Vol. 5, pp. 365–376.

[67] Williams, F. W. and Wittrick, W. H., [1970], "An Automatic Computational Procedure for Calculating Natural Frequencies of Skeletal Structures," *International Journal of Mechanical Science,* Vol. 12, pp. 781–791.

[68] Williams, F. W. and Wittrick, W. H., [1983], "Exact Buckling and Frequency Calculations Surveyed," *Journal of Structural Engineering,* Vol. 109, pp. 169–187.

[69] Williams, F. W. and Kennedy, D., [1988], "Reliable Use of Determinants to Solve Non–Linear Structural Eigenvalue Problems Efficiently," *International Journal for Numerical Methods in Engineering,* Vol. 26, pp. 1825–1841.

[70] Wilkinson, W. H., [1965], *"The Algebraic Eigenvalue Problem,"* Claredon Press, Oxford, England.

[71] Wittrick, W. H. and Williams, F. W., [1971], "A General Algorithm for Computing Natural Frequencies of Elastic Structures," *Quarterly Journal of Mechanics and Applied Mathematics,* Vol. 24, pp. 263–284.

[72] Yang, I. M., [1988], "TECHNICAL NOTE: An Iterative Method for Solving Nonlinear Eigenvalue Problems in Matrix Form," *Computers and Structures,* Vol. 29, pp. 353–354.

[73] Zienkiewicz, O. C., [1989], *The Finite Element Method,* 4th edition, McGraw Hill Book Company, New York, New York.

[74] Zienkiewicz, O. C., De, J. P., Gago, S. R. and Kelley, D. W.,[1983], "The Hierarchical Concept in Finite Element Analysis," *Computers and Structures,* Vol. 16 (1–4), pp. 53–65.

[75] Zienkiewicz, O. C., Zhu, J. Z. and Gong, N. G., [1989], "Effective and Practical $h-p$ Version Adaptive Analysis Procedures for the Finite Element Method," *International Journal for Numerical Methods in Engineering,* Vol. 28, pp. 879–891.

Shape Functions and Element Matrices

A.1 Conventional Formulation

- **Node Locations:** Nodes are located at the element ends $\eta = 0, 1$ where

$$\eta = \frac{x}{l} \text{ is the nondimensional spanwise coordinate.}$$

- **Displacement Fields:**

$$
\begin{aligned}
u_{p_c}^h &= \bar{a}_0 + \bar{a}_1 x \\
v_{p_c}^h &= a_0 + a_1 x + a_2 x^2 + a_3 x^3
\end{aligned}
\tag{A.1}
$$

- **Shape Functions for Axial Vibration:**

$$
\begin{aligned}
N_1 &= 1 - \eta \\
N_2 &= \eta
\end{aligned}
\tag{A.2}
$$

- **Shape Functions for Lateral Vibration:**

$$
\begin{aligned}
N_1 &= 1 - 3\eta^2 + 2\eta^3 \\
N_2 &= l(\eta - 2\eta^2 + \eta^3) \\
N_3 &= 3\eta^2 - 2\eta^3 \\
N_4 &= l(-\eta^2 + \eta^3)
\end{aligned}
\tag{A.3}
$$

- **Element Stiffness and Mass Matrices for Axial Vibrations:**

$$
\bar{\mathbf{K}}_{p_c}^e = \frac{EA}{l} \begin{bmatrix} 1 & -1 \\ -1 & 1 \end{bmatrix}
\tag{A.4}
$$

$$\bar{\mathbf{M}}^e_{p_c} \;=\; \frac{\bar{m}l}{6}\begin{bmatrix} 2 & 1 \\ 1 & 2 \end{bmatrix} \tag{A.5}$$

● **Element Stiffness and Mass Matrices for Bending Vibrations:**

$$\mathbf{K}^e_{p_c} \;=\; \frac{EI}{l^3}\begin{bmatrix} 12 & 6l & -12 & 6l \\ 6l & 4l^2 & -6l & 2l^2 \\ -12 & -6l & 12 & -6l \\ 6l & 2l^2 & -6l & 4l^2 \end{bmatrix} \tag{A.6}$$

$$\mathbf{M}^e_{p_c} \;=\; \frac{\bar{m}l}{420}\begin{bmatrix} 156 & 22l & 54 & -13l \\ 22l & 4l^2 & 13l & -3l^2 \\ 54 & 13l & 156 & -22l \\ -13l & -3l^2 & -22l & 4l^2 \end{bmatrix} \tag{A.7}$$
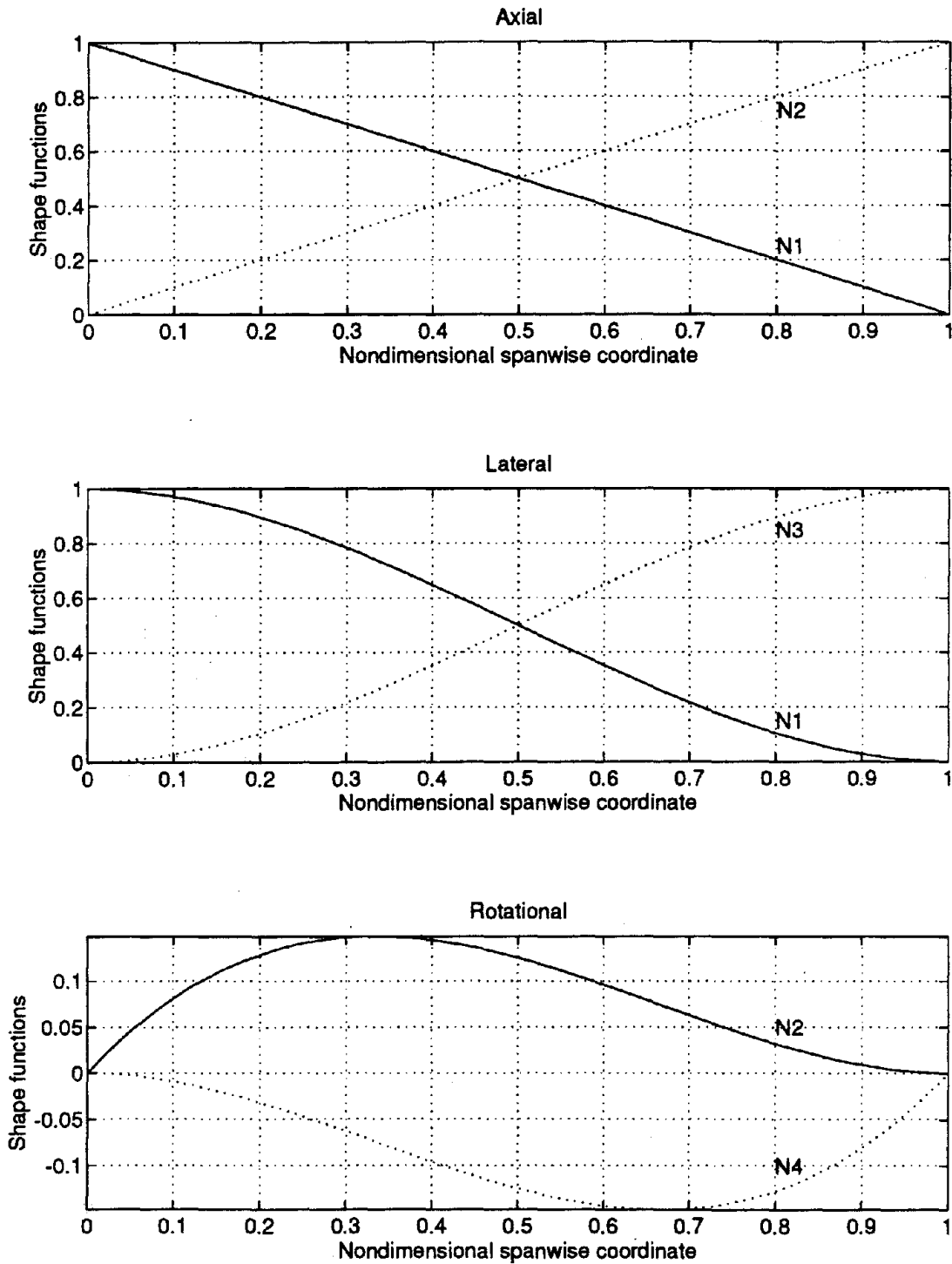
Figure A.1: Shape functions for the axial, lateral and rotational degrees-of-freedom for the conventional formulation

A.2 P_1 Formulation

- **Node Locations:** Nodes are located at the element ends $\eta = 0, 1$ and at the

    midpoint $\eta = \frac{1}{2}$.

- **Displacement Fields:**

$$
\begin{aligned}
u_{p_1}^h &= \bar{b}_0 + \bar{b}_1 x + \bar{b}_2 x^2 \\
v_{p_1}^h &= b_0 + b_1 x + b_2 x^2 + b_3 x^3 + b_4 x^4 + b_5 x^5
\end{aligned}
\tag{A.8}
$$

- **Shape Functions for Axial Vibration:**

$$
\begin{aligned}
N_1 &= 1 - 3\eta + 2\eta^2 \\
N_2 &= -\eta + 2\eta^2 \\
N_3 &= 4(\eta - \eta^2)
\end{aligned}
\tag{A.9}
$$

- **Shape Functions for Lateral Vibration:**

$$
\begin{aligned}
N_1 &= 1 - 23\eta^2 + 66\eta^3 - 68\eta^4 + 24\eta^5 \\
N_2 &= l(\eta - 6\eta^2 + 13\eta^3 - 12\eta^4 + 4\eta^5) \\
N_3 &= 7\eta^2 - 34\eta^3 + 52\eta^4 - 24\eta^5 \\
N_4 &= l(-\eta^2 + 5\eta^3 - 8\eta^4 + 4\eta^5) \\
N_5 &= 16\eta^2 - 32\eta^3 + 16\eta^4 \\
N_6 &= l(-8\eta^2 + 32\eta^3 - 40\eta^4 + 16\eta^5)
\end{aligned}
\tag{A.10}
$$

- **Element Stiffness and Mass Matrices for Axial Vibrations:**

$$
\bar{K}_{p_1}^e = \frac{EA}{3l} \begin{bmatrix} 7 & 1 & -8 \\ 1 & 7 & -8 \\ -8 & -8 & 16 \end{bmatrix}
\tag{A.11}
$$

$$
\bar{M}_{p_1}^e = \frac{\bar{m}l}{30} \begin{bmatrix} 4 & -1 & 2 \\ -1 & 4 & 2 \\ 2 & 2 & 16 \end{bmatrix}
\tag{A.12}
$$

● Element Stiffness and Mass Matrices for Bending Vibrations:

$$
\mathbf{K}^e_{p_1} = \frac{EI}{35l^3}
\begin{bmatrix}
5092 & 1138l & -1508 & 242l & -3584 & 1920l \\
1138l & 332l^2 & -242l & 38l^2 & -896l & 320l^2 \\
-1508 & -242l & 5092 & -1138l & -3584 & -1920l \\
242l & 38l^2 & -1138l & 332l^2 & 896l & 320l^2 \\
-3584 & -896l & -3584 & 896l & 7168 & 0 \\
1920l & 320l^2 & -1920l & 320l^2 & 0 & 1280l^2
\end{bmatrix}
\tag{A.13}
$$

$$
\mathbf{M}^e_{p_1} = \frac{\bar{m}l}{13860}
\begin{bmatrix}
2092 & 114l & 262 & -29l & 880 & -160l \\
114l & 8l^2 & 29l & -3l^2 & 88l & -12l^2 \\
262 & 29l & 2092 & -114l & 880 & 160l \\
-29l & -3l^2 & -114l & 8l^2 & -88l & -12l^2 \\
880 & 88l & 880 & -88l & 5632 & 0 \\
-160l & -12l^2 & 160l & -12l^2 & 0 & 128l^2
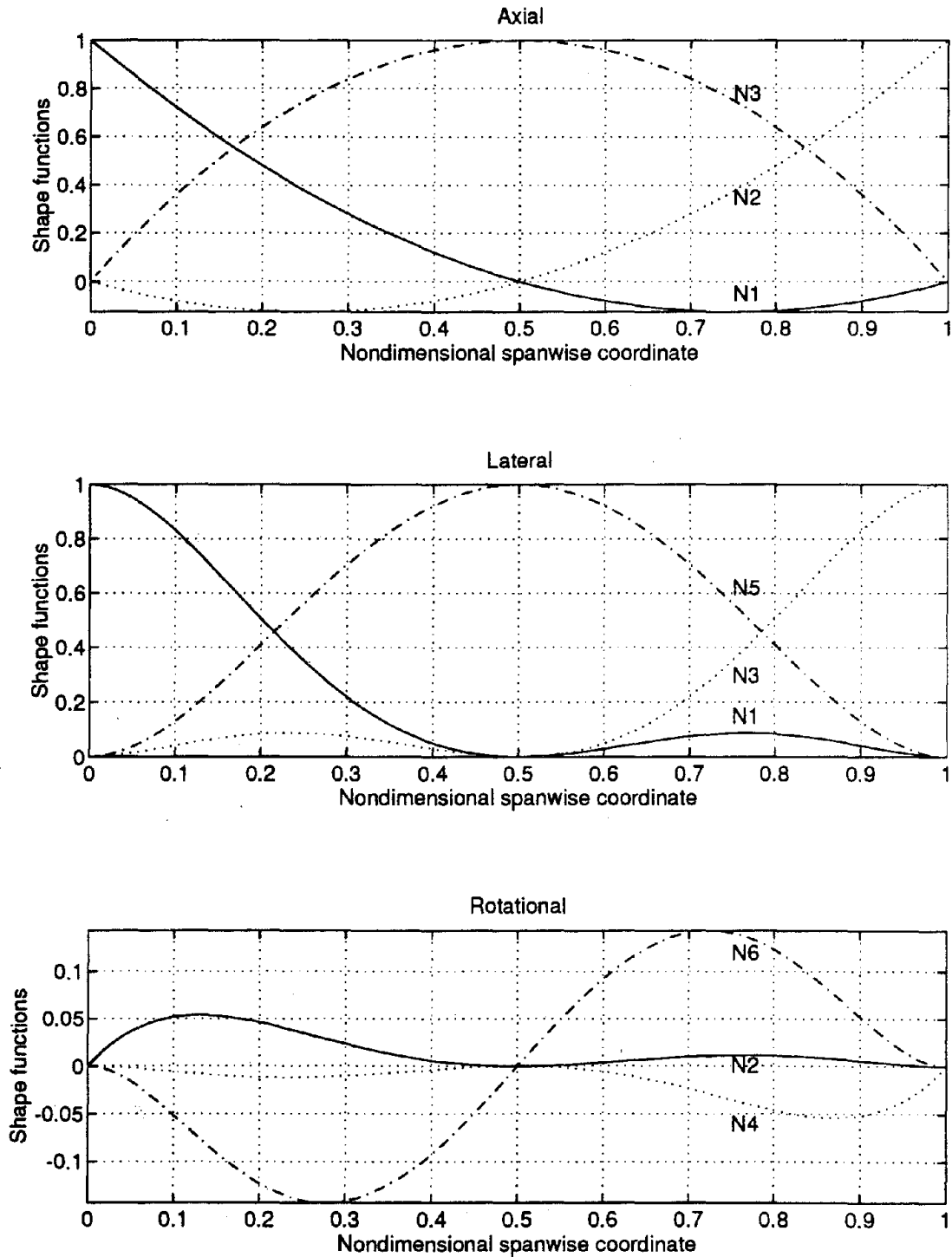\end{bmatrix}
\tag{A.14}
$$

Figure A.2: Shape functions for the axial, lateral and rotational degrees-of-freedom for the P_1 formulation

A.3 P_2 Formulation

- **Node Locations:** Nodes are located at the element ends $\eta = 0, 1$ and at the one-third points $\eta = \frac{1}{3}, \frac{2}{3}$.

- **Displacement Fields:**

$$
\begin{aligned}
u^h_{p_2} &= \bar{c}_0 + \bar{c}_1 x + \bar{c}_2 x^2 + \bar{c}_3 x^3 \\
v^h_{p_2} &= c_0 + c_1 x + c_2 x^2 + c_3 x^3 + c_4 x^4 + c_5 x^5 + c_6 x^6 + c_7 x^7
\end{aligned}
\tag{A.15}
$$

- **Shape Functions for Axial Vibration:**

$$
\begin{aligned}
N_1 &= \frac{1}{2}(2 - 11\eta + 18\eta^2 - 9\eta^3) \\
N_2 &= \frac{1}{2}(2\eta - 9\eta^2 + 9\eta^3) \\
N_3 &= \frac{1}{2}(18\eta - 45\eta^2 + 27\eta^3) \\
N_4 &= \frac{1}{2}(-9\eta + 36\eta^2 - 27\eta^3)
\end{aligned}
\tag{A.16}
$$

- **Shape Functions for Lateral Vibration:**

$$
\begin{aligned}
N_1 &= \frac{1}{4}(4 - 291\eta^2 + 1691\eta^3 - 4230\eta^4 + 5418\eta^5 - 3483\eta^6 + 891\eta^7) \\
N_2 &= \frac{l}{4}(4\eta - 44\eta^2 + 193\eta^3 - 432\eta^4 + 522\eta^5 - 324\eta^6 + 81\eta^7) \\
N_3 &= \frac{1}{4}(48\eta^2 - 476\eta^3 + 1800\eta^4 - 3231\eta^5 + 2754\eta^6 - 891\eta^7) \\
N_4 &= \frac{l}{4}(-4\eta^2 + 40\eta^3 - 153\eta^4 + 279\eta^5 - 243\eta^6 + 81\eta^7) \\
N_5 &= \frac{1}{4}(972\eta^3 - 4860\eta^4 + 8991\eta^5 - 7290\eta^6 + 2187\eta^7) \\
N_6 &= \frac{l}{4}(-108\eta^2 + 864\eta^3 - 2619\eta^4 + 3807\eta^5 - 2673\eta^6 + 729\eta^7) \\
N_7 &= \frac{1}{4}(243\eta^2 - 2187\eta^3 + 7290\eta^4 - 11178\eta^5 + 8019\eta^6 - 2187\eta^7) \\
N_8 &= \frac{l}{4}(-54\eta^2 + 513\eta^3 - 1836\eta^4 + 3078\eta^5 - 2430\eta^6 + 729\eta^7)
\end{aligned}
\tag{A.17}
$$

- **Element Stiffness and Mass Matrices for Axial Vibrations:**

$$
\bar{\mathbf{K}}^e_{p_2} = \frac{EA}{40l}
\begin{bmatrix}
148 & -13 & -189 & 54 \\
-13 & 148 & 54 & -189 \\
-189 & 54 & 432 & -297 \\
54 & -189 & -297 & 432
\end{bmatrix}
\tag{A.18}
$$

$$
\bar{\mathbf{M}}^e_{p_2} = \frac{\bar{m}l}{1680}
\begin{bmatrix}
128 & 19 & 99 & -36 \\
19 & 128 & -36 & 99 \\
99 & -36 & 648 & -81 \\
-36 & 99 & -81 & 648
\end{bmatrix}
\tag{A.19}
$$

- **Element Stiffness and Mass Matrices for Bending Vibrations:**

$$
\mathbf{K}^e_{p_2} = \frac{EI}{6160l^3}
\begin{bmatrix}
3994320 & 553740l & -746625 & 72600l \\
553740l & 98512l^2 & -72600l & 6893l^2 \\
-746625 & -72600l & 3994320 & -553740l \\
72600l & 6893l^2 & -553740l & 98512l^2 \\
-841995 & -218700l & -2405700 & 262440l \\
1363230l & 148959l^2 & -641520l & 66096l^2 \\
-2405700 & -262440l & -841995 & 218700l \\
641520l & 66096l^2 & -1363230l & 148959l^2
\end{bmatrix}
$$

$$\tag{A.20}$$

$$
\begin{bmatrix}
-841995 & 1363230l & -2405700 & 641520l \\
-218700l & 148959l^2 & -262440l & 66096l^2 \\
-2405700 & -641520l & -841995 & -1363230l \\
262440l & 66096l^2 & 218700l & 148959l^2 \\
7085880 & 918540l & -3838185 & 1640250l \\
918540l & 723168l^2 & -1640250l & 490617l^2 \\
-3838185 & -1640250l & 7085880 & -918540l \\
1640250l & 490617l^2 & -918540l & 723168l^2
\end{bmatrix}
$$

$$
\mathbf{M}^e_{p_2} = \frac{\bar{m}l}{3843840}
\begin{bmatrix}
339312 & 10520l & 23034 & -1496l \\
10520l & 416l^2 & 1496l & -90l^2 \\
23034 & 1496l & 339312 & -10520l \\
-1496l & -90l^2 & -10520l & 416l^2 \\
86670 & 5184l & 82944 & -4536l \\
-33156l & -1566l^2 & 11016l & -432l^2 \\
82944 & 4536l & 86670 & -5184l \\
-11016l & -432l^2 & 33156l & -1566l^2
\end{bmatrix}
$$

$$
\begin{bmatrix}
86670 & -33156l & 82944 & -11016l \\
5184l & -1566l^2 & 4536l & -432l^2 \\
82944 & 11016l & 86670 & 33156l \\
-4536l & -432l^2 & -5184l & -1566l^2 \\
944784 & -17496l & 275562 & -8748l \\
-17496l & 15552l^2 & 8748l & 6318l^2 \\
275562 & 8748l & 944784 & 17496l \\
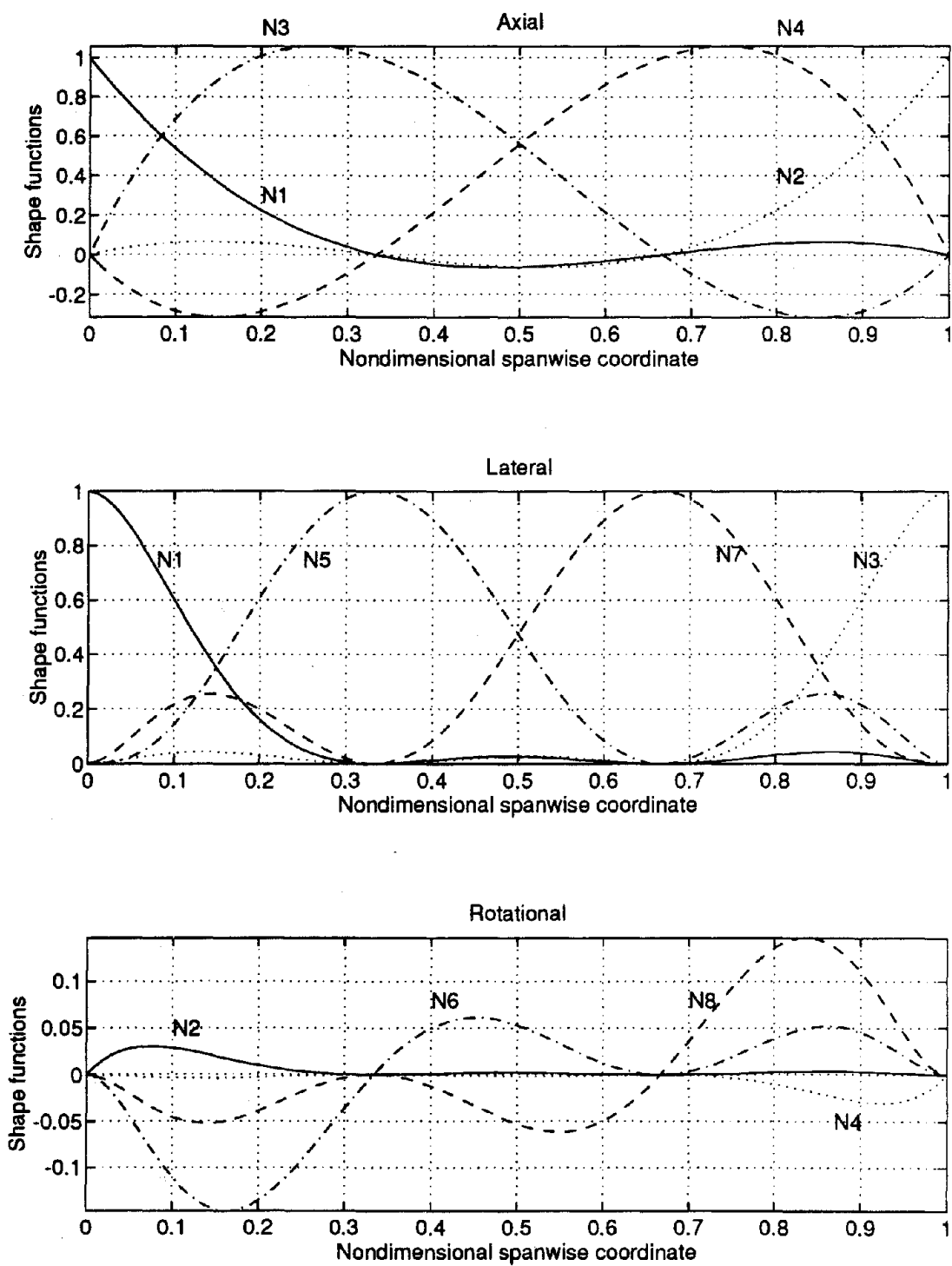-8748l & 6318l^2 & 17496l & 15552l^2
\end{bmatrix}
$$

(A.21)

Figure A.3: Shape functions for the axial, lateral and rotational degrees-of-freedom for the P_2 formulation

A.4 P_3 Formulation

- **Node Locations:** Nodes are located at the element ends $\eta = 0, 1$ and at the quarter- and mid-points $\eta = \frac{1}{4}, \frac{1}{2}\frac{3}{4}$.

- **Displacement Fields:**

$$
\begin{aligned}
u_{p_3}^h &= \bar{d}_0 + \bar{d}_1 x + \bar{d}_2 x^2 + \bar{d}_3 x^3 + \bar{d}_4 x^4 \\
v_{p_3}^h &= d_0 + d_1 x + d_2 x^2 + d_3 x^3 + d_4 x^4 + d_5 x^5 + d_6 x^6 + d_7 x^7 + d_8 x^8 + d_9 x^9
\end{aligned}
$$

$$(A.22)$$

- **Shape Functions for Axial Vibration:**

$$
\begin{aligned}
N_1 &= \frac{1}{3}(3 - 25\eta + 70\eta^2 - 80\eta^3 + 32\eta^4) \\
N_2 &= \frac{1}{3}(-3\eta + 22\eta^2 - 48\eta^3 + 32\eta^4) \\
N_3 &= \frac{1}{3}(48\eta - 208\eta^2 + 288\eta^3 - 128\eta^4) \\
N_4 &= \frac{1}{3}(-36\eta + 228\eta^2 - 384\eta^3 + 192\eta^4) \\
N_5 &= \frac{1}{3}(16\eta - 112\eta^2 + 224\eta^3 - 128\eta^4)
\end{aligned}
$$

$$(A.23)$$

- **Shape Functions for Lateral Vibration:**

$$
\begin{aligned}
N_1 &= \frac{1}{27}(27 - 4365\eta^2 + 40310\eta^3 - 171724\eta^4 + 416200\eta^5 \\
&\quad -607360\eta^6 + 528640\eta^7 - 252928\eta^8 + 51200\eta^9) \\
N_2 &= \frac{l}{27}(27\eta - 450\eta^2 + 3135\eta^3 - 11940\eta^4 + 27276\eta^5 \\
&\quad -38400\eta^6 + 32640\eta^7 - 15360\eta^8 + 3072\eta^9) \\
N_3 &= \frac{1}{27}(477\eta^2 - 7446\eta^3 + 47516\eta^4 - 160712\eta^5 \\
&\quad +311936\eta^6 - 348416\eta^7 + 207872\eta^8 - 51200\eta^9) \\
N_4 &= \frac{l}{27}(-27\eta^2 + 423\eta^3 - 2712\eta^4 + 9228\eta^5 \\
&\quad -18048\eta^6 + 20352\eta^7 - 12288\eta^8 + 3072\eta^9)
\end{aligned}
$$

$$(A.24)$$

$$N_5 = \frac{1}{27}(-4608\eta^2 + 86016\eta^3 - 541184\eta^4 + 1682432\eta^5$$
$$-2914304\eta^6 + 2871296\eta^7 - 1507328\eta^8 + 327680\eta^9)$$

$$N_6 = \frac{l}{27}(-1728\eta^2 + 21888\eta^3 - 113088\eta^4 + 311808\eta^5$$
$$-498432\eta^6 + 463872\eta^7 - 233472\eta^8 + 49152\eta^9)$$

$$N_7 = \frac{1}{27}(3888\eta^2 - 49248\eta^3 + 238896\eta^4 - 566784\eta^5$$
$$+705024\eta^6 - 442368\eta^7 + 110592\eta^8)$$

$$N_8 = \frac{l}{27}(-1944\eta^2 + 28512\eta^3 - 168696\eta^4 + 522288\eta^5$$
$$-919296\eta^6 + 926208\eta^7 - 497664\eta^8 + 110592\eta^9)$$

$$N_9 = \frac{1}{27}(4608\eta^2 - 69632\eta^3 + 426496\eta^4 - 1371136\eta^5$$
$$+2504704\eta^6 - 2609152\eta^7 + 1441792\eta^8 - 327680\eta^9)$$

$$N_{10} = \frac{l}{27}(-576\eta^2 + 8832\eta^3 - 55104\eta^4 + 181248\eta^5$$
$$-340224\eta^6 + 365568\eta^7 - 208896\eta^8 + 49152\eta^9)$$

(A.24)

● Element Stiffness and Mass Matrices for Axial Vibrations:

$$\bar{\mathbf{K}}_{p_3}^e = \frac{EA}{945l}\begin{bmatrix} 4925 & 347 & -6848 & 3048 & -1472 \\ 347 & 4925 & -1472 & 3048 & -6848 \\ -6848 & -1472 & 16640 & -14208 & 5888 \\ 3048 & 3048 & -14208 & 22320 & -14208 \\ -1472 & -6848 & 5888 & -14208 & 16640 \end{bmatrix}$$

(A.25)

$$\bar{\mathbf{M}}_{p_3}^e = \frac{\bar{m}l}{5670}\begin{bmatrix} 292 & -29 & 296 & -174 & 56 \\ -29 & 292 & 56 & -174 & 296 \\ 296 & 56 & 1792 & -384 & 256 \\ -174 & -174 & -384 & 1872 & -384 \\ 56 & 296 & 256 & -384 & 1792 \end{bmatrix}$$

(A.26)

• Element Stiffness and Mass Matrices for Bending Vibrations:

$$
\mathbf{K}^e_{p_3} = \alpha
\begin{bmatrix}
7129230844 & 691304574l & -959155196 & 64268286l & 3929022464 \\
691304574l & 85371732l^2 & -64268286l & 4196394l^2 & 157691904l \\
-959155196 & -64268286l & 7129230844 & -691304574l & -5665202176 \\
64268286l & 4196394l^2 & -691304574l & 85371732l^2 & 422916096l \\
3929022464 & 157691904l & -5665202176 & 422916096l & 23235395584 \\
2450092032l & 192407040l^2 & -836149248l & 59798016l^2 & 3932946432l \\
-4433895936 & -361812096l & -4433895936 & 361812096l & -4437835776 \\
2400935040l & 181165248l^2 & -2400935040l & 181165248l^2 & 6858915840l \\
-5665202176 & -422916096l & 3929022464 & -157691904l & -17061380096 \\
836149248l & 59798016l^2 & -2450092032l & 192407040l^2 & 3498835968l
\end{bmatrix}
$$

$$
\begin{bmatrix}
2450092032l & -4433895936 & 2400935040l & -5665202176 & 836149248l \\
192407040l^2 & -361812096l & 181165248l^2 & -422916096l & 59798016l^2 \\
-836149248l & -4433895936 & -2400935040l & 3929022464 & -2450092032l \\
59798016l^2 & 361812096l & 181165248l^2 & -157691904l & 192407040l^2 \\
3932946432l & -4437835776 & 6858915840l & -17061380096 & 3498835968l \\
1198669824l^2 & -2048053248l & 1447538688l^2 & -3498835968l & 602652672l^2 \\
-2048053248l & 17743463424 & 0 & -4437835776 & 2048053248l \\
1447538688l^2 & 0 & 2572985088l^2 & -6858915840l & 1447538688l^2 \\
-3498835968l & -4437835776 & -6858915840l & 23235395584 & -3932946432l \\
602652672l^2 & 2048053248l & 1447538688l^2 & -3932946432l & 1198669824l^2
\end{bmatrix}
$$

$$(\text{A}.27)$$

where

$$
\alpha = \frac{EI}{3648645l^3}
$$

$$\mathbf{M}^e_{p3} = \beta \begin{bmatrix}
857544924 & 17984922l & 38622110 & -1703505l & -1061888 \\
17984922l & 478728l^2 & 1703505l & -69327l^2 & 1524480l \\
38622110 & 1703505l & 857544924 & -17984922l & 206361600 \\
-1703505l & -69327l^2 & -17984922l & 478728l^2 & -6880512l \\
-1061888 & 1524480l & 206361600 & -6880512l & 2282225664 \\
-94104768l & -3070944l^2 & 18408768l & -455328l^2 & -19267584l \\
229607856 & 8072568l & 229607856 & -8072568l & 649986048 \\
-81056160l & -2495772l^2 & 81056160l & -2495772l^2 & -22339584l \\
206361600 & 6880512l & -1061888 & -1524480l & 267911168 \\
-18408768l & -455328l^2 & 94104768l & -3070944l^2 & 40501248l
\end{bmatrix}$$

$$\begin{bmatrix}
-94104768l & 229607856 & -81056160l & 206361600 & -18408768l \\
-3070944l^2 & 8072568l & -2495772l^2 & 6880512l & -455328l^2 \\
18408768l & 229607856 & 81056160l & -1061888 & 94104768l \\
-455328l^2 & -8072568l & -2495772l^2 & -1524480l & -3070944l^2 \\
-19267584l & 649986048 & -22339584l & 267911168 & 40501248l \\
38854656l^2 & -24164352l & 30689280l^2 & -40501248l & 13639680l^2 \\
-24164352l & 2909965824 & 0 & 649986048 & 24164352l \\
30689280l^2 & 0 & 55458432l^2 & 22339584l & 30689280l^2 \\
-40501248l & 649986048 & 22339584l & 2282225664 & 19267584l \\
13639680l^2 & 24164352l & 30689280l^2 & 19267584l & 38854656l^2
\end{bmatrix}$$

(A.28)

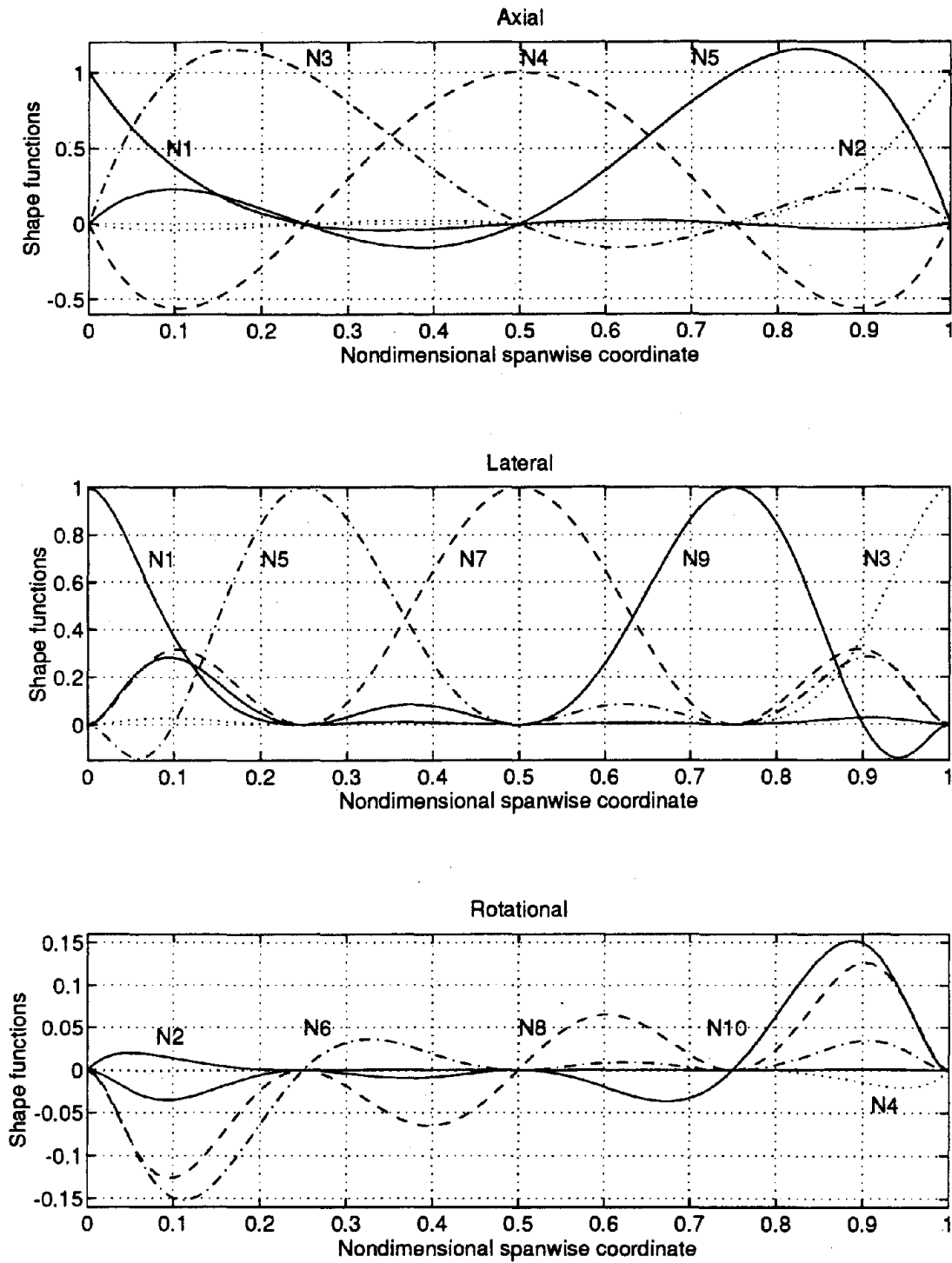where

$$\beta = \frac{\bar{m}l}{14142148020}$$

Figure A.4: Shape functions for the axial, lateral and rotational degrees-of-freedom for the P_3 formulation

A.5 Mixed Formulation

• **Node Locations:** Nodes are located at the element ends $\eta = 0, 1$.

• **Displacement Fields:** The mixed formulation uses two sets of displacement fields: the polynomial displacement fields given by Eq. (A.1), and the frequency dependent displacement fields u_e and v_e based on the exact solution to the governing differential equations of motion.

$$
\begin{aligned}
u_e &= \bar{e}_0 \cos bx + \bar{e}_1 \sin bx \\
v_e &= e_0 \cos \bar{b}x + e_1 \sin \bar{b}x + e_2 \cosh \bar{b}x + e_3 \sinh \bar{b}x
\end{aligned}
\tag{A.29}
$$

where $b = \sqrt{\dfrac{m\omega^2}{EA}}$ and $\bar{b} = \left(\dfrac{m\omega^2}{EI}\right)^{\frac{1}{4}}$.

• **Shape Functions for Axial Vibration:** The polynomial based shape functions given by Eq. (A.2) and the frequency dependent shape functions

$$
\begin{aligned}
N_{1_e} &= \cos(\theta\eta) - \frac{\sin(\theta\eta)}{\tan\theta} \\
N_{2_e} &= \frac{\sin(\theta\eta)}{\sin\theta}
\end{aligned}
\tag{A.30}
$$

where $\theta = \sqrt{\dfrac{\omega^2 m l^2}{EA}}$.

• **Shape Functions for Lateral Vibration:** The polynomial based shape functions given by Eq. (A.3) and the frequency dependent shape functions

$$
\begin{aligned}
N_{1_e} &= \frac{1}{2\Delta}\left(C_1 \cos(\phi\eta) - C_2 \sin(\phi\eta) + C_3 \cosh(\phi\eta) + C_2 \sinh(\phi\eta) \right) \\
N_{2_e} &= \frac{l}{2\phi\Delta}\left(C_4 \cos(\phi\eta) + C_3 \sin(\phi\eta) - C_4 \cosh(\phi\eta) + C_1 \sinh(\phi\eta) \right) \\
N_{3_e} &= \frac{1}{2\Delta}\left(C_5 \cos(\phi\eta) + C_6 \sin(\phi\eta) - C_5 \cosh(\phi\eta) - C_6 \sinh(\phi\eta) \right) \\
N_{4_e} &= \frac{l}{2\phi\Delta}\left(C_7 \cos(\phi\eta) + C_5 \sin(\phi\eta) - C_7 \cosh(\phi\eta) - C_5 \sinh(\phi\eta) \right)
\end{aligned}
\tag{A.31}
$$

where

$$\phi = \left(\frac{\omega^2 m l^4}{EI}\right)^{\frac{1}{4}}$$

$$\Delta = (1 - \cos\phi\cosh\phi)$$

$$C_1 = 1 + \sinh\phi\sin\phi - \cosh\phi\cos\phi$$

$$C_2 = \sinh\phi\cos\phi + \cosh\phi\sin\phi$$

$$C_3 = 1 - \sinh\phi\sin\phi - \cosh\phi\cos\phi \qquad\qquad (A.32)$$

$$C_4 = \cosh\phi\sin\phi - \sinh\phi\cos\phi$$

$$C_5 = \cos\phi - \cosh\phi$$

$$C_6 = \sin\phi + \sinh\phi$$

$$C_7 = \sinh\phi - \sin\phi$$

- **Element Stiffness and Mass Matrices for Axial Vibrations:**

$$\bar{\mathbf{K}}_e^e = \frac{EA}{l}\begin{bmatrix} 1 & -1 \\ -1 & 1 \end{bmatrix} \qquad\qquad (A.33)$$

$$\bar{\mathbf{M}}_e^e = ml\begin{bmatrix} \left(\dfrac{1}{\theta^2} - \dfrac{\cos\theta}{\theta\sin\theta}\right) & \left(\dfrac{1}{\theta\sin\theta} - \dfrac{1}{\theta^2}\right) \\[2ex] \left(\dfrac{1}{\theta\sin\theta} - \dfrac{1}{\theta^2}\right) & \left(\dfrac{1}{\theta^2} - \dfrac{\cos\theta}{\theta\sin\theta}\right) \end{bmatrix} \qquad (A.34)$$

- **Element Stiffness and Mass Matrices for Bending Vibrations:**

$$\mathbf{K}_e^e = \frac{EI}{l^3}\begin{bmatrix} 12 & 6l & -12 & 6l \\ 6l & 4l^2 & -6l & 2l^2 \\ -12 & -6l & 12 & -6l \\ 6l & 2l^2 & -6l & 4l^2 \end{bmatrix} \qquad (A.35)$$

$$\mathbf{M}_e^e = \frac{ml}{2\Delta}\begin{bmatrix} M_{11} & M_{12} & M_{13} & M_{14} \\ M_{21} & M_{22} & M_{23} & M_{24} \\ M_{31} & M_{32} & M_{33} & M_{34} \\ M_{41} & M_{42} & M_{43} & M_{44} \end{bmatrix} \qquad (A.36)$$

where

$$M_{11} = C_1 f_1 - C_2 f_2 + C_3 f_3 + C_2 f_4$$

$$M_{12} = \frac{l}{\phi} (C_4 f_1 + C_3 f_2 - C_4 f_3 + C_1 f_4)$$

$$M_{13} = C_5 f_1 + C_6 f_2 - C_5 f_3 - C_6 f_4$$

$$M_{14} = \frac{l}{\phi} (C_7 f_1 + C_5 f_2 - C_7 f_3 - C_5 f_4)$$

$$M_{21} = C_1 f_5 - C_2 f_6 + C_3 f_7 + C_2 f_8$$

$$M_{22} = \frac{l}{\phi} (C_4 f_5 + C_3 f_6 - C_4 f_7 + C_1 f_8)$$

$$M_{23} = C_5 f_5 + C_6 f_6 - C_5 f_7 - C_6 f_8$$

$$M_{24} = \frac{l}{\phi} (C_7 f_5 + C_5 f_6 - C_7 f_7 - C_5 f_8)$$

$$M_{31} = C_1 f_9 - C_2 f_{10} + C_3 f_{11} + C_2 f_{12}$$

$$M_{32} = \frac{l}{\phi} (C_4 f_9 + C_3 f_{10} - C_4 f_{11} + C_1 f_{12})$$

$$M_{33} = C_5 f_9 + C_6 f_{10} - C_5 f_{11} - C_6 f_{12}$$

$$M_{34} = \frac{l}{\phi} (C_7 f_9 + C_5 f_{10} - C_7 f_{11} - C_5 f_{12})$$

$$M_{41} = C_1 f_{13} - C_2 f_{14} + C_3 f_{15} + C_2 f_{16}$$

$$M_{42} = \frac{l}{\phi} (C_4 f_{13} + C_3 f_{14} - C_4 f_{15} + C_1 f_{16})$$

$$M_{43} = C_5 f_{13} + C_6 f_{14} - C_5 f_{15} - C_6 f_{16}$$

$$M_{44} = \frac{l}{\phi} (C_7 f_{13} + C_5 f_{14} - C_7 f_{15} - C_5 f_{16})$$

$$(A.37)$$

and

$$f_1 = \frac{12}{\phi^4} - \frac{6 \sin \phi}{\phi^3} - \frac{12 \cos \phi}{\phi^4}$$

$$f_2 = \frac{1}{\phi} + \frac{6}{\phi^3} - \frac{6 \cos \phi}{\phi^3} - \frac{12 \sin \phi}{\phi^4}$$

$$f_3 = \frac{12}{\phi^4} - \frac{6 \sinh \phi}{\phi^3} - \frac{12 \cosh \phi}{\phi^4}$$

$$f_4 = -\frac{1}{\phi} + \frac{6}{\phi^3} - \frac{6 \cosh \phi}{\phi^3} - \frac{12 \sinh \phi}{\phi^4}$$

$$(A.38)$$

$$f_5 = l \left(\frac{6}{\phi^4} - \frac{1}{\phi^2} - \frac{2\sin\phi}{\phi^3} - \frac{6\cos\phi}{\phi^4} \right)$$

$$f_6 = l \left(\frac{4}{\phi^3} + \frac{2\cos\phi}{\phi^3} - \frac{6\sin\phi}{\phi^4} \right)$$

$$f_7 = l \left(\frac{6}{\phi^4} + \frac{1}{\phi^2} + \frac{2\sinh\phi}{\phi^3} - \frac{6\cosh\phi}{\phi^4} \right)$$

$$f_8 = l \left(\frac{4}{\phi^3} + \frac{2\cosh\phi}{\phi^3} - \frac{6\sinh\phi}{\phi^4} \right)$$

$$f_9 = \frac{12}{\phi^4} + \frac{\sin\phi}{\phi} + \frac{6\sin\phi}{\phi^3} + \frac{12\cos\phi}{\phi^4}$$

$$f_{10} = -\frac{6}{\phi^3} - \frac{\cos\phi}{\phi} - \frac{6\cos\phi}{\phi^3} + \frac{12\sin\phi}{\phi^4}$$

$$f_{11} = -\frac{12}{\phi^4} + \frac{\sinh\phi}{\phi} - \frac{6\sinh\phi}{\phi^3} + \frac{12\cosh\phi}{\phi^4}$$

$$f_{12} = -\frac{6}{\phi^3} + \frac{\cosh\phi}{\phi} - \frac{6\cos\phi}{\phi^3} + \frac{12\sinh\phi}{\phi^4}$$

$$f_{13} = l \left(\frac{6}{\phi^4} + \frac{\cos\phi}{\phi^2} - \frac{4\sin\phi}{\phi^3} - \frac{6\cos\phi}{\phi^4} \right)$$

$$f_{14} = l \left(\frac{2}{\phi^3} + \frac{\sin\phi}{\phi^2} + \frac{4\cos\phi}{\phi^3} - \frac{6\sin\phi}{\phi^4} \right)$$

$$f_{15} = l \left(\frac{6}{\phi^4} - \frac{\cosh\phi}{\phi^2} + \frac{4\sinh\phi}{\phi^3} - \frac{6\cosh\phi}{\phi^4} \right)$$

$$f_{16} = l \left(\frac{2}{\phi^3} - \frac{\sinh\phi}{\phi^2} + \frac{4\cosh\phi}{\phi^3} - \frac{6\sinh\phi}{\phi^4} \right)$$

(A.38)

Taylor Series Expansion of the Frequency Dependent Matrices

B.1 The Dynamic Stiffness Matrix

The dynamic stiffness matrix for lateral vibrations is derived in Section 2.1 from the exact harmonic solution to the governing partial differential equation of motion and is given as

$$
\mathbf{D} = B \begin{bmatrix}
\bar{b}^2(cS + sC) & \bar{b}sS & -\bar{b}^2(s + S) & -\bar{b}(c - C) \\
\bar{b}sS & (sC - cS) & \bar{b}(c - C) & (S - s) \\
-\bar{b}^2(s + S) & \bar{b}(c - C) & \bar{b}^2(cS + sC) & -\bar{b}sS \\
-\bar{b}(c - C) & (S - s) & -\bar{b}sS & (sC - cS)
\end{bmatrix}
\tag{B.1}
$$

where,

$$
\bar{b} = \left(\frac{m\omega^2}{EI}\right)^{\frac{1}{4}} \qquad B = \frac{\bar{b}EI}{(1 - \cos\bar{b}l \cosh\bar{b}l)}
$$

$$
s = \sin\bar{b}l \qquad S = \sinh\bar{b}l
\tag{B.2}
$$

$$
c = \cos\bar{b}l \qquad C = \cosh\bar{b}l
$$

subject to the condition that $(1 - \cos\bar{b}l \cosh\bar{b}l) \neq 0$. For series expansion, it is better to

work with the nondimensional variable $\phi = \left(\dfrac{\omega^2 m l^4}{EI}\right)^{\frac{1}{4}}$. The first step in this analysis is to write the Taylor series expansion about $\phi = 0$ for elementary trigonometric and hyperbolic functions as given below.

$$
\begin{aligned}
\sin \bar{b}l &= \sin \phi \\
&= \phi - \frac{\phi^3}{6} + \frac{\phi^5}{120} - \frac{\phi^7}{5040} + \frac{\phi^9}{362880} - \frac{\phi^{11}}{39916800} + \mathcal{O}(\phi^{13}) \\
\sinh \bar{b}l &= \sinh \phi \\
&= \phi + \frac{\phi^3}{6} + \frac{\phi^5}{120} + \frac{\phi^7}{5040} + \frac{\phi^9}{362880} + \frac{\phi^{11}}{39916800} + \mathcal{O}(\phi^{13}) \\
\cos \bar{b}l &= \cos \phi \\
&= 1 - \frac{\phi^2}{2} + \frac{\phi^4}{24} - \frac{\phi^6}{720} + \frac{\phi^8}{40320} - \frac{\phi^{10}}{3628800} + \frac{\phi^{12}}{479001600} + \mathcal{O}(\phi^{13}) \\
\cosh \bar{b}l &= \cosh \phi \\
&= 1 + \frac{\phi^2}{2} + \frac{\phi^4}{24} + \frac{\phi^6}{720} + \frac{\phi^8}{40320} + \frac{\phi^{10}}{3628800} + \frac{\phi^{12}}{479001600} + \mathcal{O}(\phi^{13}) \\
\Delta &= (1 - \cos \phi \cosh \phi) \\
&= \frac{\phi^4}{6} - \frac{\phi^8}{2520} + \frac{\phi^{12}}{7484400} + \mathcal{O}(\phi^{13})
\end{aligned}
$$

(B.3)

Substituting the above elementary series into Eq. (B.1) gives the following power series expressions for each element of the 4×4 dynamic stiffness matrix.

$$
\begin{aligned}
D_{11} &= \frac{EI}{\Delta}(\frac{\phi}{l})^3(\cos \phi \sinh \phi + \sin \phi \cosh \phi) \\
&= \frac{12\,EI}{l^3} - \frac{13\,EI\,\phi^4}{35\,l^3} - \frac{59\,EI\,\phi^8}{161700\,l^3} - \frac{551\,EI\,\phi^{12}}{794593800\,l^3} + \mathcal{O}(\phi^{13}) \\
D_{12} &= \frac{EI}{\Delta}(\frac{\phi}{l})^2(\sin \phi \sinh \phi) \\
&= \frac{6\,EI}{l^2} - \frac{11\,EI\,\phi^4}{210\,l^2} - \frac{223\,EI\,\phi^8}{2910600\,l^2} - \frac{3547\,EI\,\phi^{12}}{23837814000\,l^2} + \mathcal{O}(\phi^{13})
\end{aligned}
$$

(B.4)

$$D_{13} = -\frac{EI}{\Delta}(\frac{\phi}{l})^3(\sin\phi + \sinh\phi)$$

$$= \frac{-12\,EI}{l^3} - \frac{9\,EI\,\phi^4}{70\,l^3} - \frac{1279\,EI\,\phi^8}{3880800\,l^3} - \frac{5801\,EI\,\phi^{12}}{8475667200\,l^3} + \mathcal{O}(\phi^{13})$$

$$D_{14} = -\frac{EI}{\Delta}(\frac{\phi}{l})^2(\cos\phi - \cosh\phi)$$

$$= \frac{6\,EI}{l^2} + \frac{13\,EI\,\phi^4}{420\,l^2} + \frac{1681\,EI\,\phi^8}{23284800\,l^2} + \frac{112631\,EI\,\phi^{12}}{762810048000\,l^2} + \mathcal{O}(\phi^{13})$$

$$D_{21} = \frac{EI}{\Delta}(\frac{\phi}{l})^2(\sin\phi\sinh\phi)$$

$$= \frac{6\,EI}{l^2} - \frac{11\,EI\,\phi^4}{210\,l^2} - \frac{223\,EI\,\phi^8}{2910600\,l^2} - \frac{3547\,EI\,\phi^{12}}{238378140000\,l^2} + \mathcal{O}(\phi^{13})$$

$$D_{22} = \frac{EI}{\Delta}(\frac{\phi}{l})(\sin\phi\cosh\phi - \cos\phi\sinh\phi)$$

$$= \frac{4\,EI}{l} - \frac{EI\,\phi^4}{105\,l} - \frac{71\,EI\,\phi^8}{4365900\,l} - \frac{127\,EI\,\phi^{12}}{3972969000\,l} + \mathcal{O}(\phi^{13})$$

$$\text{(B.4)}$$

$$D_{23} = \frac{EI}{\Delta}(\frac{\phi}{l})^2(\cos\phi - \cosh\phi)$$

$$= \frac{-6\,EI}{l^2} - \frac{13\,EI\,\phi^4}{420\,l^2} - \frac{1681\,EI\,\phi^8}{23284800\,l^2} - \frac{112631\,EI\,\phi^{12}}{762810048000\,l^2} + \mathcal{O}(\phi^{13})$$

$$D_{24} = \frac{EI}{\Delta}(\frac{\phi}{l})(\sinh\phi - \sin\phi)$$

$$= \frac{2\,EI}{l} + \frac{EI\,\phi^4}{140\,l} + \frac{1097\,EI\,\phi^8}{698544000\,l} + \frac{899\,EI\,\phi^{12}}{282522240000\,l} + \mathcal{O}(\phi^{13})$$

$$D_{31} = -\frac{EI}{\Delta}(\frac{\phi}{l})^3(\sin\phi + \sinh\phi)$$

$$= \frac{-12\,EI}{l^3} - \frac{9\,EI\,\phi^4}{70\,l^3} - \frac{1279\,EI\,\phi^8}{3880800\,l^3} - \frac{5801\,EI\,\phi^{12}}{8475667200\,l^3} + \mathcal{O}(\phi^{13})$$

$$D_{32} = \frac{EI}{\Delta}(\frac{\phi}{l})^2(\cos\phi - \cosh\phi)$$

$$= \frac{-6\,EI}{l^2} - \frac{13\,EI\,\phi^4}{420\,l^2} - \frac{1681\,EI\,\phi^8}{23284800\,l^2} - \frac{112631\,EI\,\phi^{12}}{762810048000\,l^2} + \mathcal{O}(\phi^{13})$$

$$D_{33} = \frac{EI}{\Delta}(\frac{\phi}{l})^3(\cos\phi\sinh\phi + \sin\phi\cosh\phi)$$

$$= \frac{12\,EI}{l^3} - \frac{13\,EI\,\phi^4}{35\,l^3} - \frac{59\,EI\,\phi^8}{161700\,l^3} - \frac{551\,EI\,\phi^{12}}{794593800\,l^3} + \mathcal{O}(\phi^{13})$$

$$D_{34} = -\frac{EI}{\Delta}(\frac{\phi}{l})^2(\sin\phi\sinh\phi)$$

$$= \frac{-6\,EI}{l^2} + \frac{11\,EI\,\phi^4}{210\,l^2} + \frac{223\,EI\,\phi^8}{2910600\,l^2} + \frac{3547\,EI\,\phi^{12}}{23837814000\,l^2} + \mathcal{O}(\phi^{13})$$

$$D_{41} = -\frac{EI}{\Delta}(\frac{\phi}{l})^2(\cos\phi - \cosh\phi)$$

$$= \frac{6\,EI}{l^2} + \frac{13\,EI\,\phi^4}{420\,l^2} + \frac{1681\,EI\,\phi^8}{23284800\,l^2} + \frac{112631\,EI\,\phi^{12}}{762810048000\,l^2} + \mathcal{O}(\phi^{13})$$

$$D_{42} = \frac{EI}{\Delta}(\frac{\phi}{l})(\sinh\phi - \sin\phi)$$

$$= \frac{2\,EI}{l} + \frac{EI\,\phi^4}{140\,l} + \frac{1097\,EI\,\phi^8}{698544000\,l} + \frac{899\,EI\,\phi^{12}}{28252224000\,l} + \mathcal{O}(\phi^{13})$$

$$D_{43} = -\frac{EI}{\Delta}(\frac{\phi}{l})^2(\sin\phi\sinh\phi)$$

$$= \frac{-6\,EI}{l^2} + \frac{11\,EI\,\phi^4}{210\,l^2} + \frac{223\,EI\,\phi^8}{2910600\,l^2} + \frac{3547\,EI\,\phi^{12}}{23837814000\,l^2} + \mathcal{O}(\phi^{13})$$

$$D_{44} = \frac{EI}{\Delta}(\frac{\phi}{l})(\sin\phi\cosh\phi - \cos\phi\sinh\phi)$$

$$= \frac{4\,EI}{l} - \frac{EI\,\phi^4}{105\,l} - \frac{71\,EI\,\phi^8}{4365900\,l} - \frac{127\,EI\,\phi^{12}}{3972969000\,l} + \mathcal{O}(\phi^{13})$$

$$(B.4)$$

Note that the first term in the above power series expansion is constant for all elements of the dynamic stiffness matrix. Furthermore, the matrix formed by the constant terms is exactly the same as the stiffness matrix of the conventional formulation given by Eq. (A.6). Hence, for $\phi = 0$ (i.e., $\omega = 0$) the dynamic stiffness matrix reduces to the polynomial based conventional stiffness matrix.

B.2 The Mixed Formulation Mass Matrix

In the mixed formulation both the polynomial based shape functions and frequency dependent shape functions are used to form the mass matrix. The general form of this matrix for lateral vibrations is given by Eq. (A.37). Each element of the 4×4 mixed formulation mass matrix is expressed in terms of some of the parameters C_1 through C_7 and f_1 through f_{16}. Using the trigonometric and hyperbolic series of Eq. (B.3), the power series for these parameters are derived as below.

$$
\begin{aligned}
C_1 &= 1 + \sinh\phi\sin\phi - \cosh\phi\cos\phi \\
&= \phi^2 + \frac{\phi^4}{6} - \frac{\phi^6}{90} - \frac{\phi^8}{2520} + \frac{\phi^{10}}{113400} + \frac{\phi^{12}}{7484400} + \mathcal{O}(\phi^{13}) \\[2mm]
C_2 &= \sinh\phi\cos\phi + \cosh\phi\sin\phi \\
&= 2\phi - \frac{\phi^5}{15} + \frac{\phi^9}{11340} + \mathcal{O}(\phi^{13}) \\[2mm]
C_3 &= 1 - \sinh\phi\sin\phi - \cosh\phi\cos\phi \\
&= -\phi^2 + \frac{\phi^4}{6} + \frac{\phi^6}{90} - \frac{\phi^8}{2520} - \frac{\phi^{10}}{113400} + \frac{\phi^{12}}{7484400} + \mathcal{O}(\phi^{13}) \\[2mm]
C_4 &= \cosh\phi\sin\phi - \sinh\phi\cos\phi \\
&= \frac{2\,\phi^3}{3} - \frac{\phi^7}{315} + \frac{\phi^{11}}{623700} + \mathcal{O}(\phi^{13}) \\[2mm]
C_5 &= \cos\phi - \cosh\phi \\
&= -\phi^2 - \frac{\phi^6}{360} - \frac{\phi^{10}}{1814400} + \mathcal{O}(\phi^{13}) \\[2mm]
C_6 &= \sin\phi + \sinh\phi \\
&= 2\phi + \frac{\phi^5}{60} + \frac{\phi^9}{181440} + \mathcal{O}(\phi^{13}) \\[2mm]
C_7 &= \sinh\phi - \sin\phi \\
&= \frac{\phi^3}{3} + \frac{\phi^7}{2520} + \frac{\phi^{11}}{19958400} + \mathcal{O}(\phi^{13})
\end{aligned}
\tag{B.5}
$$

$$f_1 = \frac{12}{\phi^4} - \frac{6\sin\phi}{\phi^3} - \frac{12\cos\phi}{\phi^4}$$

$$= \frac{l}{2} - \frac{l\,\phi^2}{30} + \frac{l\,\phi^4}{1120} - \frac{l\,\phi^6}{75600} + \frac{l\,\phi^8}{7983360} - \frac{l\,\phi^{10}}{1210809600}$$

$$+ \frac{l\,\phi^{12}}{249080832000} + \mathcal{O}(\phi^{13})$$

$$f_2 = \frac{1}{\phi} + \frac{6}{\phi^3} - \frac{6\cos\phi}{\phi^3} - \frac{12\sin\phi}{\phi^4}$$

$$= \frac{3\,l\,\phi}{20} - \frac{l\,\phi^3}{168} + \frac{l\,\phi^5}{8640} - \frac{l\,\phi^7}{739200} + \frac{l\,\phi^9}{94348800}$$

$$- \frac{l\,\phi^{11}}{16765056000} + \mathcal{O}(\phi^{13})$$

$$f_3 = \frac{12}{\phi^4} - \frac{6\sinh\phi}{\phi^3} - \frac{12\cosh\phi}{\phi^4}$$

$$= \frac{l}{2} + \frac{l\,\phi^2}{30} + \frac{l\,\phi^4}{1120} + \frac{l\,\phi^6}{75600} + \frac{l\,\phi^8}{7983360} + \frac{l\,\phi^{10}}{1210809600} \qquad \text{(B.6)}$$

$$+ \frac{l\,\phi^{12}}{249080832000} + \mathcal{O}(\phi^{13})$$

$$f_4 = -\frac{1}{\phi} + \frac{6}{\phi^3} - \frac{6\cosh\phi}{\phi^3} - \frac{12\sinh\phi}{\phi^4}$$

$$= \frac{3\,l\,\phi}{20} + \frac{l\,\phi^3}{168} + \frac{l\,\phi^5}{8640} + \frac{l\,\phi^7}{739200} + \frac{l\,\phi^9}{94348800}$$

$$+ \frac{l\,\phi^{11}}{16765056000} + \mathcal{O}(\phi^{13})$$

$$f_5 = l\left(\frac{6}{\phi^4} - \frac{1}{\phi^2} - \frac{2\sin\phi}{\phi^3} - \frac{6\cos\phi}{\phi^4}\right)$$

$$= \frac{l^2}{12} - \frac{l^2\,\phi^2}{120} + \frac{l^2\,\phi^4}{4032} - \frac{l^2\,\phi^6}{259200} + \frac{l^2\,\phi^8}{26611200} - \frac{l^2\,\phi^{10}}{3962649600}$$

$$+ \frac{l^2\,\phi^{12}}{804722688000} + \mathcal{O}(\phi^{13})$$

$$f_6 = l\left(\frac{4}{\phi^3} + \frac{2\cos\phi}{\phi^3} - \frac{6\sin\phi}{\phi^4}\right)$$

$$= \frac{l^2\,\phi}{30} - \frac{l^2\,\phi^3}{630} + \frac{l^2\,\phi^5}{30240} - \frac{l^2\,\phi^7}{2494800} + \frac{l^2\,\phi^9}{311351040}$$

$$- \frac{l^2\,\phi^{11}}{54486432000} + \mathcal{O}(\phi^{13})$$

$$f_7 = l\left(\frac{6}{\phi^4} + \frac{1}{\phi^2} + \frac{2\sinh\phi}{\phi^3} - \frac{6\cosh\phi}{\phi^4}\right)$$

$$= \frac{l^2}{12} + \frac{l^2\,\phi^2}{120} + \frac{l^2\,\phi^4}{4032} + \frac{l^2\,\phi^6}{259200} + \frac{l^2\,\phi^8}{26611200} + \frac{l^2\,\phi^{10}}{3962649600}$$

$$+ \frac{l^2\,\phi^{12}}{804722688000} + \mathcal{O}(\phi^{13})$$

$$f_8 = l\left(\frac{4}{\phi^3} + \frac{2\cosh\phi}{\phi^3} - \frac{6\sinh\phi}{\phi^4}\right)$$

$$= \frac{l^2\,\phi}{30} + \frac{l^2\,\phi^3}{630} + \frac{l^2\,\phi^5}{30240} + \frac{l^2\,\phi^7}{2494800} + \frac{l^2\,\phi^9}{311351040}$$ (B.6)

$$+ \frac{l^2\,\phi^{11}}{54486432000} + \mathcal{O}(\phi^{13})$$

$$f_9 = \frac{12}{\phi^4} + \frac{\sin\phi}{\phi} + \frac{6\sin\phi}{\phi^3} + \frac{12\cos\phi}{\phi^4}$$

$$= \frac{l}{2} - \frac{2\,l\,\phi^2}{15} + \frac{5\,l\,\phi^4}{672} - \frac{l\,\phi^6}{5400} + \frac{l\,\phi^8}{380160} - \frac{l\,\phi^{10}}{41277600}$$

$$+ \frac{l\,\phi^{12}}{6386688000} + \mathcal{O}(\phi^{13})$$

$$f_{10} = -\frac{6}{\phi^3} - \frac{\cos\phi}{\phi} - \frac{6\cos\phi}{\phi^3} + \frac{12\sin\phi}{\phi^4}$$

$$= \frac{7\,l\,\phi}{20} - \frac{l\,\phi^3}{28} + \frac{11\,l\,\phi^5}{8640} - \frac{13\,l\,\phi^7}{554400} + \frac{l\,\phi^9}{3773952}$$

$$- \frac{17\,l\,\phi^{11}}{8382528000} + \mathcal{O}(\phi^{13})$$

$$f_{11} = -\frac{12}{\phi^4} + \frac{\sinh\phi}{\phi} - \frac{6\sinh\phi}{\phi^3} + \frac{12\cosh\phi}{\phi^4}$$

$$= \frac{l}{2} + \frac{21\,l\,\phi^2}{15} + \frac{51\,l\,\phi^4}{672} + \frac{l\,\phi^6}{5400} + \frac{l\,\phi^8}{380160} + \frac{l\,\phi^{10}}{41277600}$$

$$+ \frac{l\,\phi^{12}}{6386688000} + \mathcal{O}(\phi^{13})$$

$$f_{12} = -\frac{6}{\phi^3} + \frac{\cosh\phi}{\phi} - \frac{6\cos\phi}{\phi^3} + \frac{12\sinh\phi}{\phi^4}$$

$$= \frac{7\,l\,\phi}{20} + \frac{l\,\phi^3}{28} + \frac{11\,l\,\phi^5}{8640} + \frac{13\,l\,\phi^7}{554400} + \frac{l\,\phi^9}{3773952}$$

$$+ \frac{17\,l\,\phi^{11}}{8382528000} + \mathcal{O}(\phi^{13})$$

$$f_{13} = l\left(\frac{6}{\phi^4} + \frac{\cos\phi}{\phi^2} - \frac{4\sin\phi}{\phi^3} - \frac{6\cos\phi}{\phi^4}\right)$$

$$= \frac{-l^2}{12} + \frac{l^2\,\phi^2}{60} - \frac{l^2\,\phi^4}{1344} + \frac{l^2\,\phi^6}{64800} - \frac{l^2\,\phi^8}{5322240} + \frac{l^2\,\phi^{10}}{660441600} \qquad \text{(B.6)}$$

$$- \frac{l^2\,\phi^{12}}{114960384000} + \mathcal{O}(\phi^{13})$$

$$f_{14} = l\left(\frac{2}{\phi^3} + \frac{\sin\phi}{\phi^2} + \frac{4\cos\phi}{\phi^3} - \frac{6\sin\phi}{\phi^4}\right)$$

$$= -\frac{l^2\,\phi}{20} + \frac{l^2\,\phi^3}{252} - \frac{l^2\,\phi^5}{8640} + \frac{l^2\,\phi^7}{554400} - \frac{l^2\,\phi^9}{56609280}$$

$$+ \frac{l^2\,\phi^{11}}{8382528000} + \mathcal{O}(\phi^{13})$$

$$f_{15} = l\left(\frac{6}{\phi^4} - \frac{\cosh\phi}{\phi^2} + \frac{4\sinh\phi}{\phi^3} - \frac{6\cosh\phi}{\phi^4}\right)$$

$$= \frac{-l^2}{12} - \frac{l^2\,\phi^2}{60} - \frac{l^2\,\phi^4}{1344} - \frac{l^2\,\phi^6}{64800} - \frac{l^2\,\phi^8}{5322240} - \frac{l^2\,\phi^{10}}{660441600}$$

$$- \frac{l^2\,\phi^{12}}{114960384000} + \mathcal{O}(\phi^{13})$$

$$f_{16} = l \left(\frac{2}{\phi^3} - \frac{\sinh \phi}{\phi^2} + \frac{4 \cosh \phi}{\phi^3} - \frac{6 \sinh \phi}{\phi^4} \right)$$

$$= -\frac{l^2 \phi}{20} - \frac{l^2 \phi^3}{252} - \frac{l^2 \phi^5}{8640} - \frac{l^2 \phi^7}{554400} - \frac{l^2 \phi^9}{56609280} \qquad (B.6)$$

$$- \frac{l^2 \phi^{11}}{8382528000} + \mathcal{O}(\phi^{13})$$

Substituting the power series expressions for C_1 through C_7 and f_1 through f_{16} into Eq. (A.37), and simplifying and regrouping equal powers of ϕ gives the power series expansion of the mass matrix.

$$M_{11}^e = (\frac{ml}{2\Delta})(C_1 f_1 - C_2 f_2 + C_3 f_3 + C_2 f_4)$$

$$= \frac{13 \, l \, m}{35} + \frac{59 \, l \, m \, \phi^4}{161700} + \frac{551 \, l \, m \, \phi^8}{794593800} + \mathcal{O}(\phi^{13})$$

$$M_{12}^e = (\frac{ml}{2\Delta})\frac{l}{\phi}(C_4 f_1 + C_3 f_2 - C_4 f_3 + C_1 f_4)$$

$$= \frac{11 \, l^2 \, m}{210} + \frac{223 \, l^2 \, m \, \phi^4}{2910600} + \frac{3547 \, l^2 \, m \, \phi^8}{23837814000}$$

$$+ \frac{4215149 \, l^2 \, m \, \phi^{12}}{142288865278560000} + \mathcal{O}(\phi^{13})$$

$$M_{13}^e = (\frac{ml}{2\Delta})(C_5 f_1 + C_6 f_2 - C_5 f_3 - C_6 f_4) \qquad (B.7)$$

$$= \frac{9 \, l \, m}{70} + \frac{1279 \, l \, m \, \phi^4}{3880800} + \frac{5801 \, l \, m \, \phi^8}{8475667200}$$

$$+ \frac{417329273 \, l \, m \, \phi^{12}}{3035495792609280000} + \mathcal{O}(\phi^{13})$$

$$M_{14}^e = (\frac{ml}{2\Delta})\frac{l}{\phi}(C_7 f_1 + C_5 f_2 - C_7 f_3 - C_5 f_4)$$

$$= \frac{-13 \, l^2 \, m}{420} - \frac{1681 \, l^2 \, m \, \phi^4}{23284800} - \frac{112631 \, l^2 \, m \, \phi^8}{762810048000}$$

$$- \frac{41460911 \, l^2 \, m \, \phi^{12}}{1400998058127360000} + \mathcal{O}(\phi^{13})$$

$$M_{21}^e = (\frac{ml}{2\Delta})(C_1 f_5 - C_2 f_6 + C_3 f_7 + C_2 f_8)$$

$$= \frac{11\, l^2\, m}{210} + \frac{223\, l^2\, m\, \phi^4}{2910600} + \frac{3547\, l^2\, m\, \phi^8}{23837814000}$$

$$+ \frac{4215149\, l^2\, m\, \phi^{12}}{142288865278560000} + \mathcal{O}(\phi^{13})$$

$$M_{22}^e = (\frac{ml}{2\Delta})\frac{l}{\phi}(C_4 f_5 + C_3 f_6 - C_4 f_7 + C_1 f_8)$$

$$= \frac{l^3\, m}{105} + \frac{71\, l^3\, m\, \phi^4}{4365900} + \frac{127\, l^3\, m\, \phi^8}{3972969000}$$

$$+ \frac{20403571\, l^3\, m\, \phi^{12}}{320149994676760000} + \mathcal{O}(\phi^{13})$$

$$M_{23}^e = (\frac{ml}{2\Delta})(C_5 f_5 + C_6 f_6 - C_5 f_7 - C_6 f_8)$$

$$= \frac{13\, l^2\, m}{420} + \frac{1681\, l^2\, m\, \phi^4}{23284800} + \frac{112631\, l^2\, m\, \phi^8}{762810048000} \qquad \text{(B.7)}$$

$$+ \frac{41460911\, l^2\, m\, \phi^{12}}{140099805812736000} + \mathcal{O}(\phi^{13})$$

$$M_{24}^e = (\frac{ml}{2\Delta})\frac{l}{\phi}(C_7 f_5 + C_5 f_6 - C_7 f_7 - C_5 f_8)$$

$$= \frac{-(l^3\, m)}{140} - \frac{1097\, l^3\, m\, \phi^4}{69854400} - \frac{899\, l^3\, m\, \phi^8}{28252224000}$$

$$- \frac{5220181117\, l^3\, m\, \phi^{12}}{8195838640045056000} + \mathcal{O}(\phi^{13})$$

$$M_{31}^e = (\frac{ml}{2\Delta})(C_1 f_9 - C_2 f_{10} + C_3 f_{11} + C_2 f_{12})$$

$$= \frac{9\, l\, m}{70} + \frac{1279\, l\, m\, \phi^4}{3880800} + \frac{5801\, l\, m\, \phi^8}{8475667200}$$

$$+ \frac{417329273\, l\, m\, \phi^{12}}{3035495792609280000} + \mathcal{O}(\phi^{13})$$

$$M_{32}^e = (\frac{ml}{2\Delta})\frac{l}{\phi}(C_4 f_9 + C_3 f_{10} - C_4 f_{11} + C_1 f_{12})$$

$$= \frac{13\,l^2\,m}{420} + \frac{1681\,l^2\,m\,\phi^4}{23284800} + \frac{112631\,l^2\,m\,\phi^8}{762810048000}$$

$$+ \frac{41460911\,l^2\,m\,\phi^{12}}{140099805812736000} + \mathcal{O}(\phi^{13})$$

$$M_{33}^e = (\frac{ml}{2\Delta})(C_5 f_9 + C_6 f_{10} - C_5 f_{11} - C_6 f_{12})$$

$$= \frac{13\,l\,m}{35} + \frac{59\,l\,m\,\phi^4}{161700} + \frac{551\,l\,m\,\phi^8}{794593800}$$

$$+ \frac{753689\,l\,m\,\phi^{12}}{547264866456000} + \mathcal{O}(\phi^{13})$$

$$M_{34}^e = (\frac{ml}{2\Delta})\frac{l}{\phi}(C_7 f_9 + C_5 f_{10} - C_7 f_{11} - C_5 f_{12})$$

$$= \frac{-11\,l^2\,m}{210} - \frac{223\,l^2\,m\,\phi^4}{2910600} - \frac{3547\,l^2\,m\,\phi^8}{23837814000} \qquad (B.7)$$

$$- \frac{4215149\,l^2\,m\,\phi^{12}}{14228886527856000} + \mathcal{O}(\phi^{13})$$

$$M_{41}^e = (\frac{ml}{2\Delta})(C_1 f_{13} - C_2 f_{14} + C_3 f_{15} + C_2 f_{16})$$

$$= \frac{-13\,l^2\,m}{420} - \frac{1681\,l^2\,m\,\phi^4}{23284800} - \frac{112631\,l^2\,m\,\phi^8}{762810048000}$$

$$- \frac{41460911\,l^2\,m\,\phi^{12}}{140099805812736000} + \mathcal{O}(\phi^{13})$$

$$M_{42}^e = (\frac{ml}{2\Delta})\frac{l}{\phi}(C_4 f_{13} + C_3 f_{14} - C_4 f_{15} + C_1 f_{16})$$

$$= \frac{-(l^3\,m)}{140} - \frac{1097\,l^3\,m\,\phi^4}{69854400} - \frac{899\,l^3\,m\,\phi^8}{28252224000}$$

$$- \frac{5220181117\,l^3\,m\,\phi^{12}}{81958386400450560000} + \mathcal{O}(\phi^{13})$$

$$M_{43}^e = (\frac{ml}{2\Delta})(C_5 f_{13} + C_6 f_{14} - C_5 f_{15} - C_6 f_{16})$$

$$= \frac{-11\, l^2\, m}{210} - \frac{223\, l^2\, m\, \phi^4}{2910600} - \frac{3547\, l^2\, m\, \phi^8}{23837814000}$$

$$- \frac{4215149\, l^2\, m\, \phi^{12}}{14228886527856000} + \mathcal{O}(\phi^{13})$$

$$M_{44}^e = (\frac{ml}{2\Delta})\frac{l}{\phi}(C_7 f_{13} + C_5 f_{14} - C_7 f_{15} - C_5 f_{16})$$

$$= \frac{l^3\, m}{105} + \frac{71\, l^3\, m\, \phi^4}{4365900} + \frac{127\, l^3\, m\, \phi^8}{3972969000}$$

$$+ \frac{20403571\, l^3\, m\, \phi^{12}}{320149946876760000} + \mathcal{O}(\phi^{13})$$

(B.7)

From Eqs. (B.4) and (B.7) it is seen that the final power series expressions for both the dynamic stiffness matrix and the mixed formulation mass matrix involve on ϕ^{4n} terms. As defined before, $\phi = \left(\frac{\omega^2 m l^4}{EI}\right)^{\frac{1}{4}}$, hence, $\phi^{4n} = \left(\frac{ml^4}{EI}\right)^n \omega^{2n}$. Therefore, the foregoing analysis verifies that only even powers of the natural frequency ω appear in expansion of the frequency dependent mass and stiff matrices.

Term by term comparison shows that $i, j \in \{1, 2, 3, 4\}$,

$$\varepsilon_{ij} = \mathbf{D}_{ij} - (\mathbf{K}_{ij}^e - \omega^2 \mathbf{M}_{ij}^e)$$

$$\approx \mathcal{O}(\phi^{13})$$

(B.8)

where $\mathbf{D}$ is the dynamic stiffness matrix and $\mathbf{K}^e$ and $\mathbf{M}^e$ are the mixed formulation stiffness and mass matrices. Additional analyses shows that the difference ε_{ij} can be made arbitrarily small by using more and more terms in power series expansions.

Rajesh Kumar Singh

MAILING ADDRESS: At & Post – Pali
Gorakhpur – 273209, U.P.
INDIA

PLACE AND DATE OF BIRTH: Gorakhpur, India on April 30, 1967

EDUCATION:

Doctor of Philosophy, January, 1994
Stanford University
Stanford, California, U.S.A.

Master of Applied Science, June, 1989
University of British Columbia
Vancouver, B.C. V6T 1W5, Canada

Bachelor of Technology, May, 1987
Indian Institute of Technology
Kanpur – 208016, U.P., India

PUBLICATIONS:

- H. A. Smith and R. K. Singh, "An Arnoldi-based Eigensolution Technique For Damped Free Vibration Analysis Using Frequency Dependent Formulation," *35th Structures, Structural Dynamics, and Materials Conference, Hilton Head, South Carolina*, April, 1994.

- R. K. Singh and H. A. Smith, "A Comparison of Computational Effectiveness of the Finite Element Formulations in Free Vibration Analysis," accepted for publication in the *Computers and Structures*.

- R. K. Singh and H. A. Smith, "Performance Comparison of the Mixed, $h-$ and $p-$formulations of the Finite Element Method for Vibration Analysis," *34th Structures, Structural Dynamics, and Materials Conference, La Jolla, California*, April, 1993.

- H. A. Smith, D. C. Sorensen, and R. K. Singh, "A Lanczos-based Eigensolution Technique for Exact Vibration Analysis," *International Journal for Numerical Methods in Engineering*, Vol. 36, 1987–2000, 1993.

- H. A. Smith, D. C. Sorensen, and R. K. Singh, "A Nonlinear Eigensolver for Exact Vibration Analysis," *Proceedings of the Ninth Conference on Engineering Mechanics, ASCE*, Texas A & M University, 920–923, May, 1992.

- R. K. Singh, "Finite Element Analysis of Period Viscous Flow in a Constricted Pipe," dissertation submitted to the *Department of Civil Engineering, The University of British Columbia, Vancouver, BC*, June, 1989.

- R. K. Singh, R. Pipraiya, et al.,"Planning and Design of a Grade Separated Traffic Interchange System," project report submitted to the *Department of Civil Engineering, Indian Institute of Technology, Kanpur*, April, 1987.

AWARDS:

1988 – 90	University Graduate Fellowship
1987 – 90	Research Assistantship
Spring '86	Certificate of Merit
1983 – 87	Institute Merit Scholarship
Winter '83	2nd position in "Pratibha Khoj Pariksha" (Talent Search Examination)
1981 – 87	National Merit Scholarship
1979 – 81	U.P. Government Provincial Merit Scholarship